PRODUCTION AND CHARACTERIZATION OF ACTIVATED CARBON FROM PISTACHIO-NUT SHELL

A THESIS SUBMITTED TO
THE GRADUATE SCHOOL OF NATURAL AND APPLIED SCIENCES
OF
THE MIDDLE EAST TECHNICAL UNIVERSITY

BY

GAMZENUR ÖZSİN

IN PARTIAL FULFILLMENT OF THE REQUIREMENTS
FOR
THE DEGREE OF MASTER OF SCIENCE
IN
CHEMICAL ENGINEERING

JANUARY 2011

Approval of the thesis:

PRODUCTION AND CHARACTERIZATION OF ACTIVATED CARBON FROM PISTACHIO-NUT SHELL

submitted by **GAMZENUR ÖZSİN** in partial fulfillment of the requirements for the degree of **Master of Science in Chemical Engineering Department, Middle East Technical University** by,

Prof. Dr. Canan ÖZGEN _____

Dean, Graduate School of **Natural and Applied Sciences**

Prof. Dr. Deniz ÜNER _____

Head of Department, **Chemical Engineering**

Prof. Dr. Hayrettin YÜCEL _____

Supervisor, **Chemical Engineering Dept., METU**

Dr. Ahmet Kemal BEHLÜLGİL

Co-Supervisor, **Central Lab., METU** _____

Examining Committee Members:

Prof. Dr. Gürkan KARAKAŞ _____

Chemical Engineering Dept., METU

Prof. Dr. Hayrettin YÜCEL _____

Chemical Engineering Dept., METU

Dr. Ahmet Kemal BEHLÜLGİL _____

Central Lab., METU

Prof. Dr. Zeki AKTAŞ _____

Chemical Engineering Dept., Ankara University

Dr. Cevdet ÖZTİN _____

Chemical Engineering Dept.,METU **Date:** 24.01.2011

I hereby declare that all information in this document has been obtained and presented in accordance with academic rules and ethical conduct. I also declare that, as required by these rules and conduct, I have fully cited and referenced all material and results that are not original to this work.

Name, Last Name: Gamzenur ÖZSİN

Signature:

ABSTRACT

PRODUCTION AND CHARACTERIZATION OF ACTIVATED CARBON FROM PISTACHIO-NUT SHELL

ÖZSİN, Gamzenur
M.Sc., Department of Chemical Engineering
Supervisor: Prof. Dr. Hayrettin YÜCEL
Co-Supervisor: Dr. Ahmet Kemal BEHLÜLGİL

January 2011, 190 pages

In this study production and characterization of activated carbon from an agricultural waste, pistachio-nut shells, was investigated. To determine optimum production conditions by chemical activation method, effect of tempreature (300, 500, 700 and 900 ^{o}C) and effect of impregnation ratio (1:1, 2:1 and 3:1 as activation agent:sample) were investigated by applying two different methods (raw material activation and char activation) and with two different activation agents (phosphoric acid and potassium hydroxide).

To produce activated carbon, all the impregnated samples were heated to the final activation temperature under a continuous nitrogen flow (100 cm^3/min) and at a heating rate of 10 ^{o}C/min and were held at that temperature for 1 hour.

Pore structures of activated carbons were determined by N_2 adsorption and micro-mesopore analysis was made by "Non-local Density

Functional Theory" and "Monte Carlo Simulation" method (NLDFT-Monte Carlo Simulation Method). BET surface areas of produced activated carbons were found from N_2 adsorption data in the relative pressure range of 0.01 to 0.15.

BET surface areas of phosphoric acid activated carbons by raw material activation method were found between 880 and 1640 m^2/g. The highest value of the BET surface area was obtained in the case of the activated carbon which was produced with an impregnation ratio of 3/1 (g H_3PO_4/g raw material), at an activation temperature of 500 ^oC. The repeatibility was also investigated on phosphoric acid activated carbons which were produced with conventional raw matererial activation method. Results showed that, both the BET surface area values and pore size distributions were consistent among themselves.

On the other hand char activation experiments with phosphoric acid produced activated carbons having lower BET surface areas than the ones obtained with raw material activation method by creating mesoporous structure. When the same char activation method was tried with potassium hydroxide, it was concluded that elevated temperatures could help in producing activated carbons with high BET surface areas by creating microporous structure.

Results also showed that properties of activated carbon such as ash content, slurry pH value, true density, elemental composition, methylene blue number and surface morphology were strongly affected by both production conditions and production method, as pore structure was affected considerably.

Keywords: Activated carbon, Pistachio-nut shell, Phosphoric acid, Potassium hydroxide, Pore structure, Activation

ÖZ

ANTEP FISTIĞI KABUĞUNDAN
AKTİF KARBON ÜRETİMİ VE KARAKTERİZASYONU

ÖZSİN, Gamzenur
Yüksek Lisans, Kimya Mühendisliği Bölümü
Tez Yöneticisi: Prof. Dr. Hayrettin YÜCEL
Ortak Tez Yöneticisi: Dr. Ahmet Kemal BEHLÜLGİL

Ocak 2011, 190 sayfa

Bu çalışmada, tarımsal bir atık olan antep fıstığı kabuklarından aktif karbon üretimi ve karakterizasyonu incelenmiştir. Kimyasal aktivasyon yöntemi ile optimum üretim koşullarını belirlemek için sıcaklığın (300, 500, 700 and 900 ^{o}C) ve doyurma oranının (1:1, 2:1 ve 3:1; aktivasyon maddesi :numune) etkisi iki farklı yöntem (hammaddenin aktivasyonu ve kömür aktivasyonu) uygulanarak ve iki farklı aktivasyon maddesi (fosforik asit ve potasyum hidroksit) kullanılarak incelenmiştir.

Aktif karbon üretmek için, kimyasalla doyurulmuş örnekler sürekli bir azot akışında (100 cm^3 / dak) ve 10 ^{o}C/dak ısıtma hızında aktivasyon sıcaklığına kadar ısıtılmış ve bu sıcaklıkta 1 saat süreyle bekletilmiştir.

Aktif karbonların gözenek yapıları N_2 adsorpsiyonu ile belirlenmiş ve mikro ve mezogözenek analizleri "Lokal Olmayan Yoğunluk Fonksiyonu Teorisi" ve "Monte Carlo Simülasyon Yöntemi" ile belirlenmiştir. Üretilen

aktif karbonların BET yüzey alanları bağıl basıncın 0.01 ile 0.15 olduğu bir aralıkta N_2 adsorpsiyon verilerinden bulunmuştur.

Hammadde aktivasyonu yöntemi uygulanarak, fosforik asit ile aktive edilmiş aktif karbonların BET yüzey alanları 880 ile 1640 m^2/g arasında bulunmuştur. En yüksek BET yüzey alanı, 3/1 doyurma oranı (g H_3PO_4/g hammadde), 500 ^oC aktivasyon sıcaklığında aktif karbon üretilmesi durumunda elde edilmiştir. Geleneksel olarak uygulanan, hammadde aktivasyonunun uygulandığı yöntem ile üretilen, fosforik asit ile aktive edilmiş aktif karbonların tekrarlanabilirliği de incelenmiştir. Sonuçlar, hem BET yüzey alanı değerlerinin hem de gözenek boyutu dağılımlarının kendi aralarında tutarlı olduğunu göstermiştir.

Diğer taraftan, fosforik asit ile yapılan char aktivasyon deneyleri ile, mezogözenekli bir yapı oluşturularak, hammaddenin aktive edildiği yöntemden daha düşük BET yüzey alanlarına sahip olan aktif karbonlar üretilmiştir. Aynı kömür aktivasyonu yöntemi potasyum hidroksit ile denendiğinde ise, yüksek sıcaklıklarda mikrogözenekli yapı oluşturularak, yüksek BET yüzey alanlarına sahip aktif karbonlar üretilebileceği sonucuna varılmıştır.

Sonuçlar, gözenek yapısı gibi, aktif karbonun kül içeriği, bulamaç pH değeri, gerçek yoğunluğu, elementel bileşimi, metilen mavi sayısı gibi özelliklerinin de, hem üretim koşulları hem de üretim yöntemi ile önemli oranda etkilendiğini göstermiştir.

Anahtar kelimeler: Aktif karbon, Antep fıstığı kabuğu, Fosforik asit, Potasyum hidroksit, Gözenek yapısı, Aktivasyon

To My Family…

ACKNOWLEDGEMENTS

First of all, I want to express my deepest appreciation to my supervisors Prof. Dr. Hayrettin YÜCEL and Dr.Ahmet Kemal BEHLÜLGİL for their support, guidance and suggestions during my research. Working with them is a great honor for me.

I am very grateful to my parents Zehra ÖZSİN and Gürsel ÖZSİN for their endless love, trust and sacrifices for me.

I should mention Prof. Dr. Zeki AKTAŞ and Assoc. Prof. Dr. Emine YAĞMUR from Ankara University for sharing their experiences and comments with me.

I also want to thank my undergraduate teachers at Anadolu University for encouraging me to graduate studies and conducting me to the academic life.

I would like to thank Kerime GÜNEY for her moral support and Mihrican AÇIKGÖZ and Gülten ORAKÇI for helping me in the analysis of the products.

Explaining my feelings to my friends is the most difficult part of this writing. I want to thank Eda Oral, Berk Baltacı, Nur Sena Yüzbaşı, Bijen Kadaifci, Merve Başdemir, Didem Polat, A. İrem Balcı, Aslı & Efe Boran, Ş.Seda Yılmaz, Saltuk Pirgalioğlu, Sibel Dönmez, Wissam Abdallah, Birsu Aydoğdu, Ahmet Naiboğlu, Emre Yılmaz, Hasan Zerze and many others. I want to thank all of my colleagues at METU for their friendship. I also want to mention my colleague Baraa Abbas Ali who died dramatically in Iraq after a very short time from his graduation. Rest in peace Baraa….

I also want to thank my best friends Esra İnce Özsoy, Merih Kasap and Ekin Özakar for their endless support and friendship. I'm so lucky for having such lovely sisters which will make me so strong during my life.

Finally, I want to say how much that I loved my grandfather, Recep Doğu ÖZSİN, who died 10 days before my jury. Rest in peace…

TABLE OF CONTENTS

APPENDICES

LIST OF TABLES

TABLES

LIST OF FIGURES

FIGURES

LIST OF SYMBOLS

A_m : Cross-sectional area of the adsorbate, m^2

C : A constant BET equation

C_o : Initial concentration of solution, mg/L

C_{blank} : Concentration of solution in blank experiment, mg/L

CSA_{N2} : Cross sectional area of nitrogen molecule, m^2

D_p : Pore diameter, μm

E_i : Adsorption potential, KJ/mole

ΔG : Gibbs free energy change of the reaction, KJ/mole

I : Intercept of the BET plot

K : A constant in DR equation

M : Adsorbate molecular weight, g/mol

N : Amount adsorbed, moles

N_A : Avagadro's constant, $6.023*10^{23}$ molecules/mol

P_i : Partial pressure of the gas, I

P : Pressure, atm, Pa, psia, mmHg

P_o : Saturation pressure, mmHg

q_1 : Heat of adsorption of the second and subsequent layers

q_2 : The gas constant, $8.314x10^7$erg/mole-K, $8.314x10^{-3}$ KJ/mole-K

r_p : Actual pore radius, mean radius of the liquid meniscus, nm or μm

r_K : Kelvin radius

r_{KAVE} : Average Kelvin radius

r_{PAVE} : Average pore radius

S : Slope of the BET plot

S_{BET} : BET surface area, m^2/g

S_{MESO} : Mesopore surface area, m^2/g

T : Thickness of the adsorbate layer

t_m : Thickness of the monolayer

T : Temperature, °C

T_c : Critical temperature of the adsorption, °C

V : Volume adsorbed, cm^3/g

V_{CEL} : Cell volume, cm^3

V_{EXP} : Expansion volume, cm^3

V_{SAMP} : Volume of the sample, cm^3

V_o : Micropore Volume, cm^3/g

V_m : Monolayer volume, cm^3/g

V_{meso} : Mesopore volume, cm^3/g

V_{mol} : Molar volume of nitrogen, $34.6x10^{24}$ A^3/mol at -195.6°C

ΔV_{gas} : Incremental molar adsorbed gas volume, cm^3/g

ΔV_{Liq} : Incremental molar adsorbed liquid volume, cm^3/g

W : Pore width, Å

W : Limiting adsorption space volume value

W_o : Limiting adsorption space volume value

W_a : The quantity of adsorbed at a particular relative pressure

W_m : The quantity of adsorbed at correspond to BET monolayer

Greek Letters

μm : Micrometer (10^{-6} meter)

Å : Angstrom (10^{-10} meter)

ρ : Liquid density, g/cm^3

B : Affinity coefficient in DR method

ρ_{He} : Helium (True) Density, g/cm^3

Θ : Contact angle of mercury, 130° and Fraction of surface occupied by adsorbate

γ : Surface tension

CHAPTER I

INTRODUCTION

Although it has been invented many years ago, activated carbon is still one of the most popular adsorbents throughout the world due to its high adsorptive capacity. The thing that makes activated carbon such a special and broadly used adsorbent is its porous texture. The pores of the activated carbon have intense forces that cause the adsorption phenomena on its surface (Marsh and Rodriguez-Reinoso, 2006).

The term activated carbon belongs to a large family of carbons which includes carbon blacks, carbon fibers and so forth. But the general definition can be given as the amorphous carbonaceous material that possesses very high porosity with an extended surface area (Balcı 1992; Bansal and Goyal, 2006).

The adsorption characteristics of activated carbons are dependent on their chemical and physical structure. The porous network and the dimensions of the pores are crucial for the sustainment of the enough penetration of adsorbed phase to the pores of the adsorbent. Since activated carbon has a polymodal pore size distribution including macropores, mesopores and micropores, adsorption of various components in many applications is feasible by activated carbon. Besides, the non-polar properties of the activated carbons give a hydrophobic character that makes adsorption from aqueous solutions or humid streams possible (Crittenden and Thomas,1998).

The pore classification of porous materials, which has been proposed by IUPAC (Table 1) distinguishes the pore sizes of activated carbon and determines the adsorption properties.

Table 1.1 Classification of Pores According to Their Sizes (IUPAC, 1985)

Classification	**Pore Diameter**
Macropores	D_p >50 nm (or D_p >500 Å)
Mesopores	50 nm > D_p > 2 nm (or 500 Å > D_p > 20 Å)
Micropores	2 nm > D_p (or 20 Å >D_p)

Activated carbon is used in many fields both in industry and daily life of every person. The drinking water treatment, medical usage, taste and color removal in food industry, usage in catalysis, filtration are the most commonly known applications of activated carbon. Also natural gas storage, usage in capacitors and in the manufacturing of special products are less known than the other application fields but undoubtedly, these less known and still growing fields of activated carbon applications will have enormous importance for amelioration of productive goods and processes.

Indispensible utilization of activated carbon in industry necessitates the lowering of the production costs to keep the competitiveness on the

market. Lowering the production costs can be possible by both replacement of the raw materials with the cheap and abundant ones and by optimizing the process conditions that could minimize the operating costs. Furthermore, products that have high quality with a wide variety of activated carbon products for specific applications, should be supplied. That's why remarkable investigations and research should be done on the alternative sources and processes for the activated carbon production.

Activated carbon can be produced from many materials like biomass, resins, different coals with different ranks including peat, lignite, anthracite or synthetic macromolecular systems. In the selection of the raw material, reliability of the source is as important as the quality and the cost of the raw material. Biomass is one of the major and inexhaustible source for organic fuels, chemicals and new-generation materials. It has a complex structure including cellulose, hemicellulose and lignin, therefore it is also called as a lignocellulosic material. Conversion of the lignocellulosic biomass to a form of activated carbon is also easy and widely used and especially environment friendly technique. Notably, by evaluating agricultural wastes in the production of activated carbon, the conversion of such worthless wastes to valuable products can be achieved. This waste management also makes an important contribution for the sustainment of a healty environment by using activated carbon produced in the purification of contaminants from liquid and gas streams that evolved from the industrial and domestic sources (Pütün and Apaydın-Varol, 2010).

Mainly, the production of activated carbon includes two steps, namely carbonization and activation which involve the dehydration, carbonization and oxidation of the raw material. Although many raw materials are used in the preparation of activated carbon in the laboratory, the commercialized ones are limited (Balcı, 1992; Yahşi, 2004).

Carbonization is the pyrolysis of raw material in the absence of air which aims the maximization of the char product formed from the parent material and the increasing the carbon content for the activated carbon production. At the time of the carbonization, hundreds of co-current reactions occur because of the complex and the heterogeneous origin of the lignocellulosic biomass. During these reactions a little porosity is created but this porosity is not enough for most of the adsorption processes because of its low adsorption capacity. For this purpose the carbonization step is followed by activation process for creating further porosity. The temperature, heating rate, atmosphere that reactions takes place in, catalyst usage, reactor configuration and carbonization time are the important process parameters in the pyrolysis or carbonization process that should be carefully selected and controlled.

The activation can be done either physically or chemically. Physical activation involves the reaction of the carbon structure created by carbonization with air, oxygen, steam or carbon dioxide. Gas activation or thermal activation term is usually used instead of the physical activation, because the heat treatment is carried out at very high temperatures and carbonaceous material is treated with gases for further pore development. Since the air and oxygen activation reactions are difficultly controlled, steam activation and carbon dioxide activation is generally used in the commercial scale.

On the other hand, some disadvantages of physical activation can be handled by the chemical activation methods, or methods including the combination of the physical and chemical activation. Since the chemical activation is carried out in a single step and reaches higher yields and well developed microporosity, preferred activation mechanism may be selected as the chemical activation. Besides, in many conditions, the activated carbons can be produced at lower temperatures than the temperatures used in the physical activation. This offers an important decrease in the energy cost in the production by influencing the operating costs of the overall process. Notwithstanding the advantages of chemical

activation, there are some disadvantages of this method, such as removing the excess chemicals after carbonization, possible impurities remained in the structure, additional cost payment to the chemical agents, and additional time and energy required to provide enough contact with the chemicals. But both physical and chemical or the combination of these two activation methods is used in modern technologies depending on the requirement (Balcı, 1992).

In the chemical activation, the raw material or carbonized products is mixed with the activating agents and then activated with an additional heat treatment. Up to now, there are a few chemicals tried for activated carbon production but three chemicals are important; phosphoric acid, zinc chloride and potassium hydroxide. Each chemical behaves different on the different parent material depending on the structure and the conditions but they all effect the course of the carbonization (Marsh and Rodriguez-Reinoso, 2006; Yahşi, 2004).

Pore characteristics such as surface area, pore volume and pore size distribution with the chemical surface properties are the main considerations that should be taken into account in the determination of the quality and application fields. These properties undoubtedly depend on both the raw material and carbonization and activation methods. Agricultural raw materials are desirable when they are compared with the other precursors in the activated carbon production according to their adsorptive properties. Besides, low ash and high carbon including precursors are more preferable than the others.

The objective of this study is production of chemically activated carbons from an agricultural waste; pistachio-nut shell, by phosphoric acid and potassium hydroxide activation with two different methods and characterization of the produced activated carbons in terms of surface area, pore volume and pore size distribution. The novelty achieved in this work is the phosphoric activation of pistachio nut shells and investigation by two different methods that have not been tried with this material and

activator. These two methods are activation of raw material and activation of carbonized product. Also effects of the temperature and the chemical to raw material impregnation ratio were investigated to find optimum production conditions of activated carbon from pistachio-nut shells.

CHAPTER II

LITERATURE SURVEY

Since activated carbon plays an important role on adsorption processes in many fields, extensive studies and innovations have been made on both in the production methods and forms of the activated carbon. In this study, requirements that have to be possessed by activated carbons to be an effective sorbent is explained, and the methods of the production are described.

2.1. ACTIVATED CARBON

2.1.1 Definition and Properties

The term activated carbon includes many carbonaceous materials which are amorphous. But, the general definition of activated carbon can be defined as a microcrystalline, non-graphitic form of carbon with a large surface area that derives from its porosity.

According to the X-ray analysis, the structure of activated carbon is much more irregular than the graphite's structure. Active carbons have crystallites only a few layers in thickness and less than 10 nm in width (Smisek and Cerny, 1970).

The property which makes activated carbon so unique, useful and popular among the other sorbents is its large surface area. The high surface area is a result of the microporous structure and the thing which makes this microporous structure is the voids between the crystallites. The internal surface area of an activated carbon varies between 250 and 2500 m^2/g. There are also some activated carbons with a surface area more than 2500 m^2/g that can be feasible for special applications which necessitates a very high accessible surface area. In Figure 2.1, SEM micrographs of surface of an activated carbon can be seen.

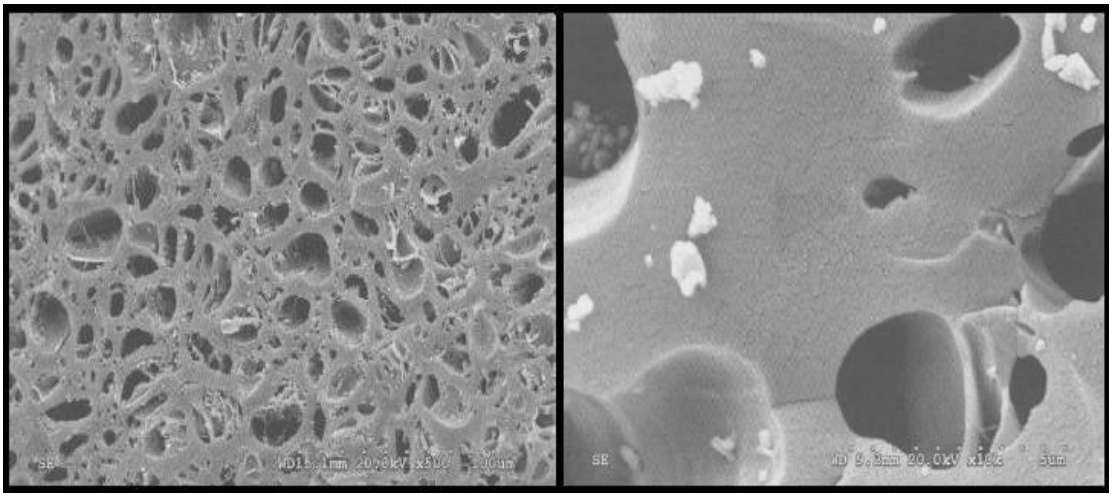

Figure 2.1 SEM Micrographs of a Surface of an Activated Carbon (Marsh and Rodriguez-Reinoso, 2006)

Activated carbons are used for a multitude separation and purification applications by adsorption. Adsorption is the accumulation of substances on the interface of a solid. That means, the concentration of a substance at the interface between a fluid and a solid tends to be higher than the concentration in the fluid due to the forces in the adsorption process. The adsorption process can be either physical or chemical, and sometimes the term physical and chemical adsorption can renamed as

physisorption and chemisorption, respectively, depending on the nature of the surface forces (Akgün, 2005; Balcı 1992).

Table 2.1 Differences Between Chemisorption and Physisorption (Inglezakis and Poulopoulos, 2006)

	Chemisorption	**Physisorption**
Temperature range over which adsorption occurs	Virtually unlimited; however, a given molecule can be effectively adsorbed only over a small range	Near or below the condensation point of the gas
Adsorption enthalpy	Wide range, related to the chemical bond strength, typically 40-800 kJ/mol	Related to factors like molecular mass and polarity, but typically 5-40 kJ/mol
Nature of adsorption	Often dissociative and may be irreversible	Non-dissociative and reversible
Saturation uptake	Limited to monolayer	Multilayer uptake is possible
Kinetics of adsorption	Variable; often it is an activated process	Fast, because it is a non-activated process

In physisorption, the adsorbates hold on to the adsorbent surface by weak van der Waals forces and electrostatic forces between the adsorbate species and adsorbent surface. Whereas, in chemisorption the forces are not weak like in physisoption, and the adsorption only occurs on the active sites of the adsorbents surface. Chemisorption includes an exchange of electrons that causes chemical bonding on the specific sites. And, if a comparision between the interaction energies of these two types

of adsorption is carried out, it will be obviously seen that interaction energies in chemisorption is stronger than in the physisorption. The most discriminative properties between chemisorption and physisorption are mono or multilayer formation on the adsorbent, activation energy, reversibility and the specificity of the adsorption towards to the interacting surfaces. These main differences between physisorption and chemisoption are summarized in Table 2.1 (Inglezakis and Poulopoulos, 2006).

The adsorption capacity and the adsorption kinetics are both distinct and interlinked concepts which should be considered in the adsorption processes. These two concepts are directly related the porous structure of the adsorbent. And the porous structure of the adsorbent is influenced by the parent material and its production procedure. Undoubtedly, porous structure is main, but it is not only the requirement to satisfy the adsorption process effectively. The surface area limits the amount and the pore volume limits to the size of the molecules or atoms of the adsorbed species. Besides, the adsorbent should be selective to the adsorbate with a high adsorption capacity (Do, 1998).

The most reliable techniques to characterize the adsorbents' adsorptive properties are again possible with techniques developed on the basis of adsorption, like nitrogen adsorption. Internal surface area can be determined by nitrogen adsorption, which is used extensively. But the results obtained from the nitrogen adsorption may not agree with the real available surface, hence pore size distribution is a necessity for an activated carbon characterization.

2.1.2 History

From the time of the invention of active carbons, they have found very wide application fields that influenced the mankind's life. It is believed that history of activated carbons goes back to ancient times. It

is known, father of medicine, Hyppocrates used activated carbon in digestion problems and that application is still used in the modern medicine. But in the contemporary sense, inventor of activated carbon is admitted a Russian researcher, Raphael Ostrejko who got patents of activated carbon. Another important application including activated carbon is the usage in the gas masks in World War I. With this usage of activated carbon, soldiers were protected against the poisonous gases (Marsh and Rodriguez-Reinoso, 2006; McKetta and Cunningham, 1978).

In 1900's, two important process patents from wood and peat were granted in Europe and then these developments followed by the entire world. Recent innovations are still developing and most of the researches are focused on the recycling of waste materials to protect environment by converting them activated carbon forms (Kirk Othmer, 2001).

2.1.3 Applications of Activated Carbons

The applications of activated carbons can be categorized in two broad subtitles as liquid-phase applications and gas-phase applications.

The liquid-phase carbons mostly have pores near or larger than 3 nm in diameter. On the other hand, gas-phase active carbons are mostly in the range from 1 to 2.5 nm in diameter. Because of the larger sizes of many dissolved adsorbates and the slow diffusion rates of molecules in the liquid than the diffusion rates of molecules in the gas for the equal dimensions, liquid-phase applications require larger pores in the activated carbons. Also, granular form of activated carbons are generally used in the adsorption in the gaseous phase, on the contrary, powdered activated carbons are more preferable in the liquid-phase applications (Yang, 1997; Ullmann, 2002).

Purification of sugar and corn sugar in the sugar industry, potable water treatment to improve taste, smell and the color of water, industrial and municipal wastewater treatment, groundwater remediation, impurity

removal in food and beverage industry, useage in chemical processing and mining operations in industry, usage in pharmaceutical processes and purification of wastewaters in electroplating industry can be denoted as the main liquid phase applications of the activated carbons. Gas phase applications include solvent recovery, catalysis, gas storage, gasoline emission control, flue gas treatment, protection against hazardous atmospheric contaminants and so on and so forth. Meanwhile, the producers are still developing specialized products to extend applications of activated carbons not only by improving separation and purification capabilities, but also finding innovative application fields such as using the carbons as energy storage medium in the capacitors.

2.1.4 Physical Structure of Activated Carbon

Carbon is a unique element which possesses different allotropes depending on the hybridization type. Graphite or graphitic carbon has graphene layers that are arranged parallel to each other in tridimensional crystalline network. On the contrary to graphitic carbon, non-graphitic carbon does not have a long range tridimensional network even if it has been treated in graphitization process. The non-graphitic carbons then subdivided to graphitizing (graphitizable) and non-graphitizing (non-graphitizable) carbons (Bottani and Tascon, 2008).

Franklin (1951) defined two different classes of non-graphitic carbons obviously and shematic representations of these non-graphitic carbons is given in Figures 2.2 and 2.3.

It was concluded that, matters which has little hydrogen or much oxygen in their structure result in non-graphitizing carbons. By heating these matters, at low temperatures, there is a development of a strong system of crosslinking which immobilize the structure and crystalline units in a rigid mass. The random orientations of of crystallites with crosslinking make up a porous structure. The non-graphitizing carbons

can not be transformed into graphitic form by a high temperature treatment under atmospheric pressure.

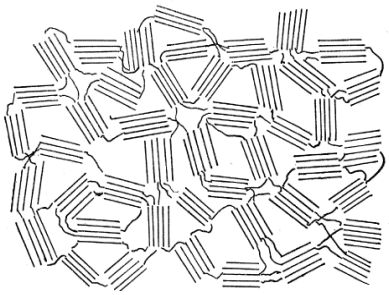

Figure 2.2 Schematic Representation of the Structure of a Non-graphitizing Carbon (Franklin, 1951)

On the other hand, graphitizing carbons can be converted to a form of graphitic carbon. In general, graphitizing carbons are created from substances containing more hydrogen. During the early stages of carbonization, the crystallites stay relatively mobile and cross-linking formation occurs weakly. The neighbouring crystallites tend to lie nearly parallel to another by allowing only small voids between them. As a consequence, the carbons formed are much softer and less porous than the non-graphitizing carbons (Franklin,1951).

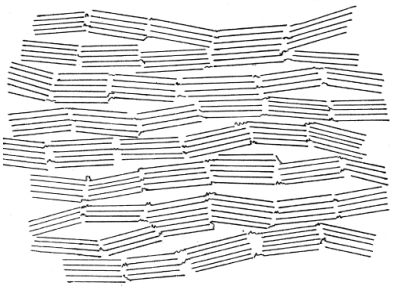

Figure 2.3 Schematic Representation of the Structure of a Graphitizing (but non-graphitic) Carbon (Franklin, 1951)

The basic structure of activated carbon resembles the structure of pure graphite but it is different from the graphite. The graphite crystal consists of layers of fused hexagons that are held approximately 0.335 nm apart by the effects of van der Waals forces and this structure of graphite is given in Figure 2.4 (Smisek and Cerny,1970).

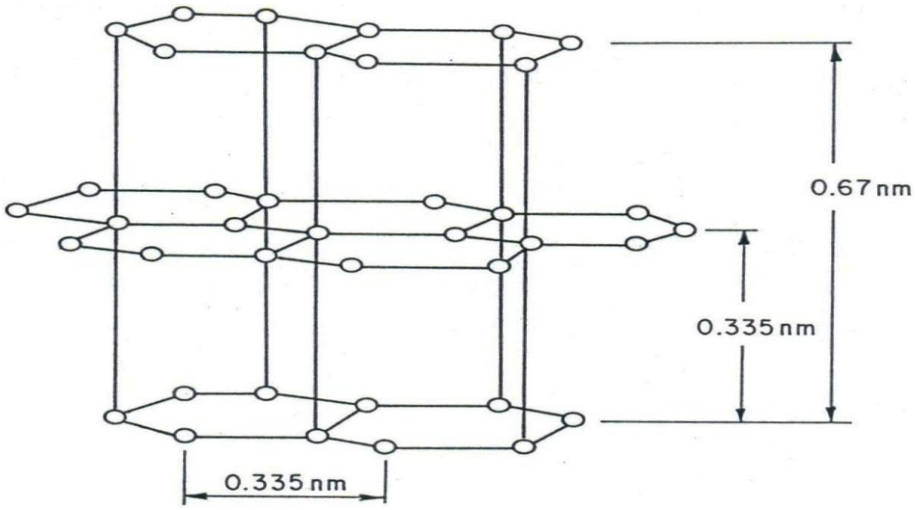

Figure 2.4 Arrangements of Carbon Atoms in the Graphite Crystal (Smisek and Cerny,1970)

At the time of carbonization process to produce activated carbon, several atomic nuclei which have a structure same with the graphite's structure are formed. Distance of planar separation is nearly 0.36 nm in carbon. From the X-ray spectrograph, these structures of carbon have been interpreted as microcrystallite consisting of fused hexagonal rings of carbon atoms. Hence, activated carbon is considered to contain a rigid interlinked groups of microcrystallites and each of these microcrystallites includes a stack of graphite planes. Also there are interconnections of microcrystallites by fuctional groups that destroy the graphitic planes in the structure. In summary, activated carbon has a non-graphitic,

amorphous and a randomly crosslinked structure (Abdallah, 2004; Balcı 1992).

2.1.5 Chemical Structure of Activated Carbon

The chemical structure of activated carbon has an important effect on the adsorptive properties. The adsorption capacity of activated carbons is affected by the chemical structure besides the physical or porous structure.

There are many carbons that have different adsorption capacity to the same adsorbate although they have very similar characteristics in terms of surface area and pore size distribution. This explains that adequate porous structure is a necessity for adsorption but it should be considered with the chemical structure of the carbon.

Activated carbon includes two types of admixtures. These are inorganic part of the product called ash and chemically bounded elements which make up the organic structure with the carbon atoms. The chemically bounded structures consist of mainly oxygen and hydrogen elements and these structures are derived from the parent material and remained in the structure due to the imperfect carbonization or chemical bonding to the surface during activation. Roughly, the chemical composition of an activated carbon can be stated as 85-90 % C, 5 % O, 0,5 % H, 0,5 % N and 1 % S. The remaining 5-6 % corresponds to the inorganic constituents (Yahşi, 2004).

Activated carbon can be defined as a twisted network of defective hexagonal carbon layer planes. These layer planes are cross-linked by aliphatic bridging groups. There are heteroatoms, the atoms other than carbon both into the network and on the surroundings of the planes. The heteroatoms on the surface of activated carbon have a significant key role in the surface chemistry by influencing the adsorption properties.

The presence or absence of the surface groups of activated carbon effects the adsorbent-adsorbate interaction (Yang, 2003).

Heterogeneous nature of activated carbon is a result of the many surface functional groups which are formed by the interactions of the free radicals during carbonization and activation. The nature of these functional groups is determined by both activation method and the type of the raw material. Mainly oxygen containing and hydrogen containing functional groups are present in the surface of the activated carbon. Other than hydrogen and oxygen elements, nitrogen, calcinated sulphur, chlorine and other elements can also be present in the structure.

The surface functional group effects both the hydrophobic/hydrophilic and the acidic/basic character of the activated carbon (Bandosz, 2006).

2.1.5.1 Oxygen Containing Functional Groups

In the structure of an activated carbon, carbon atoms at the edges of the basal planes are unsaturated because of the unpaired electrons. These sites not only increase the surface groups by chemical bonding of heteroatoms but also define the chemical characteristics of the activated carbon. Oxygen-containing functional groups are very common surface groups in the activated carbon structure.

The oxygen-containing surface groups effect both surface characteristics such as polarity, wettability, acidity, and physicochemical properties like catalytic, electrical and chemical reactivity of the material (Bansal and Goyal, 2006).

The oxygen content of the raw material has an enormous effect on the arrangement and the size of the elementary crystallites formed in the carbonaceous sorbents. High oxygen containing materials cause smaller distances between the parallel graphitic layers. Also, course of the

carbonization and carbonization temperature highly depend on the oxygen content of the starting material (Balcı, 1992; Çuhadar 2004).

Activated carbons (non-graphitizable carbons) have also a relatively large edge area that causes a strong tendency for oxygen chemisorptions. The oxygen of oxidizing gases dissociates into atoms and reacts with carbon structure and as a consequence bonding at the edge of the layer planes and makes up the oxygen surface oxides (Bandosz, 2006).

Activated carbons have variable oxygen content between 1 % and 25 %. The amount of the oxygen is changeable with the activation temperature, generally increasing activation temperature causes a decline on the amount of the oxygen (Yahşi, 2004).

The most common oxygen containing surface functional groups found on carbon surfaces are given in Figure 2.5.

Carbons activated at low temperatures (200 ^{o}C - 500 ^{o}C) are generally termed as L-carbons, while those activated at high temperatures (800 ^{o}C - 1000 ^{o}C) are termed as H-carbons. The L-carbons will develop acidic surface oxides which mainly includes phenolic hydroxyl groups. Chemical treatment in aqueous solutions with oxidizing agents like chloride, permanganate, persulfate, hydrogen peroxide and nitric acid also causes activated carbons that have same characteristics as L-carbons. On the other hand, H-carbons will develop basic surface oxides. The acidic or basic surface oxides influence the adsorption of electrolytes. Although, activated carbons are amphoteric by nature with the coexistence of the acidic and basic sites together, the overall acidity or basicity depends on the strengths and the amounts of these sites (Bandosz, 2006; Balcı 1992).

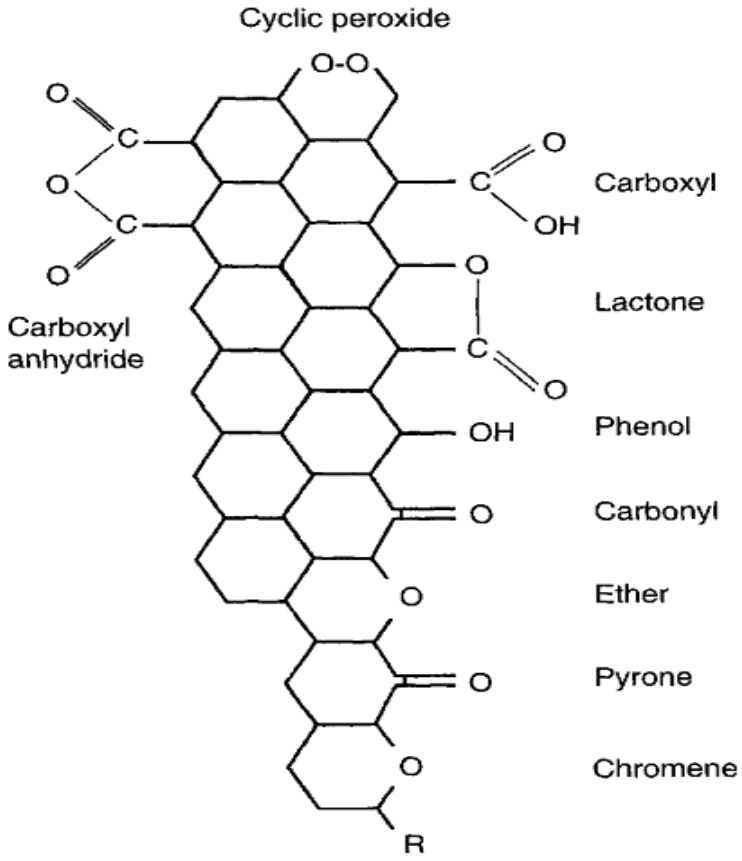

Figure 2.5 Oxygen Functional Groups on Carbon Surfaces (Marsh and Rodriguez-Reinoso, 2006)

The existence of the polar surface oxygen complexes gives a polar character with an increase in hydrophilicity. This is explained as the hydrogen bonding of the oxygen atoms of the carbon surface. Thus, adsorption of polar organic compounds is affected by the oxygen containing functional groups (Bandosz, 2006).

2.1.5.2 Hydrogen Containing Functional Groups

Before the activation, the starting material also includes hydrogen in the form of hydrocarbon chains and rings that are attached to border atoms of the hexagon planes. The removal of the most of the hydrogen

from the structure occurs at the time of activation below 950 ^{o}C. But some hydrogen is still held after the activation process and the removal of this hydrogen necessitates higher temperatures. The evolution of the latter portion of the hydrogen at very high temperatures also causes a decrease in adsorptive power (Abdallah, 2004).

It is also known that hydrogen is more strongly chemisorbed than oxygen. Infrared studies showed that the hydrogen is found in the form of aromatic and aliphatic hydrogen. The aromatic hydrogen is suggested to form covalent bonds to the carbon atoms at the periphery of the aromatic basal planes. On the other hand, the aliphatic hydrogen is proposed to be in the form of aliphatic chains and alicyclic rings connected to the peripheral aromatic rings (Balcı, 1992).

2.1.6 Porous Structure and Adsorption Properties of Activated Carbon

Activated carbons have a well-developed porous structure with a random arrangement of microcrystallites. The cross-linking between crystallites contributes the porous texture. Activated carbons have a low degree of graphitization and relatively low density which is generally less than 2 g/cm^3. The porous structure of activated carbon is a result of carbonization and activation processes which cause the removal of tarry substances from the spaces between the elementary crystallites. The resulting pores are enhanced and disorganized carbon is removed by activation (Bansal and Goyal, 2006).

Results have indicated that pores can be in the shape of capillaries, in the shape of more or less typical slits between two planes, v-shaped, tapered and other geometrical forms. In most cases, accurate determination of the pore shapes is challenging. But, assuming cylindrical capillary shaped pores approximates the real values in the calculation of pore dimensions (Balcı, 1992).

Pores that make up the activated carbon's surface have variable dimensions, these can be less than a nanometer to several thousand nanometers. It's known that accessible surface area of the carbon determines the adsorption properties but the surface area of activated carbon without pore size distributions is meaningless to interpretation of the adsorption properties.

A convenient classification of pores according to their sizes was first proposed by Dubinin and than officially done by International Union of Pure and Applied Chemistry (IUPAC). This classification includes the definitions of micro, meso and macropores according to their dimensions.

The IUPAC classification makes up a basis that each size range of pores corresponds to characteristic adsorption effects. Pores with a diameter larger than 50 nm are called macropores. Although, the macropores do not contribute adsorption capacity and surface area of the adsorbent significantly, they are important in the kinetics of adsorption. Since, macropores allow the adsorbate molecules to diffuse into the adsorbent with a minimum diffusional resistance, they are called transport arteries (Walker, 1968).

The mesopores have diameters in the range of 2 nm to 50 nm. These pores are also called transitional pores since they are between the macropores and mesopores like a passway. In mesopores capillary condensation occurs with the formation of a meniscus of the liquefied adsorbate. This capillary condensation exhibits characteristics hysteresis loop on the adsorption isotherm. The surface area of mesopores does not reach the 5 % of the total surface area but it is also possible to prepare activated carbons with an enhanced mesoporosity (Balcı, 1992; Bansal, 2006).

The pores that have a diameter less than 2 nm are called micropores. The contribution to the surface area and adsorption capacity of micropores is very high. In micropores transportation of molecules which are small enough to penetrate occurs with the molecular sieve

effect. In micropores, the interaction potential between adsorbent and adsorbate is higher than in wider pores because of the proximity of the pore walls, hence at a given relative pressure the amount adsorbed is enhanced (Gregg and Sing,1982).

Micropores can be further divided to supermicropores and narrow or ultramicropores specifically. These ultramicropores have a diameter less than 0.7 nm and make up a highly porous texture.

In the activated carbon micro, meso and macropores can all be found as it can be seen in Figure 2.6 and the distribution of these pores has a specific function to determine the adsorption properties.

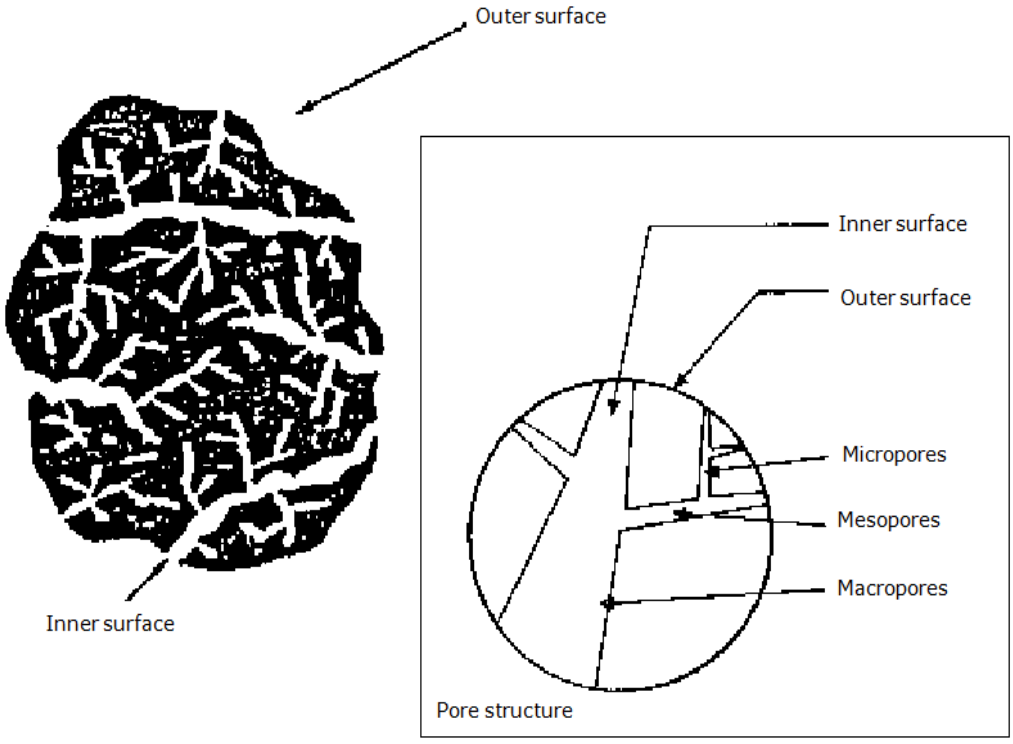

Figure 2.6 Pore Structure of Activated Carbon (Akikol, 2005)

Since separation with the adsorption processes are based on the three mechanisms as steric, equilibrium and kinetic, pore structure of the adsorbent has a decisive importance with the adsorbent-adsorbate interaction and adsorption conditions. In steric separation mechanism, the porous sorbent has to possess proper pore dimensions that could allow small molecules to take in while larger ones are excluded. The equilibrium mechanism arises from the accommodation of different species with different adsorption abilities on the adsorbent. Thus, preferential removal of the stronger adsorbing species occurs. On the other hand, the kinetic mechanism based on the different diffusion rates of various species (Do, 1998).

2.1.7 Mechanical Properties of Activated Carbon

Mechanical properties of activated carbons are also important to determine its performance on the adsorption processes. Mass related expressions are generally used to determine the mechanical properties of activated carbons. If volume related expressions are necessary, the bulk density or tapped density are needed to do conversion calculations.

Grain size distribution and bulk density are the most common properties to evaluate the mechanical properties of activated carbons.

Distribution of grain size is improtant to determine the resistance of layer of activated carbon to the gas or liquid steams during adsorption. Also, fineness of the grinding of activated carbon influences the filtration properties (Ullmann, 2002).

The bulk density is a feature that should be taken into account which is determined by the displacement method. It is dependent to grain size of material, filling technique and application and the geometry of the vessel used in the measurement. In the case of higher tapped densities, a defined tapping and shaking is included (Abdallah, 2004).

2.2 ACTIVATED CARBON PRODUCTION

Activated carbon can be produced by removal of some compounds from the structure of a suitable carbon containing parent material. Basically, raw material selection and preparation, pyrolysis (carbonization) and activation are the steps followed in the manufacture of the activated carbon.

2.2.1 Raw Materials

Although many investigations have proposed to use many raw materials in the activated carbon production, commercialized precursors are limited. Due to the process economics and product quality, the precursors should be carefully analyzed before the production in the large scale.

The key factors in the selection of the raw material are economy, processability and consistency of the material. The range of the parent material is diverse and widespread such as peat, coal, lignite, petroleum based residues, woody biomass, agricultural by-products and old tyres. Environmental concerns have also turned the producers' attention to waste materials obtained from food and wood industry. By this way, evaluating waste materials in the activated carbon production contributes to the lowering the production costs by using worthless materials. The activated carbon sources are still expanding by the researches carried out on both finding suitable precursors and optimizing the production with these precursors.

Biomass can be defined as plants that make up earth’s flora that can be grown into less than hundred years and plant derived wastes from industries like wood and food industry. There are lots of biomass samples tried as source materials for activated carbon manufacture such as rice hulls, fruit pits, waste cereals, coconut shells, corncobs and nut shells. Due to high availability, abundance and low cost lignocellulosic

biomass can take part adsorption processes both being a parent material of activated carbon and using as a biosorbent itself. Besides, biomass is a strategic energy source and this energy can be obtained from biomass either direct burning or thermochemical conversion to the alternative fuels. The biomass resource is an organic matter and in this organic matter energy of sunlight is stored in the chemical bonds. In the case of breaking bonds between adjacent carbon, hydrogen and oxygen molecules by combustion, decomposition or digestion, the stored chemical energy is released. When the biomass is evaluated as an energy source, it offers many advantages compared to fossil fuels, as being environmentally friendly and renewable (McKendry,2002).

Biomass has a very complex structure but the main constituents of of a plant cell wall are cellulose, hemicelluloses and lignin that make biomass a natural composite material. Also mineral content of biomass and organic extractives are included in the structure, but the relative amounts are very small since cellulose, hemicellulose and lignin contribute the mass of biomass they are called lignocellulosic. Generally, these structures are composed of 70-90% cellulose and hemicelulose and the remaining lignin molecules. The cellulose and hemicellulose are tightly bound to lignin molecules mainly by hydrogen bonds and some covalent bonds and this biomass cell wall model is given in Figure 2.7 (Lee, 1997; Özmak, 2010).

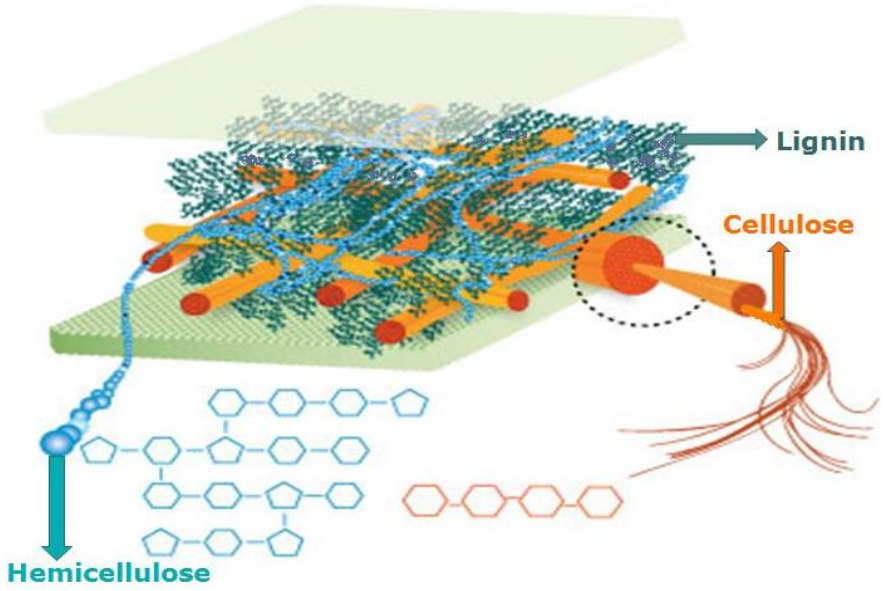

Figure 2.7 Biomass Cell Wall Model (Özmak, 2010)

Cellulose is the framework substance which contributes to the biomass in the form of microfibrils. It has a crystalline and a strong structure because of the hydrogen bonding in the structure. Hemicelluloses are the branched, matrix substances that possess a heteregeneous, amorphous structure with a little strength. They bind tightly to the surface of each cellulose microfibril non-covalently. On the other hand lignin is a large crosslinked polymer and has an amorphous, structure that is covalently bounded to the hemicellulose molecules. These three components of the plant cell wall give mechanical support and transport properties in plant cells by a combination of them in the structure. Put another way, cellulose, hemicelluloses and lignin resemble to the construction materials like iron core, cement and buffering material to improve bonding, respectively (Hon and Shiraishi 2001; Karamanlıoğlu 2008, Mckendry 2002).

2.1.1 Pistachio-nut Shell as a Biomass

Pistachios are edible nuts or fruits of Pistachia vera. Each fruit is covered by a kernel and a hard coat, named pistachio-nut shells. The chemical composition of pistachio shells determined Yeganeh et al. (2006) is given in Table 2.2. The chemical composition of the shells may differ depending on the geographical site and the season of cultivation.

Table 2.2 Chemical Composition of Pistachio-nut Shells (Yeganeh et al., 2006)

Component (wt. %)		
Cellulose	Lignin	Extractables
56.5	22.5	7.95

Turkey is one of the top producers of pistachios throughout the world according to the statistics of Food and Agricultural Organisation of United Nations in 2008. Specific weather conditions are required for cultivation of pistachio trees and this reason limits the suitable lands to cultivate pistachios in the world. Also, Turkey has a non-uniform product distribution of pistachios, that has became denser in the southern east part of Anatolia, especially Gaziantep (FAO website, 2010; Bektaş 2006).

Table 2.3 Top Pistachio Producer Countries (FAO Website,2010)

Country	Production (MT)
Iran	192269
USA	126100
Turkey	120113
Syria	52600
China	40000

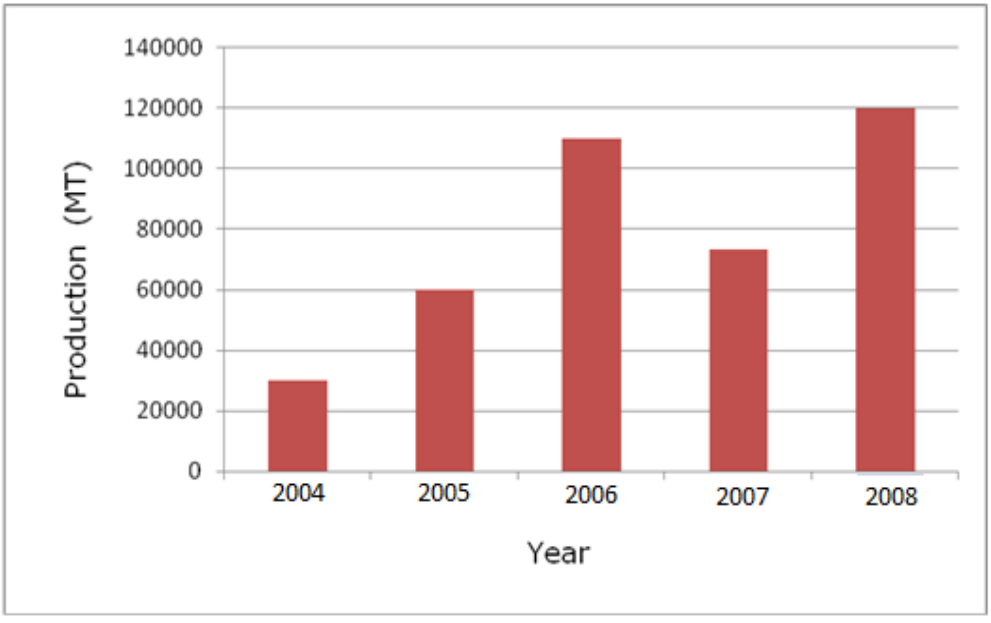

Figure 2.8 Pistachio Production of Turkey by Years (FAO website,2010)

If production of pistachios in recent years is investigated, quantity of produced in Turkey seems to have an increasing trend from 2004 to 2008 and this can be seen in Figure 2.8 apparently. So, the wastes of these pistachios can be a consistent precursor material to produce activated carbon in recent years if conversion of the pistachio-nut shells to an adsorbent material can be accomplished.

2.2.2 Pyrolysis (Carbonization)

Biomass can be converted to fuels or chemicals by thermochemical processes like gasification, liquefaction and combustion, and biochemical processes like fermentation, anaerobic digestion, and mechanical extraction. Among these processes pyrolysis is a method to convert to organics to several products by heating in the absence of air.

The thermal decomposition of the organic matrix in the pyrolysis yields three types of products as chars, tars and gases. The char obtained from pyrolysis has a high carbon content that can be suitable to use in the activated carbon production. If activated carbon manufacturing is aimed in the pyrolysis process, char is the desirable product in the process. Also the char can be used in the burning since they have higher heating values than the parent material due to the splitting of volatiles from the structure. The tar or bio-oil is a miscible mixture of polar organics and water. Generally pyrolysis focuses on this bio-oil and efforts have been made to enhance the characteristics and the amounts of the tarry substances. On the other hand gaseous fraction obtained by pyrolysis includes lower molecular weight products as H_2, CO, CO_2, CH_4, C_2H_6, C_2H_4 and trace amounts of higher gaseous organics with water (Yaman, 2004).

The terms carbonization and pyrolysis are used without any distinction, since these two processes are almost identical and refer to the total or partial volatilization of organic substances in the absence of

air. But, the differences arise from the objectives, that means, pyrolysis is generally used when the gaseous and tarry compounds evolved from the material are objected and all the process conditions are focused to maximize the yields or these products. To put it another way, when the thermal treatment focuses on the final properties and amounts of the char, regardless of the tarry and gaseous products, the carbonization term is used instead of the pyrolysis (Bandosz, 2006).

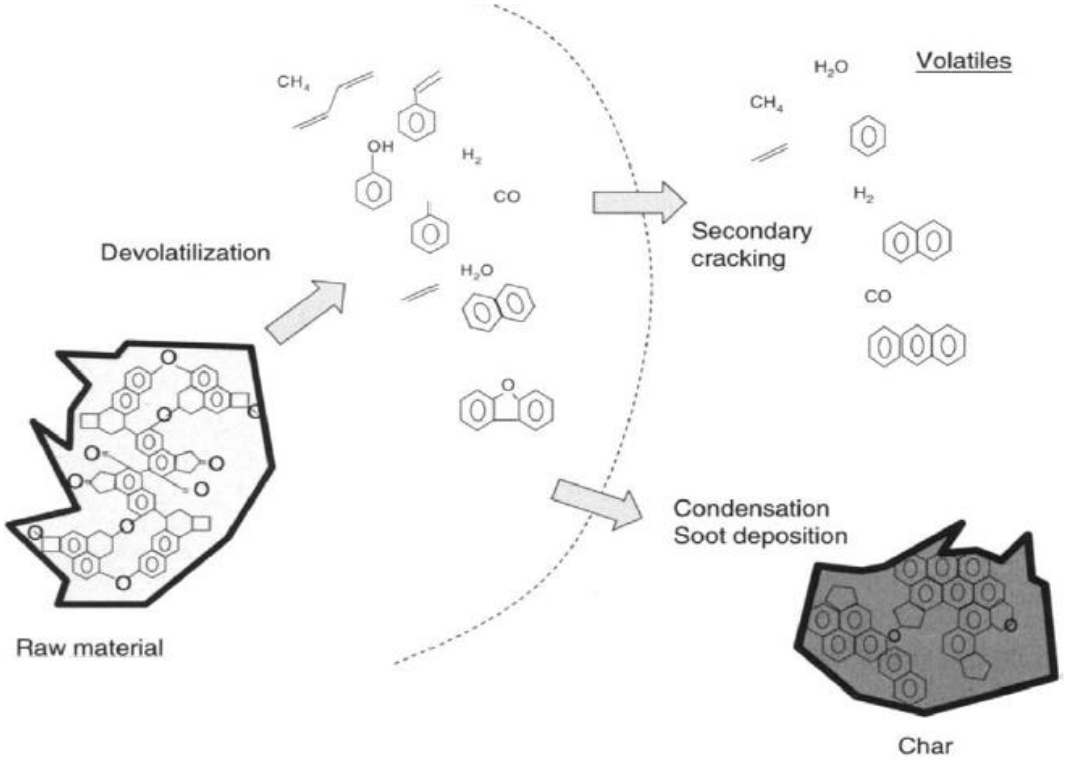

Figure 2.9 Typical Carbonization Scheme of a Carbonaceous Material (Bandosz, 2006)

During the pyrolysis of biomass, many complex reactions occur because of the heterogeneous structure of the lignocellulosic materials. Dehydration, cracking, isomerisation, dehydrogenation, aromatization, coking and condensation reactions takes place and rearrangments occur in the structure of the parent material. According to the mechanisms proposed, the primary products are formed by the evolvement of gases

and vapors from the fragments of the structure in the early stages. So, there are many radical species on the carbonaceous material which can react among themselves according to the process conditions, as it can be seen in Figure 2.9 . Secondary cracking products then formed by the reactions of primary products. After the stabilization of products tar, gases and chars are formed (Klass, 1998; Bandosz, 2006).

Pyrolysis process is sensitive to the process conditions such as temperature, heating rate, pressure, atmosphere that reactions take place in, residence time and reactor configuration, also raw material properties like moisture, ash, composition and particle size.

According to the heating rates used in the pyrolysis process, slow, fast and flash pyrolysis techniques are used and that techniques are separated from each other by influencing the product distribution. High heating rates and short residence times tend to trigger the formation of the liquid and gaseous products. By this way, the process can afford up to 70 % yields of the tarry products. On the contrary slow heating rates caused the decrement of the liquid and gaseous products while maximizing the yield of char. Thus lower heating rates are more favorable for activated carbon production (Onay and Kockar, 2003; Klass, 1998).

During carbonization, pyrolytic decomposition of biomass is first started by the evolvement of the non-carbon elements (hydrogen, oxygen, traces of sulphur and nitrogen) from the structure. By the removal of hydrogen and oxygen, the freed atoms of elementary carbon are grouped into an organized crystallographic formation and constituted elementary graphitic crystallites. And the final carbonized product, char, includes irregular mutual arrangements of the crystallites; that’s why, free gaps remain between the crystallites. Because of the deposition and decomposition of tarry substances these gaps between crystallites become filled or blocked by disorganized (amorphous) carbon. The char formed by carbonization or pyrolysis has a more aromatized and porous

structure and includes more carbon content than the parent material. Despite having high carbon content, the char formed by the carbonization process have not enough capabilities for taking part in adsorption processes effectively. Removing of the tarry products can be possible by partial activation by heating in an inert atmosphere, or by extraction or by a chemical reaction (Wigmans, 1989).

The method of carbonization of raw material, has an enormous effect on both carbonized intermediate product, char and on the final product.

2.2.3 Activation

The resulting product from the carbonization has small adsorption capacity. Thus, it's not suitable for use as an activated carbon. Under specific conditions, chars can be used as an adsorbent without any further processing. But activated products have more developed porous structure that influences adsorption capacity enormously than the non-activated products.

The activation is carried out in many ways including creation of further porosity, opening the existing porosity, modifications to the surfaces of porosities and also modifying the existing porosity. Two methods are used both separately and together to activate the carbonized products. These methods are physical and chemical activation. Sometimes by a combination of physical and chemical activation, the chemically activated carbon is subjected to additional physical activation with a gaseous enviroment to increase the number of wider pores (Marsh, 2006; Balcı 1992).

In modern technologies both chemical and physical activation are preferred extensively, depending on the conditions. Undoubtedly, the quality of the products of these two activation processes will not be same. Since it is not possible to forecast which activation procedure gives

better product, too much and detailed research should be done before industrial production.

2.2.3.1 Physical Activation

Physical activation is also known as thermal activation and gas activation because heat treatment at elevated temperatures near 900 ^{o}C is required and suitable oxidizing gases in the activation processes are used.

Generally, physical activation is a two-step process including the carbonization of raw material followed by activation.

The gases as activating agents are mainly steam and carbon dioxide and mixtures of both. Air, oxygen, flue gases are rarely used as activating gases, due to challenging control of activation with these gases.

On the physical activation, reaction occurs between the activation agent and carbon. The active oxygen in the activating gases burns away the more reactive part of the carbon skeleton by yielding carbon dioxide and carbon monoxide. The physical activation occurs in two stages. In the initial stage, burn-off degree is lower than 10 percent. In this stage, disorganized carbon burns preferentially and plugged pores between the crystallites are freed. Then, by the removal of disorganized carbons, the surface of elementary cyrstallites becomes ready to contact with the activating gases. The burning out of crystallites occurs at different reaction rates on the different regions of the surface that are exposed to gases. If the burning does not proceed by such a way, new pores can't be formed. The departing of non-organized and non-uniform burnout elementary crystallites from the structure causes the formation of new pores and constitution of a meso and macroporous structure. This is done by widening of the existing porosity or formation of larger pores by the

complete burnout of the walls of the neighbouring micropores (Abdallah, 2004).

Activation with steam and carbon dioxide occurs usually at a temperature range between 800 and 1000 ^{o}C with a series of heterogeneous reactions. Although the reaction equations seem very simple, the overall kinetics includes further details. Temperature of the activation must be carefully chosen and adjusted to make the rate determining factor during the reactions. Since lower temperatures influence reaction kinetics adversely due to the endothermic reactions, the temperature should be high. In kinetics control region, reactions occur at the interior surface of the carbon and the carbon removal from the pore walls gives rise to pore widening and enlargement. But, very high temperatures cause the reactions which are diffusion controlled and in this situation reactions occur on the outer surface of the carbon particle. It should be noted that when oxygen or air is used as an activating gas, due to the high reactivities, they cause very fast reactions with carbon by resulting an uncontrolled combustion. This combustion leads to great amount of losses from the carbon surface and causes a large amount of surface oxides. Because of these difficulties and drawbacks, oxygen or air activation is not preferred so much as steam and carbon dioxide (Balcı,1992; Ullmann, 2002).

The endothermic reactions that occur during the activation with steam, carbon dioxide and oxygen can be summarized as followed;

$$H_2O + C_x \rightarrow CO + H_2 + C_{x-1}$$

$$2\ H_2O + C_x \rightarrow CO_2 + 2\ H_2 + C_{x-1}$$

$$CO_2 + C_x \rightarrow 2\ CO + C_{x-1}$$

$$O_2 + C_x \rightarrow 2\ CO + C_{x-2}$$

$$O_2 + C_x \rightarrow CO_2 + C_{x-1}$$

Other than the temperature of the reaction, the adsorptive powers of physically activated carbons are determined by the chemical nature and concentration of oxidizing gases, the extent to which the activation is carried out and the amount and type of the mineral matter in the raw material and in the char (Hassler, 1974).

In the physical activation of some materials, small amounts of various compounds speeds up the activation. As a catalyst, caustic potash and potassium carbonate is sometimes used to accelerate the activation in industry (Ullmann, 2002).

There are some difficulties arising from bringing the raw material to an intimate contact with activating gases on the furnaces or reactors at the exact activation temperature. Also uncontrolled burn-off gives rise to uncontrolled pore development on the quality of the carbon and yield decrease on the production. Besides two separate processes of carbonization and activation at high temperatures causes a high energy cost.

2.2.3.2 Chemical Activation

Chemical activation is another method developed to produce highly porous carbons with a single step operation. The chemical activation is roughly defined as adding chemical activation agents to the precursor or the carbonized product before the heat treatment. Generally it has been done by mixing the raw material and performing both carbonization and activation in a single step. There are studies done by treating char instead of raw material with the chemicals.

The chemical activation includes co-carbonization of the precursor with the suitable substances such as zinc chloride, potassium hydroxide and phosphoric acid. There have been many chemicals reported in the literature as chemical activation agents but extensively used ones are these three of them. The chemistry and the mechanisms of these

chemicals on the precursors are different from each other. But these three chemicals offer many advantages compared to the physical activation. Since the chemicals restrict the formation of tar during pyrolysis, higher yields can obtained by chemical activation. Contrary to the physical activation, chemical activation at lower temperatures and at shorter times can achieve highly porous texture. This means energy required in activated carbon processes can be lowered by chemical activation process. Chemical activation also promotes a better and controlled porosity development. Under such a condition of chemical activation, smaller elementary crystallites are formed.

On the other hand, chemical activation requires an additional washing step to recover the agents used. Environmental concerns about the remaining chemicals in the porous carbon can be handled by an effective washing.

Since the chemicals used in the chemical activation are mainly zinc chloride, potassium hydroxide and phosphoric acid, there are numerous studies done to understand the overall mechanism of these chemicals and to investigate their effects on the porosity.

It is known that zinc chloride promotes the extraction of water molecules from the lignocellulosic structures. During impregnation with zinc chloride, the chemical reaches the inner parts of the raw material and triggers hydrolysis reactions. This effect causes to the structural changes like weight loss, volatiles removal, increase in elasticity and weakening of the carbonaceous structure. Also, zinc chloride impregnation causes particle swelling. During carbonization of the zinc chloride impregnated precursor, tar formation decreases, so yield of the product increases. Apparently zinc chloride tends to remove hydrogen and oxygen atoms in the form of water instead of the hydrocarbons and oxygenated organic compounds. And after the removal of non-carbon elements from the structure, carbon skeleton is remained largely untouched with a well-developed porosity. Despite obtaining highly

porous carbons, zinc chloride activation has some disadvantages like corrosion problems, low recovery efficiencies, the presence of residual zinc in the carbon structure and environmental problems (Allen, 1998; Bandosz, 2006).

Potassium hydroxide acts on the precursor differently than zinc chloride. When potassium hydroxide impregnation is carried out on a carboneous material it does not act until a heat treatment, it does not behave like a dehydrating agent on the precursor. Potassium hydroxide also does not inhibit the shrinkage of the particles upon heat treatment. Reaction between the carbonized material and potassium hydroxide starts at temperatures above 700 ^{o}C,. Besides the impregnation of the raw material, impregnation of char gives well-developed porosity on the activated carbon production. Reaction mechanisms of potassium hydroxide have been proposed for different materials and they are proved that during reactions hydrogen, metallic potassium, carbon monoxide, carbon dioxide and potassium oxide are detected. In this situation, potassium hydroxide seems to react with carbon skeleton, and a carbon-burn out occurs for further porosity development. In the literature there is an agreement on the reaction mechanism as;

$$6\ KOH + 2\ C \leftrightarrow 2\ K + 3\ H_2 + 2\ K_2CO_3$$

The proposed reactions also continue with the decomposition of the potassium carbonate further to form potassium oxide and carbon dioxide. There are also some chemical activation studies by using potassium carbonate as an activation agent, and this chemical can create a porous structure by itself (Marsh and Rodriguez-Reinoso, 2006; Bandosz, 2006; El-Hendawy, 2009; Lillo-Rodenas et al., 2004).

The activation mechanism of phosphoric acid has been studied by several researchers. There is a convincing proof that impregnation with phosphoric acid makes the lignocellulosic structure elastic and this phenomenon can be explained with the separation of the cellulose fibers and a partial depolymerization of hemicelluloses and lignin. Thus,

swelling of the particle and tar formation on the surface of the particle is observed. The depolymerization of cellulose is followed by dehydration and condensation and these reactions cause tar formation and lead to more aromatic and more reactive products with some cross-linked structure. The phosphoric acid treatment is carried out on both carbonized and uncarbonized raw material. The yields that are obtained by the phosphoric acid activation is higher than the yield of pyrolyzing the starting material. Another advantage of phosphoric activation is that the recovery of phosphoric acid in large amounts can be possibble by multiple stage extraction (Marsh and Rodriguez-Reinoso, 2006; Ullmann, 2002; Bandosz, 2006; Çetinkaya, 2009).

In a study of Jagtoyen and Derbyshire (1998) two different woody biomass samples named yellow poplar and white oak have been activated with phosphoric acid and the activation mechanism have been investigated. The raw materials have a complex lignocellulosic structure, that means cellulose, hemicellulose and lignin constitute the main structure of these two woody biomass samples. To define the reactions between this structure and phosphoric acid, three temperature region have been studied differently.

At the lower temperature conclusions are as follows: When the phosphoric acid is mixed with the precursor, the reactions start instantaneously and when the temperature reaches at 50 ^{o}C, physical and chemical changes can be observed clearly. In the lignocellulosic structure, phosphoric acid firstly penetrates and attacks to lignin and hemicelluluse due to the easiness to taking in amorphous biopolymers than the crystalline cellulose. The acid in the cellulose and hemicellulose, hydrolyzes the glycosidic linkages and in the lignin cleaves aryl ether bonds. These reactions then continue by further chemical reactions that include dehydration, degradation and condensation. By reason of these reactions, molecular weights of the biopolymers decrease (Jagtoyen and Derbyshire, 1998).

At the intermediate temperatures following comments are presented: Releasing of volatile components and water-soluble product formation with polymerisation cause a considerable weight loss. Above 150 ^{o}C, water insoluble char formation and the expansion of the structure occur while the weight loss rate slows down. The stabilisation and expansion of the structure brings about pore development while the crosslinking, bond cleavage and depolymerisation reactions continue. The dilation of the structure contribute porosity development considerably. Below 200 ^{o}C, phosphoric acid inhibites the formation of a volatile component, levoglucosan and decreases weight loss from the material. Below 450 ^{o}C, phosphoric acid prevents the shrinking during thermal treatment by occupying surface of the material; this can be possible with formation of phosphate and polyphosphatic bridges that connect and crosslink to biopolymer fragments (Jagtoyen and Derbyshire, 1998).

At higher temperatures Jagtoyen and Derbyshire conclude that carbon skeleton starts to contract after 450 ^{o}C because of the breaking down of the phosphate linkages which become thermally unstable (Jagtoyen and Derbyshire, 1998).

It should be taken into account that impregnation ratio has an important factor in the chemical activation studies with the other process parameters. This ratio is the weight ratio of the activation agent to the dry materials.

A combination of chemical activation followed by a physical activation process increases the amount of wider pores (Öztürk,1999).

2.3 CHARACTERIZATION METHODS OF ACTIVATED CARBONS

2.3.1 General

In the characterization of porous materials such as activated carbon, pore structure is the principal feature that determines the properties of material. Due to the complexity of many solid surfaces, a combination of different methods can be used in the characterization.

Because of the polymodal pore size distribution of activated carbon, macropores, mesopores and micropores are present in the structure and the distribution of these pores along the surface and pore volumes with the total surface is required to be known for a complete characterization of the adsorption properties.

Numereous techniques may be applied to fulfill the requirements of a quantitative characterization of pore structure of an activated carbon. But adsorption of gases and vapors by standart gravimetric and volumetric techniques are more convenient and reliable.

Both adsorption equilibrium and adsorption kinetics should be taken into account to use a porous solid as an adsorbent. The material has to possess a highly porous structure with high pore volume and high surface area to meet requirements as an adsorbent. Hence, transfer rate of the adsorbate molecules to the interior surface of particle and adsorption capacity are increased (Do, 1998).

It is certain that most efficient approach to determine the adsorption characteristics is to use adsorption method itself to obtain information. Since activated carbon includes pores in a wide range, combination of different methods is necessary to complete the characterization of pore structure of activated carbon (Marsh and Rodriguez-Reinoso, 2006).

The following sections of this part contain the main theory and methods used to characterize activated carbons.

2.3.2 Adsorption Phenomena and Standard Isotherms

The pore analyses of porous solids are mostly determined by methods belonging to gas adsorption. In these methods, gases employed should be completely inert and should not have any interaction with the surface. For this purpose, N_2, CO_2, Ar and He are used frequently. The method is based on retention of the gas molecules on solid surface by physical adsorption. The gas adsorption enables assessment of a wide range of pore sizes. Also, it is not a cost intensive method that makes it the most convenient method among the other techniques in the characterization of porous solids such as adsorbents, catalysts, ceramics and pigments.

To initiate the gas adsorption process, an outgassed solid (adsorbent) is surrounded by the adsorbate gas. Due to the forces between the solid surface and the gas molecules, the adsorbate gas molecules are transferred and accumulated on the surface. These intermolecular forces are attractive dispersion forces and at very short distances repulsive forces in addition to the contribution from the polarization and electrostatic forces between the permanent electric moment and electric field of the solid (Yahşi, 2004).

Undoubtedly, the amount of adsorbed gas on the surface is related with the pressure, temperature and the interaction potential. Hence, at same equilibrium and temperature, the relationship between weight of gas adsorbed per unit weight of adsorbent and pressure is referred as the adsorption isotherm of a particular gas-solid interface (Lowell et al., 2006).

Based upon extensive studies and researches, the adsorption isotherms are classified according to the molecular interactions between the gas and adsorbent surface. After the explanation of 5 isotherms by Brunauer et al. (1940), IUPAC (1985) published the types of the adsorption isotherms and stated the differences among them with an

additional isotherm cited by Gregg and Sing (1982). Typical shapes of isotherms are given in Figure 2.10.

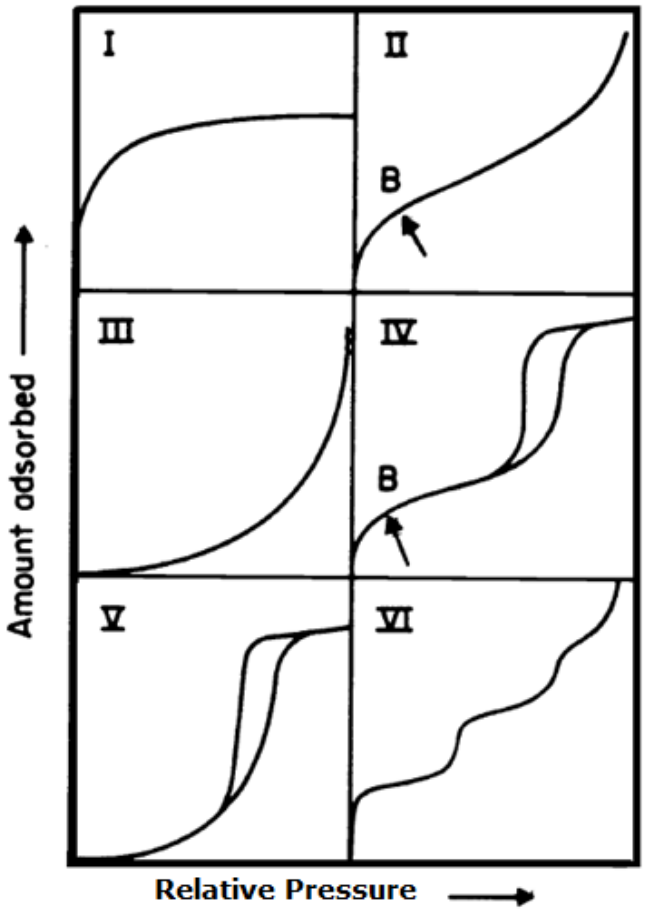

Figure 2.10 IUPAC Classification of Isotherms

Adsorption in a microporous solid leads to an isotherm of Type I. This isotherm is a concave curve which approaches a limiting value as relative pressure (P/P_o) goes to the unity. This isotherm is observed in chemisorption also and indicates that all of the active sites are covered at the limiting value. In physisorption on microporous materials, the uptake does not increase continuously. At lower pressures, high uptake values are acquired due to the narrow pore width and high adsorption potential. After micropore filling at higher pressures, the limiting value of uptake is

obtained by a plateau that is nearly or quite horizontal to the P/P_o axis. (IUPAC, 1985).

Type II isotherms belong to non-porous or macroporous solids. This reversible isotherm type indicates the unrestricted monolayer-multilayer adsorption. The inflection point B on the curve represents the stage where the monolayer coverage ends and multilayer coverage is initiated. (IUPAC, 1985; Gregg and Sing, 1982) .

Type III isotherm is a convex curve towards to the relative pressure axis without any inflection point. These type of isotherms are not very common but they are characteristic of weak gas-solid interactions. These isotherms are seen when the adsorbate interaction with an adsorbed layer is more than the interaction with the adsorbent surface. Thus, the adsorbate-adsorbent interaction plays a significant role in such cases. Adsorption of nitrogen on polyethylene and adsorption of water vapor on the clean basal plane of graphite are examples of these type of isotherms (Lowell et al.,2006; IUPAC,1985).

Type IV isotherms occur in adsorption on the mesoporous materials. A characteristic property of this type isotherm is its hysteresis loop. The exact shape of the hysteresis varies from one adsorption system to another. The hysteresis formation is related with the capillary condensation. The complete pore filling causes a plateau in these isotherms and the limiting uptake value is reached (Lowell et al.,2006; IUPAC,1985).

Type V isotherm is also characterized by convexity like Type III isotherm in the initial part. However, this convexity is not persistent throughout the curve. There is an inflection point so that the isotherm bends over and then reaches a plateau. This isotherm exhibits pore condensation and hysteresis and indicates weak attractive interactions between the adsorbent and adsorbate (Condon 2006; IUPAC,1985).

The last type of isotherms is Type VI which is a special case. This isotherm represents stepwise multilayer adsorption on a uniform non-porous surface. The sharpness of the steps is related with the surface homogeneity, adsorbate and the temperature. For each adsorbed layer, the step height represents the monolayer capacity of that layer (IUPAC,1985).

The hysteresis formation in the multilayer range of adsorption isotherms is usually related with capillary condensation in the mesopores. The shapes of the hysteresis loops are also useful in identification of the pore structures.

2.3.2.1 The Brunauer, Emmet and Teller Theory (BET)

Brunauer, Emmet and Teller developed a generalized and extended form of the Langmuir's theory which expresses the adsorption of gases in multimolecular layers evidently. This BET theory has been used for many years widely due to its simplicity and ability to describe types of isotherms (Brunauer et al, 1938).

Langmuir's theory instructed many researchers by investigating the nature of adsorption and stating the assumptions which leads to finding surface areas of porous solids and amount of adsorbed molecule at complete monolayer coverage. According to this theory, adsorption is limited to a monolayer. Adsorbate molecules stick on a fixed number of localized sites and each of these sites can hold only one adsorbate molecule. The sites on the adsorbent molecule are energetically uniform and there are not any interaction between the adsorbate molecules on neighbouring locates. When a final assumption that express the equilibrium rates of adsorption and desorption equivalently is done, the Langmuir model comes into existence.

BET Theory accepts also some assumptions of Langmuir such as surface homogeneity and defectiveness of lateral interactions among the

adsorbed molecules. Generalization of Langmuir's theory with several additional assumptions lead to multilayer adsorption which represents mutual interactions in vertical direction. Within each adsorbed molecule layer a dynamic equilibrium occurs and for the layers above the first layer heat of adsorption is equal to the latent heat of condensation. When the pressure reaches to saturation vapor pressure, the adsorbate vapor condenses on the adsorbed film like an ordinary liquid, so that the numbers of the adsorbed layers became infinite. To obtain the final form of BET equation, condensation rate of gas molecules that are adsorbed on a layer is equalized to the rate of vaporization from the same layer. After generalizing these equalities for the infinite number of layers and linearization, final form of BET equation is obtained as;

$$\frac{P}{V[P_O - P]} = \frac{1}{VmC} + \frac{C-1}{V_mC}\frac{P}{P_O} \qquad (2.1)$$

where; "V" and "Vm" are expressed as volume adsorbed at the relative equilibrium pressure P/Po and monolayer capacity, respectively. "C" is a constant used for linearization that includes the heat of adsorption at the first and subsequent layers. "C" constant is expressed as;

$$C = \exp\left[(q_1 - q_2)/RT\right] \qquad (2.2)$$

"q1" and "q2" terms in Equation 2.2 are heat of adsorption of the first layer and heat of adsorption of the second and consecutive layers, respectively.

BET theory and experimentally obtained isotherms are usually in a good agreement in the region of the relative pressures near the completion of the monolayer. This enables a practical method for the estimation of surface areas of porous materials. A plot of P/ V (P-Po) versus P/Po will give a straight line according to the equation 2.1 in a relative pressure range of 0.05 < P/Po < 0.35. The slope "S" and the intercept "I" of this line will give;

$$S = \frac{[C-1]}{V_m C} \qquad \text{and} \qquad I = \frac{1}{V_m C} \tag{2.3}$$

Rearrangements of Equations in 2.3 for "Vm" and "C" give;

$$V_m = \frac{1}{S} + I \qquad \text{and} \qquad C = S + \frac{1}{I} \tag{2.4}$$

At relative pressures higher than 0.35, the BET equation does not yield accurate values due to the capillary condensation effect. On the other hand, relative pressures lower than 0.05 also causes inaccuracy because the amount of adsorbed gas is too small to be measured with enough accuracy. If the mean cross-sectional area occupied by one molecule of adsorbate gas, "A_m", is known, then the specific surface area may be obtained from the equation;

$$S_{BET} = \frac{V_m N_A A_m}{V_{mol}} \tag{2.5}$$

The value of "C" constant is generally between 50 and 300 for nitrogen adsorption. Too high or negative C values indicate a microporous material. For materials with such conditions, usage of BET equation directly is not suitable. The BET equation is arranged with some additional assumptions to obtain another form. Firstly, very small value of the term 1/(Vm.C) is neglected. By this way BET plot passes from the origin. The reason behind the small value of this neglected term comes from the "C" constant. Since C>>1 and C-1≈C, the BET equation is obtained in another form as;

$$\frac{P}{V[P_O - P]} = \frac{1}{V_m}\left(\frac{P}{P_O}\right) \qquad (2.6)$$

Nitrogen at 77 K is generally considered as an ideal adsorbate that is suitable for standard surface area determination. It shows an unusual property on almost all surfaces so due to its small "C" value which is small enough to obstruct localized adsorption and large enough to prevent the adsorbed layer from behaving as a two dimensional gas. Another advantage of nitrogen is that its multilayer adsorption isotherm is not very sensitive to differences in adsorbent structure. Because of these unique features of nitrogen, it is accepted a standard adsorbate universally with an assigned cross sectional area of 0.162 nm^2 at its boiling point of -195.6 ^oC. Other than the nitrogen, argon, krypton and carbon dioxide are also used in determination of surface area and properties of these gasses are given in Table 2.4 (Rouquerol et al.,1999 ; Yahşi, 2004 and Lowell et al., 2006).

Table 2.4 The Gases Used in the Surface Area Determination and Pore Analysis (Ozmak, 2010)

Gas	**Temperature (K)**	**Surface Area of Molecule (nm/molecule)**
Nitrogen	77	0.162
Krypton	77/195	0.152 / 0.297
Argon	77	0.142 – 0.15
Carbon dioxide	195	0.163 – 0.206

2.3.2.2 Pore Analysis by Adsorption / Desorption

Porous texture of an adsorbent can be understood from the shape of adsorption and desorption isotherm. It is basically explained that adsorption and desorption branches of isotherms are not coincident throughout pressure range for porous materials. The isotherms provide a description for assessment of porous texture. The adsorption/desorption isotherms also include information about the geometries of pores besides pore dimensions of the adsorbent.

Since hysteresis loop on the adsorption/desorption isotherms is related with the morphology of the adsorbent, interpretation of the nature of adsorption processes requires a careful isotherm analysis including hysteresis types. IUPAC classifies types of hysteresis also and states the differences.

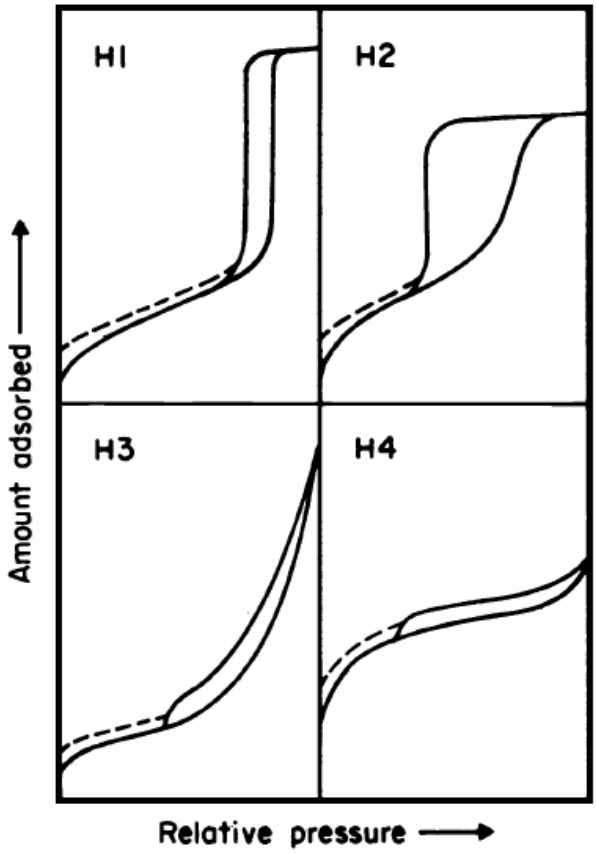

Figure 2.11 Types of Hysteresis Loops

As it can be obviously seen in Figure 2.11, there are two extreme shapes as H1 and H4. H1 hysteresis possesses almost vertical branches of adsorption and desorption, on the other hand in the H4 type hysteresis these two curves are nearly parallel over a wide range of relative pressures. The other types of hysteresis, H2 and H3 are considered as intermediate between the extreme cases. It is hard to understand factors affecting the adsorption hysteresis but it is accepted that shapes of loops are associated with specific pore structures. H1 hysteresis is a fairly narrow and related with capillary condensation in open-ended cylindrical pores. The formation of a cylindrical meniscus takes place at a higher relative pressure than the emptying process, which continues through the evaporation from a hemispherical meniscus.

H2 loop is difficult to guess but spheroidal cavities or voids as well as ink-bottle pores are recognized from the interpretation of H2 hysteresis loops. But this recognition of H2 loops is oversimplified. The pore textures of materials which have these loops, have more complex pore structures with interconnected networks. Until relative pressure is decreased to allow evaporation from the neck, the liquid seems to be trapped in the body of the pore; therefore, the release of condensate is limited by the dimension of the neck radius. H3 loops do not indicate a limiting adsorption value at P/Po =1 and these loops are given by porous materials which have slit-shaped pores. H4 types of loops also indicate to slit-shaped pores but in the case of microporous materials (IUPAC,1985; Rouquerol et al.,1999; Yahşi, 2004).

The hysteresis formation is based on capillary condensation phenomena and hysteresis part of isotherms includes information about the mesopores. Because of the condensation and evaporation phenomena, there exist a relationship between shape and position of isotherm and pore geometry as it was stated before. Kelvin equation was based on the capillary condensation concept, which is given by;

$$r_P = \frac{-2\sigma V_{mol} Cos\theta}{RT \ln[P/P_o]} \quad (2.7)$$

In the equation above "r_p", "σ" and "θ" represent the mean radius of the liquid meniscus, surface tension and contact angle between the condensed phase and surface of the solid, respectively. "T" is absolute temperature and "R" is the gas constant in the equation. Also, the thickness of the adsorbate layer, "t" is necessary to consider for finding the pore radius by Kelvin equation. The actual pore radius, "r_p", is then given by;

$$\mathbf{r_P = r_k + t} \quad (2.8)$$

The term "rk" is called Kelvin radius or critical radius which condensation occurs into, at the required relative pressure. Since adsorption has already occurred on the pore wall before the condensation, the process causes a center core or radius, "rk". Hence, Kelvin radius can not be stated as the actual pore radius. Similarly, an adsorbed film remains on the pore wall when evaporation of the center core occurs during desorption. An analytical expression which relates the thickness of layer "t" with the relative pressure has been developed by Halsey (1948);

$$\mathbf{t = t_m\left[\frac{5}{\ln(P/P_o)}\right]^{1/3}} \quad (2.9)$$

In the equation above, the term "tm" is the thickness of the monolayer. A combination of equations (2.6), (2.7) and (2.8) with nitrogen as the adsorbate at its normal boiling point of -195.6 ^{o}C and with "tm" as 0.354 nm, yields another equation as;

$$\mathbf{r_P = \frac{4.15}{\log(Po/P)} + 3.54\left[\frac{5}{2.303\log(P_O/P)}\right]} \quad (2.10)$$

In the derivation of equation (2.9), a closely packed hexagonal liquid structure is assumed for the nitrogen molecules.

Calculation of the size distribution of the mesopores from the adsorption/desorption data enables to determine mesopore surface area for a symmetrical pore geometry easily. The relative pressure data obtained from isotherms during adsorption or desorption is used to calculate the corresponding mesopore radius. Pores of various dimensions contribute surface area and by assuming precise pore geometry pore size distributions can be found. Detailed derivations and equations are given in Appendix A.

2.3.2.3 Methods Used to Determine Pore Structure of Activated Carbon

Due to non-uniform structures of porous materials which include micropores, mesopores and macropores together, several methods have been developed to determine the porous texture of materials by several investigators.

Gas adsorption includes information about pore structure and shape, pore volume besides the surface area of the porous material and this information is obtained from theories applied on the specific regions of the isotherms which is also given in Figure 2.12

There are many methods to analyse pore structure. Most recognized methods can be stated as t–plot, α_s method, Dubinin Radushkevich (DR), Dubinin Astakhov (DA), Horvath-Kawazoe (HK), Saito Foley (SF), Barrett, Joyner, Halenda (BJH) methods and Density Functional Theory (DFT).

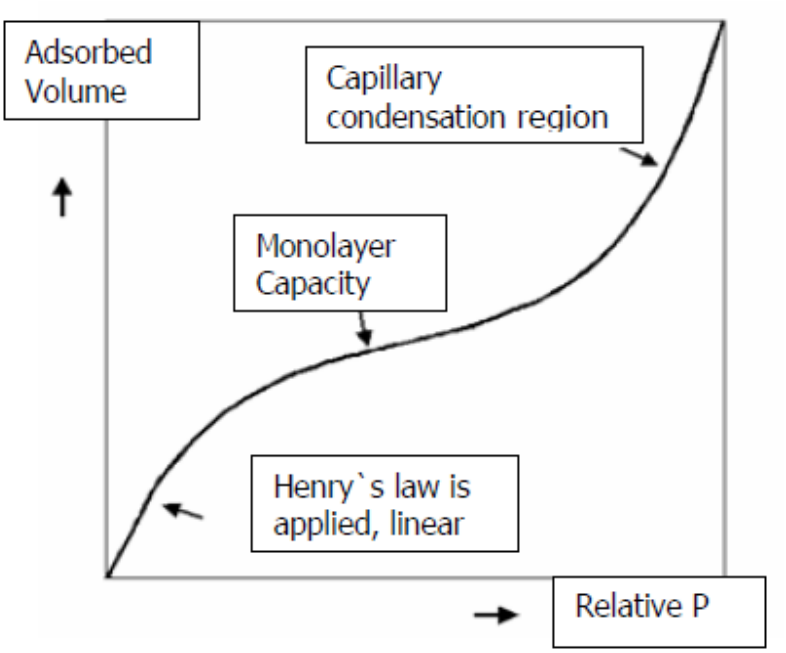

Figure 2.12 Regions on Physisorption Isotherms (Ok, 2005)

The t-plot method

The t-plot method is used in the determination of micro and mesopores on the basis of modeling a multilayer formation. In this method statistical layer thickness is calculated as a function of relative pressure according to the several mathematical expressions like de Boer, Halsey and Harkins methods. t-plot curve is obtained as a graphical representation of the relationship between volume adsorbed and statistical thickness at each relative pressure value. The linear range occurs between monolayer formation and capillary condensation. Hence, it is possible to estimate the complete micropore filling and initiation of the mesopore filling by the plot. Also the external area of the porous material (area of mesopores, macropores with the outside surface area) and micropore volume and area can be derived from the plot.

α_s Method

In the α_s method, a comparison between the tested isotherm and a normalized reference isotherm obtained from a sample of known surface area, is carried out. Without any assumption or calculation of statistical thickness as it is been in t-plot method, a plot of the amount adsorbed versus α_s values is obtained. Similar to t-plot, linear range of plot occurs between monolayer and capillary condensation. Assessment of microporosity with mesoporosity is also possible.

Dubinin Radushkevich (DR) Method

Dubinin and Radushkevich proposed an equation that is based on the Polanyi's potential theory and micropore filling. The expression is given by;

$$\log W = \log(W_O) - k\left[\log\left(\frac{P_O}{P}\right)\right]^2 \qquad (2.11)$$

k and Wo are defined as;

$$k = 2.303K\left(\frac{RT}{\beta}\right)^2 \qquad (2.12)$$

and

$$W_o = V_o \rho \qquad (2.13)$$

"W", "ρ" and "Vo" are weight adsorbed, liquid adsorbate density and micropore volume, respectively.

An identical degree of filling of the volume of adsorption space is stated by Dubinin and Raduskewich and called the affinity coefficient, "β", which is a constant as the ratio of adsorption potentials of any two vapors. The term "K" is also a constant that was determined by the shape of the pore size distribution.

Dubinin Astakhov (DA) Method

DA method is related with DR method. In the case of non-homogeneous surface and texture, DA method is more preferable. This method is also based on the micropore filling mechanism. Dubinin-Astakhov parameter and average adsorption energy are considered in the method. Dubinin-Astakhov parameter depends on surface heterogenity and effects the width of the resulting pore size distribution.

Horvath-Kawazoe (HK) Method

Horvath-Kawazoe (HK) method is a semi-emprical, analytical method which is based on micropore filling mechanism The calculation depends on slit-shaped pore model assumption for activated carbons. HK method considers the effect of pore geometry and the strength of the attractive adsorptive-adsorbent interaction on the adsorption potential. But imperfection of this method comes from that it does not differentiate the thermophysical properties of bulk fluid from the fluid in the pores. Also, mesopore analysis is not applicaple by this method. Calculation of pore size distributions from the low relative pressure region of adsorption isotherms is possibble by an expession derived which is a relationship between pore size and relative pressure and this expression also includes magnetic susceptibility of adsorbent and adsorbate molecules.

Saito-Foley (SF) Method

Since HK method has been developed for slit-shaped pores, another expression like HK was developed for cylindrical pore geometry. Calculation of SF method is also restricted to micropore region as it was in HK method.

Barrett, Joyner, Halenda (BJH) Method

BJH method is also cited as the modified form of Kelvin equation and measures mesopore size distribution. This method is based on a combination of physical adsorption and capillary condensation mechanism (Kelvin equation for hemispherical meniscus). It includes the analysis of desorption isotherm instead of adsorption isotherm. But, some studies with this method includes the study of both desorption and adsorption branch of isotherms although it can't be justified theoretically (Barrett et al., 1951).

The deficiency of this method is that it does not consider the fluid-solid interactions on capillary condensation. But it is still a convenient method and it is considered one of the main methods in the pore size distributions despite the questions raised about its validity and limitations (Ravikovitch and Neimark, 2001).

Detailed information and formulas of BJH Method is given in Appendix A.

Density Functional Theory (DFT)

Instead of other methods used in determination of pore structure, DFT is based on statistical thermodynamics on a molecular level. This method associates microscopic properties of the system such as fluid-fluid and fluid-solid interaction parameter, pore size, pore geometry and temperature with the adsorption isotherms. Complex modeling of microscopic system properties results in more realistic density profiles as a function of pressure and temperature. By this way, amount adsorbed, transport properties of the system and heat of adsorption can be derived from density profiles closely to the actual value.

In summary, DFT method includes constructing an equation called a grand potential functional of the average density of the adsorbate and

find equilibrium density profile to obtain quantity of adsorbed at each pressure that yields isotherms (Valladares et. al., 1998).

For a wide variety of materials, pore geometries and analysis conditions for individual isotherms have created for specific adsorbent/adsorbate pairs and these isotherms are available by software programs. Hence, it is possible to find pore size distribution of materials such as activated carbon by matching the isotherm with the tested material.

Although DFT is an important achievement in the determination of pore size distribution, isotherms used require an improvement to incorporate the surface heterogeneity effect (Kruk et al., 1998).

2.4 PREVIOUS STUDIES DONE ON THE CHEMICAL AND PHYSICAL ACTIVATION

There have been numereous studies on the activated carbon production and characterization for many years. A lot of parameters that influences the final texture have been investigated and reported by several authors. This part includes some recent studies that present the effects of different parameters in the physical and the chemical activation.

2.4.1. Studies Done on Physical and Chemical Activation

Chang et al. (2000) prepared activated carbon from an agricultural waste, corn cob, by physical activation under CO_2 and steam atmosphere and investigated the effects of burn-off degree and activation temperature on the characteristics of activated carbons produced. The produced carbons were characterized by nitrogen adsorption and scanning electron microscopy (SEM). According to the results, BET surface area, pore volume and average pore diameter increased with the

extent of burn-off in both steam and CO_2 activation. Activation temperature showed similar behaviour with burn-off degree. Highest BET surface area was obtained as 1705 and 1315 m^2/g by steam and CO_2 activation, respectively. It was also stated that microporous activated carbon production was feasible with this waste corn cob and adsorption capacity could reach as high as those it commercial activated carbons.

Zhang et al. (2004) carried out physical activation of different forest residues including oak wood, corn hulls and corn stover with CO_2. The raw materials were pyrolysed under nitrogen atmosphere at 500 ^oC then activated with carbon dioxide at 700 and 800 ^oC for 1 and 2 hours. The burn-off degrees were determined for every condition. Nitrogen adsorption were performed on both activated carbons and on the chars obtained without any activation process to observe the effects of the activation conditions. Pore size distributions of the activated carbons were determined by Non-Local Density Functional Theory (NLDFT). As a conclusion, both surface area and the nature of the porosity were effected by the starting material and process conditions. The maximum BET surface area was attained 1010 m^2/g by using corn hulls as a raw material and activating at a temperature of 800 ^oC for 1 h.

Bouchelta et al. (2008) produced activated carbon from date stones by physical activation with steam and characterized the products with nitrogen adsorption, scanning electron microscope (SEM), X-ray diffraction (XRD) and Fourier transform infrared spectroscopy (FTIR). The effects of pyrolysis and activation temperature, activation holding time were investigated. As the pyrolysis temperature, activation temperature and activation holding time were increased, yield of activated carbons decreased obviously. After the pyrolysis and activation of date stones, aromatization on the structure occurred. The highest BET surface area was attained at a value of 635 m^2/g when the raw material was pyrolyzed at 700 ^oC under nitrogen atmosphere and activated under steam flow at the same temperature for 6 h.

Yang et al. (2010) proposed a different activation method to produce activated carbon from coconut shells by physical activation. The raw coconut shells were carbonized at a temperature of 1000 ^{o}C with a heating rate of 10 ^{o}C/min under nitrogen atmosphere. After cooling down, the chars obtained from carbonization were activated in a special microwave reactor at 900 ^{o}C. Steam and carbon dioxide were used both separately and together as activating gases under the microwave treatment. Structural characterization of the carbons was done by nitrogen adsorption and NLDFT was used to determine pore size distribution. The microwave assisted physical activation method had a marked effect on both pore development and the yield of the activated carbon production. When microwave assisted activation results were compared with other activation methods applied coconut shells, the best results were observed with the method used in this study. BET surface areas exceed 2000 m^2/g with this proposed method in shorter activation periods. Besides, this method caused the development of ultramicropores. When a comparison was carried out among the activating gases, it was seen that CO_2 activation contributed pore development more than steam activation.

In a study of Moreno-Castilla et al. (2001) chemical activation with phosphoric acid and potassium hydroxide and physical activation with carbon dioxide were investigated together. Olive-mill waste was used as a raw material in the study and the prepared activated carbons were characterized with nitrogen and carbon dioxide adsorption. Also, ultimate analysis was performed and pH of the point of zero charge was determined. In the chemical activation studies, carbonization was done and obtained chars were treated with activating agents. Activation of chars yielded a well-developed porosity by potassium hydroxide treatment, whereas phosphoric acid treatment of chars did not increase porosity as much as potassium hydroxide. On the other hand, physical activation with various degrees of burn-off caused porosity development

but it was also less than the porosity development in the potassium hydroxide activation.

Teng et al. (2000) produced activated carbons from phenol-formaldehyde resins with chemical and physical activation methods. They used potassium hydroxide in the chemical activation and carbon dioxide in the physical activation of the resin. During the chemical activation studies, precursor was directly impregnated without any carbonization step and the effects of impregnation ratio, activation holding time, activation temperature were investigated. On the other hand, physical activations at 900 ^{o}C with carbon dioxide at various burn-off degrees were performed. Characterization of the porosity was done by nitrogen adsorption and SEM analysis. Results of the physical and chemical activation were compared and it was concluded from the results that microporous carbons with very high porosity could be prepared from phenol-formaldehyde resins. Both of two methods resulted in BET surface areas more than 2000 m^2/g. And the optimum conditions were stated for both methods in the study. Also SEM micrographs exhibited a more compact surface in the CO_2 activation than the KOH activation.

A study including both physical and chemical activation was done by Valix et al. (2004). In the study, sugarcane bagasse was used as a raw material and chemical activation with sulfuric acid at a ratio of 4:3 (wt.) was done. After impregnation of material with sulfuric acid, the material exposed to a heat treatment under air flow with a heating rate of 10 ^{o}C/min, until the final temperature had reached 160 ^{o}C and the temperature held constant for 2 h at this temperature. Also, activation of the chars was carried out under a carbon dioxide flow at 900 ^{o}C. Various gasification periods were used to investigate the effects of the activation holding time on activated carbon characteristics. The results were compared with the previous studies done with sugarcane bagasse and acid blue dye adsorption capacity was compared with a commercial activated carbon. Results showed that, despite a high ash content, sugarcane derived activated carbon production could be possible with a

low temperature chemical carbonization and gasification method. Also those produced activated carbons exhibited a higher adsorption capacity of the acid dye than the commercial one.

An interesting study to compare chemical and physical activation was presented by Okada et al. (2003) by using waste newspapers as a precursor in the activated carbon production. Three types of papers were used and, depending on the pretreatments done, those papers were categorized and called suction paper, sediment paper and as received paper. Chemical activations were performed by following four different paths as single step activation, two-step activation (oxidation followed by activation), another two-step activation (carbonization followed by oxidation) and three-step activation (oxidation, carbonization and activation steps respectively). Li_2CO_3, Na_2CO_3, K_2CO_3, Rb_2CO_3, Cs_2CO_3, NaOH and KOH were used as chemical activation reagents and during experiments impregnation ratio, activation temperature, activation time, nitrogen flow rate were varied to determine the effects on the activated carbon characteristics. The physical carbonization of the samples were done by both single-step and two-step methods. And those single-step and two-step methods were differentiated only in the cooling of the carbonized material before the activation step. Activation temperature, holding time, steam concentration in the wet nitrogen and steam flow rates were studied as parameters in the physical activation of the samples. Nitrogen adsorption, thermo gravimetric analysis (TGA), X-ray photoelectron spectroscopy (XPS), SEM and XRD were used to characterize the products. Results showed that, all the paper wastes could be used in the activated carbon production. Both in the chemical and physical activation, single-step activation gave the best results on the pore development. BET surface areas were changed dramatically with the activation reagent and activation conditions. When K_2CO_3, Rb_2CO_3, Cs_2CO_3, and KOH were used as activation agents, BET surface areas exceed 1000 m^2/g. But Li_2CO_3, Na_2CO_3, and NaOH caused lower BET surface area values than the other agents. The differences arised in BET

surface area values were suggested to be related with the ionic radius of the alkalis used. K_2CO_3 resulted in better porous structures with a highest BET surface area of 1740 m^2/g of when it was compared with other agents used in the chemical activation. Optimum conditions were stated for both chemical and physical activation studies, separately.

Gonzalez et al. (2009) obtained physically activated carbons from walnut shells by steam and carbon dioxide. Steam activation was carried out at a temperature interval from 700 to 900 ^oC for different activation periods. Carbon dioxide activations were done at 850 ^oC with activating the material at an activation time range between 60 and 480 min. The burn-off degrees of the produced carbons varied 12 to 76 % depending on the process conditions. After the characterization of the products by nitrogen adsorption, carbon dioxide adsorption, scanning electron microscopy, mercury porosimetry, helium pycnometry and Fourier transform infrared spectroscopy, the influences of the two activation mechanism were discussed. Steam caused an increase in mesoporosity by increase in the activation time. Carbon dioxide caused highly microporous carbons and widening of this microporosity occurred only for long activation periods. On the other hand, since steam was more reactive than CO_2, adsorption capacity of the steam activated carbons for N_2 was found higher than the carbon dioxide activated carbons according to the adsorption isotherms.

Mendez-Linan et al. (2010) used a char residue obtained from the polycarbonate pyrolysis to produce activated carbon by chemical and physical activation methods. Pyrolysis of polycarbonate was done at 950 ^oC with a heating rate of 5 ^oC/min and a holding time of 1 h. The produced char was then used in physical and chemical activation. Physical activation was carried out under carbon dioxide flow at 950 ^oC for 1, 4 and 8 h. For chemical activation, the char residue obtained from the pyrolysis was impregnated with KOH in three different ratios as 1:1, 4:1 and 6:1 (KOH/char) (wt.) and activation temperatures of 600 and 800 ^oC were used in the experiments. The characterization of carbons

was done with mercury porosimetry, N_2 and CO_2 adsorption and pore size distribution was then analyzed by a molecular simulation method called Monte Carlo. The results showed that KOH activation resulted in activated carbons which were dominantly microporous but CO_2 activation generated mesopores along with the microporous structure. The carbons were tested whether they could be used in methane and hydrogen storage. Methane and hydrogen storage capacities were found with a high-pressure adsorption system. Microporous structure was found suitable for both hydrogen and methane adsoption. Also, narrow micropores in the structure contributed to increase the hydrogen adsorption effectively, although they could not be characterized with nitrogen and carbon dioxide adsorption. The reason behind this phenomenon was that those narrow micropores were inaccessible to nitrogen molecules at 77 K and caused diffusion resistances for CO_2 molecules at 273 K.

Production of physically activated carbons from olive-waste cakes and optimization of the preparation parameters was presented in a study of Baçaoui et al. (2001). They used steam activation on olive-waste cakes and an experimental design method called Doehlert matrix was used to optimize conditions. Characteristics of the prepared activated carbons were investigated by N_2 and CO_2 adsorption and mercury porosimetry. Adsorption of methylene blue and iodine was performed to denote adsorption capacity of the produced activated carbons. Optimization studies aimed the maximum yield and surface area with the highest adsorption capacity. The model used determined the optimum point at an activation temperature of 822 ^{o}C an activation holding time of 68 min.

A study for preparation of activated carbon from a material other than biomass was done by Ariyadejwanich et al. (2003). They used waste tyres that were separated from rubber and carbonized this material under nitrogen atmosphere at 500 ^{o}C. During carbonization, three different heating rates as 0.5; 5 and 20 ^{o}C/min were applied. Physical activation of the carbonized samples was carried out under steam flow at 850 ^{o}C and

with a heating rate of 20 °C/min. The activation temperature was changed from 1 to 4 hour to study activation holding time as another parameter. Besides, by a hydrochloric acid treatment before steam activation, the effect of acid was studied. The acid treatment did not influence carbonization yield but decreased ash content of the products considerably. Before activation, pore properties of chars were determined with N_2 adsorption. It was seen that surface area values of chars did not exceed 100 m^2/g. After activation, the BET surface area values found between 4 to 7 times of the surface area values obtained from the unactivated chars. Also, acidic treatment before steam activation improved both micro and mesoporosity of the activated carbons. Moreover, phenol and a dye called Black 5, adsorption was carried out aqueous solutions to determine adsorption performance of the activated carbons and the results were compared with a commercial activated carbon. Activated carbon from waste tyres adsorbed phenol slightly lower than the commercial one. But Black 5 adsorption with the prepared activated carbon showed a better performance than the commercial one.

Apaydın (2007) carried a detailed study which included both physical and chemical activation studies of four different biomass samples as soybean cake, corn stalks, peanut shells and pine cones. Physical activation studies with carbon dioxide and stream together were carried out at 600, 700, and 800 °C for all the biomass samples. After the pyrolysis without any activation, BET surface areas of the samples were found to be between 2.1 and 211 m^2/g and they did not exhibited a well-developed porosity. The best results are obtained at temperatures of 700 and 800 °C under both steam and carbon dioxide activation and pine cones gave the best results considering the physical activation studies. After physical activation chemical activation of pine stones was studied with phosphoric acid, potassium hydroxide and zinc chloride. The phosphoric acid showed best performance among the other chemicals on the pine cones and the highest value of BET surface area was reached to 1372 m^2/g by phosphoric acid activation. When the surface areas were

compared with the values attained in the physical activation, it was seen that they were much higher than those obtained by both steam and carbon dioxide activation and they required lower activation temperatures. With the all activated carbons produced, the nickel adsorption from aqueous solutions was done and promising results were achieved.

Yağmur et al. (2008) presented a novel method for chemically activated carbon production with phosphoric acid. They used microwave energy in the pre-carbonization of the tea wastes. They put forward a method that included heating of the impregnated raw material under microwave energy without any inert gas flow, followed by the conventional heating under nitrogen atmosphere with a heating rate of 20 ^{o}C/min. They also investigated the effects of carbonization temperature and impregnation ratio on the pore development. They studied at a temperature interval from 250 to 700 ^{o}C by impregnating material at different ratios varied from 1:1 to 3:1 (H_3PO_4/raw material). They also carried out the conventional method by impregnation material without any microwave treatment. Then the characterization of products were done by SEM and FTIR. There was a convincing evidence that microwave treatment resulted in important changes in the structure by improving pore properties in a very short time period, when the microwave method was compared with the conventional method. Maximum BET surface area was stated as 1157 m^2/g in the case of microwave assisted method with an impregnation ratio of 3:1 and at a carbonization temperature of 350 ^{o}C. When the sample was prepared at the same conditions without microwave treatment, this value was able to achieve only 929 m^2/g.

A comprehensive study on the chemical activation with phosphoric acid was published by Toles et al. (2000). They activated almond shells by using six different activation and activation/oxidation methods. Physical, chemical and adsorptive properties are compared both with each other and with two different commercial activated carbons and cost

estimations of the all methods were done. They used an impregnation ratio of 1:1 (H_3PO_4/shells) and they used a relatively low temperature as 170 ^oC in the methods including heat treatment. They termed the methods as; activation only method, standard method, continuous method, air activation method, modified air method and quench method. Among these methods variable parameters that differentiated the processes were; temperature treatment, initial and final washing step, oxidation conditions and flowing gas type during the activation period. By taking into account of shell input rate, H_3PO_4 input rate, natural gas, water and electricity usage in the process, operating days per year, active operating hours per day and daily carbon output rate, they estimated the cost of activated carbon production of all methods. By adsorption of Cu^{2+} and organics included benzene, toluene, 1,4-dioxane, acetonitrile, acetone and methanol, they determined the adsorptive properties of each carbon that was produced. By considering physical, chemical and adsorptive properties with the cost of the production, they concluded that the best activated carbon was prepared with air activation method with a production cost of 2.45 $/kg and a BET surface area of 1283 m^2/g.

Baquero et al. (2003) used coffee bean husks as a raw material in the production of chemically activated carbon by phosphoric acid. They carried out all pyrolysis experiments under argon atmosphere with a constant heating rate of 10 ^oC/min. They performed pyrolysis at a temperature of 500 ^oC for 1 h. They investigated the effect of impregnation ratio, by impregnating the raw material at the ratios of 30, 60, 100 and 150 wt. % with phosphoric acid. The characterization of the products was then performed by the nitrogen and carbon dioxide adsorption and pore size distribution was obtained by Density Functional Theory (DFT), Dubinin-Raduskevich (DR) and Dubinin-Raduskevich-Kaganen (DRK) methods. Maximum BET surface area was attained by impregnation of material 150 % weight as 1402 m^2/g. They concluded that lower impregnation ratio caused microporous activated carbons and

while impegnation ratio was increased, pore widening occured. When high impegnation ratios were used mesoporous carbons were obtained with the enlargement of the pore volume.

In a study of Lim et al. (2010), textural characteristics of activated carbons produced from palm shells by phosphoric acid activation was investigated with the yields of the production. They impregnated raw shells with phosphoric acid at ratios between 1:2 and 3:1 (H_3PO_4/shells). A semi-carbonization of shells was done by heating impregnated samples in an oven at 170 ^oC for 1 h. Then, the samples were heated to 425 ^oC without the flow of any inert gas and held at that temperature for 30 min. Products were characterized by nitrogen and iodine adsorption to determine BET surface area, micropore volume, pore size distribution and iodine number. The structural characteristics of activated carbons developed with increasing the impregnation ratio up to 2:1. After this optimum point, the adsorption characteristics which were exhibited by iodine number, started to decline. An important point that emphasized in the study was that the yield of activated carbon production did not change with the impregnation ratio substantially. The yields of activated carbons produced in this study were found around 50% for all conditions.

In order to produce activated carbon from agricultural wastes including bagasse, apricot stones, almond, walnut and hazelnut shells, Soleimani et al. (2007) investigated the effects of preparation conditions on the product yield and the adsorption properties of the activated carbon. They determined the effects of the final activation temperature, activation time, impregnation ratio and the properties of raw materials on the activated carbon yield, percent recovery of the phosphoric acid used, iodine number and BET surface area. They obtained best adsorption properties by using apricot stones as a raw material with achieving the highest BET surface area as 1387 m^2/g. Finally, they made a comparison between activated carbon produced by apricot stones and three different commercial activated carbons by performing gold adsorption experiments. Gold recovery by the adsorption of the produced activated

carbon from apricot stones reached 98.15% by showing the highest among the other activated carbons used in the adsorption experiments.

A rapid-growing plant named arundo donax was used as a raw material in the production of the chemically activated carbon by Vernersson et al. (2002). After impregnation of the raw samples with phosphoric acid at a ratio of 3:2 and 2:1 (H_3PO_4/raw material) they activated at the temperatures between 400 and 550 ^oC with a heating rate of 3 ^oC/min. Investigations were also done on the effect of the activation holding time. The novelity of this study was that, they did activation both under nitrogen atmosphere and under self-generated atmosphere. The self-generated atmosphere was created with the combination of air that was got in to the reactor while the sample was placed and recycling of the released gases during the carbonization period. The differences of BET surface areas were not considerable when the two atmospheric conditions were compared. But, ash and phosphorous content and pore size distributions changed notably when the two methods were compared. Under nitrogen atmosphere, ash and phosphorous contents of the activated carbons increased, on the other hand mean pore radius decreased with causing more microporous structure. It was also stated that the temperature above 500 ^oC caused the reduction in porosity development for all the conditions investigated and this phenomenon was explained with the thermal breakdown of phosphate ester cross link from the structure. Besides, high impregnation ratio caused an adverse effect on the pore development due to the possibility of the weakening of the carbon structure in the case of use of phosphoric acid in excess amounts.

In a study of Budinova et al. (2006) , activated carbon from woody biomass birch was produced by modifying different activation procedures. They used three methods as following: In the first method, impregnation of raw material by phosphoric acid followed by pyrolysis at 600 ^oC under the nitrogen flow. The second method included the pyrolysis of phosphoric acid impregnated precursor under nitrogen atmosphere at

600 ^{o}C following activation by steam at the same temperature. And in the last method, phosphoric acid impregnated samples were directly subjected to steam pyrolysis at 700 ^{o}C. For the characterization of the products, iodine number, pore properties in terms of BET surface area and pore volumes and oxygen-containing functional groups were determined. Furthermore, mercury adsorption studied were done to observe adsorption capacities of activated carbons towards to Hg(II) ion. The best porous structure with the highest surface area of 1360 m^2/g was achieved by applying directly steam pyrolysis to the phosphoric acid impregnated samples. This method also caused the decrement of the phosphorous content of the activated carbon and the carbons produced with this direct steam pyrolysis exhibited good adsorption properties for Hg(II) ion removal from the aqueous solutions.

Puziy et al. (2002; a,b, and 2003) prepared a series of articles related to the synthetic carbon activation by phosphoric acid. During the studies, styrene-divinylbenzene copolymer, chloromethylated, sulfonated copolymer of styrene and divinylbenzene used. In the first study, surface chemistry and the binding properties analysed with a detailed characterization with the combination of various methods. Second study possessed investigations on the pore structure. And, in the last study an integrated chemical activation with physical air activation was included. The resulting activated carbons had exhibited cation-exchange properties considerably and that property distinguished this study from the biomass based activated carbon production researchs.

Zuo et al. (2009), published an interesting research on the chemical activation of a lignocellulosic biomass sample called China fir wood. Phosphoric acid was used as an activation agent and 475 ^{o}C was selected for activation temperature during the experiments. They carried out experiments in a container which was put in a furnace and an inert atmosphere was obtained by supplying a nitrogen flow to the furnace. The weight of the material put into the container and the open and close state of the lid of the container was changed to investigate their effects.

Covered and uncovered states were named depending on the position of lid. On the covered state, yield of activated carbon, elemental carbon content and BET surface areas reached higher values than the uncovered state. The increase in the weight of the starting raw material showed the similar trend, while the amount of material increased, yield, elemental carbon content and BET surface areas increased. On the other hand, ash content decreased by using covered state with higher amounts of material. This phenomenon was explained as the closed state prevented the removal of the volatiles from the container. Increasing the starting material caused difficulties for the removal of the volatiles from the container too because of the mass transfer limitations. Thus, the contact with the phosphoric acid increased in the case of putting the starting material in larger amounts to the container and also using closed state of the container during the pyrolysis.

Girgis et al. (2002), investigated date pits as an alternative raw material in the activated carbon production. By impregnating date pits with different impregnation ratios, they performed the pyrolysis at 300, 500 and 700 ^{o}C with a heating rate of 5 ^{o}C/min and held at that temperature for 2 hours. Pore characteristics were determined with nitrogen adsorption and methylene blue, iodine and phenol numbers were found by the adsorption of these components. Thermo gravimetric analysis was also carried out to investigate the phosphoric acid effect on the weight loss behavior at different impregnation ratios and different temperature intervals. It was concluded from the thermo gravimetric analysis that degradation behavior was influenced with the phosphoric acid treatment dramatically by causing early dehydration and later degradation of the structure. This behavior was explained with the formation of a resistant polymeric structure because of the impregnation. Up to 600 ^{o}C, evolving of the volatiles also delayed with the higher activated carbon yields. Nitrogen adsorption results showed that, treatment of raw material with phosphoric acid in excess amount caused a reduction on the pore development and this was because of the

possible formation of a solid layer that prevented activation. Up to the impregnation ratio of 50 %, the temperature increment also increased the surface area.

An investigation of a chemically activated carbon with phosphoric acid was done by Hazourli et al. (2009). Three different methods were performed to produce activated carbon from date stones. In the first method, raw material was subjected to steam pyrolysis at 600 ^{o}C without any previous chemical treatment. The other two methods involved the treatments of the raw material with nitric acid and phosphoric acid followed by the carbonization under steam flow at 600 ^{o}C too. Nitrogen adsorption to determine porosity and pore properties; Boehm titration method to determine total acidity and alkalinity; XPS to determine the composition of the surface and SEM analysis to determine surface morphology were done on the products. The applied methods in the activated carbon production caused significant differences in the overall characteristics of the products formed. Phosphoric acid treated process caused the highest surface area among the other methods and that proved the increase of the porosity could be possible by phosphoric acid impregnation before the heat treatment.

In another study of Soleimani et al. (2008), recovery of gold ions from a gold-plating waste water was studied with an activated carbon produced from apricot stones. Phosphoric acid was used as an activation agent by impregnation the material at a ratio of 1:1. Carbonization of the impregnated samples was done at 400 ^{o}C. Production efficiency, recovery of the phosphoric acid after the process, attrition percentage of the carbon were calculated and elemental composition, ash content, bulk density, specific surface area, conductivity and iodine number of the product were determined. After the determination of the characteristics of the activated carbon produced, gold adsorption experiments were performed. The results showed that an activated carbon produced from apricot stones could recover gold ions effectively, by achieving a removal percentage as 98.15% at the optimum conditions.

Fierro et al. (2010) used rice straw in the production of the activated carbon. By impregnating the raw material with ortho-phosphoric acid, they investigated the effects of the activation temperature, time and impregnation ratio. The activated carbons were then characterized by the nitrogen adsorption, SEM-EDX and methylene blue adsorption. By using Langmuir and Freundlich isotherms in the methylene blue adsorption experiments, the adsorption performance was observed. An activation temperature of 450 ^{o}C, an impregnation ratio of 1:1 and an activation holding time of 1 h was stated the optimum point as considering the yield of the production with the pore characteristics together.

Suarez-Garcia (2002) et al. obtained activated carbon from apple pulp by chemical activation. They used phosphoric acid with different impregnation ratios between 20 and 150 % by weight. Carbonization and activation experiments were conducted under the argon atmosphere with a heating rate of 10 ^{o}C/min. Carbonization temperatures of 400, 500 and 600 ^{o}C and holding times of 1, 4 and 8 h were used to investigate the effects of temperature, holding time and impregnation ratio together. Products were then characterized by nitrogen adsorption, elemental analysis and X-ray diffraction. As a consequence, low impregnation ratios seemed to be appropriate for micropore development. But when the impregnation ratios were increased, pores were enlarged and at the high ratios mesoporous activated carbons were obtained. It was also stated that, too high temperatures or too long holding times had an adverse effect to the porous structure development.

Girgis et al. (2009) carried out a study on the pilot production of activated carbon by phosphoric acid. As a raw material cotton stalks were used and two different impregnation ratios were investigated during the study. Carbonization was carried out in a rotary drum carbonizer and batch mode production was performed. Nitrogen adsorption, helium pycnometry, scanning electron microscopy, fourier transform infrared spectroscopy, techniques used for characterization with determination of

iodine number, methylene blue number, pH of the products and total acidity. Also, Pb(II) adsorption was carried out with the produced activated carbons and good adsorptive properties towards to the Pb(II) ion were observed. They emphasized the feasibility of the production of activated carbons from cotton stalks on the large scale.

Jibril et al. (2008) studied the effects of phosphoric acid and potassium hydroxide activation of the stem of date palm which was a lignocellulosic material. The two stage activation method was applied in the experimental part of the study. In the first stage, impregnated samples were heated to 85 ^{o}C with a heating rate of 15 ^{o}C/min under the nitrogen atmosphere. After the cooling the products obtained from the first stage, additional carbonization was carried out after a heating to 100 ^{o}C with a heating rate of 10 ^{o}C/min for the moisture removal. Then the second stage was performed with an additional heating to the final carbonization temperatures with a heating rate of 50 ^{o}C/min. When the final carbonization temperatures (400, 500 and 600 ^{o}C) were achieved, the temperature was held constant at that temperature for 2 h. The same procedure was also followed without any impregnation step which resulted in a carbonized solid product, char. The final carbonization temperatures which were investigated in the experiments were 400, 500 and 600 ^{o}C. The products were then characterized by nitrogen adsorption, helium pycnometry, scanning electron microscopy and oil adsorption studies from an oil-water emulsion. The fibrous structure of the raw material and solid char formed was replaced with a decayed fibrous structure after the chemical activation with both phosphoric acid and potassium hydroxide. And the best porous structure was obtained at a temperature of 500 ^{o}C with the phosphoric acid activation process with a BET surface area of 1100 m^2/g.

Molina-Sabio et al. (2003) published a study on an integrated chemical and physical activation method for the activated carbon discs production and methane storage was investigated on those activated carbon discs. At different ratios, olive stones were mixed with phosphoric

acid for impregnation and then pressed at 100 ^{o}C. After that, those discs were carbonized under the nitrogen atmosphere up to 450 ^{o}C, with a heating rate of 1 ^{o}C/min. Some of the discs were heated to 800 ^{o}C under the nitrogen atmosphere, while the others were activated with carbon dioxide at 750 ^{o}C physically. After the characterization of activated carbon discs produced, methane storage capacity of the discs was measured. A maximum methane storage capacity of 130 v/v was achieved with phosphoric acid activation and when an additional CO_2 activation were done on the phosphoric acid activated discs, this value increased to 150 v/v. They concluded that the activated carbon discs could be advantageous in the methane storage because of the cheapness of the discs produced.

2.4.2. Studies Done with Pistachio-Nut Shells

Kazemipour et al. (2008) investigated almond, walnut, hazelnut, pistachio nut shells and apricot stones to prepare activated carbon for heavy metal removal from wastewaters. After carbonization of the precursors, physical, chemical and surface properties determined without any activation process. With pistachio nut shell, a surface area of 635 m^2/g, a bulk density of 0.54 g/ml and a yield of 20% attained. This pistachio nut shell based product was then tried to adsorb heavy metals from both synthetic waste water and from real industrial waste water. From synthetic waste water, removal efficiencies of Zn, Cu, Pb and Cd were found as 63.4, 83.0, 52.7 and 33.8 %, respectively, for pistachio-nut based carbon. In the case of adsorption from a real waste obtained from a copper industry used in adsorption studies and removal efficiencies of Cu and Zn from copper industry found as 95.6 and 87.9% respectively. They concluded that pistachio shells could be used in the adsorption of heavy metals from waste waters with having advantages of their cheapness and easy production.

Hayashi et al. (2002) used almond shell, coconut shell, oil palm shell, walnut shell and pistachio-nut shell as raw material to produce chemically activated carbon with potassium carbonate. They studied the effects of carbonization temperature and weight loss behaviour of these five precursors and determined pore structures of activated carbons by N_2 adsorption. In their study, they impregnated shells with potassium carbonate at a ratio of 1/1 (K_2CO_3 / raw material) without any carbonization step before. During their experiments, heating rate was 10 ^oC/min and an holding time was 1 h. Pistachio nut shells exhibited the highest specific surface areas at all the temperatures between 500 and 900 ^OC. Selection of pistachio nut shells among other precursors used in this study seems to be appropriate to produce activated carbon. They also stated that all the activated carbons reached maximum surface area values at 800 ^oC and at this temperature pistachio nut shell based activated carbon has a surface area about 1800 m^2/g.

Lua and Yang (2004; a) prepared activated carbon from pistachio nut shells by potassium hydroxide activation. They used chars that were previously prepared by carbonization of shells under nitrogen atmosphere at 500 ^oC. After impregnation of chars at a ratio of 0.5 wt. (KOH/shells), they investigated the effects of temperature of activation on pore development, yield and the structure of the activated carbons. They examined microstructure by scanning electron microscope, surface chemistry by Fourier transform infrared spectroscopy, crystallinity structure by X-ray diffraction and pore structures by nitrogen adsorption. They emphasized the necessity of high temperatures for a highly porous texture, although very high temperatures caused high burn-off that results in meso and macro pores instead of micropores. Maximum BET surface area of the activated carbons produced came close to a value of 2000 m^2/g with potassium hydroxide activation. Also, obtained activated carbons were tested for SO_2 adsorption. They compared SO_2 adsorption capacities of hydroxide activated carbon with physically activated carbon of pistachio nut shells and three commercial activated carbons. In terms

of SO_2 adsorption capacity, pistachio nut shell based chemically activated carbon with potassium hydroxide gave the best result among other activated carbons tested.

In another study of Lua and Yang (2004; b), pistachio-nut shells were used as a raw material and effects of vacuum pyrolysis conditions on both the char and activated carbon by physical activation method was presented. They studied at a temperature interval between 350 to 1000 ^{o}C applying vacuum to the reactor and investigated the effects of holding time and heating rate on the properties of chars and activated carbons. After carbonization they carried out an additional step for chars to activate them with carbon dioxide. In the activation step, a temperature of 900 ^{o}C and a holding time of 1 h was kept constant. By nitrogen adsorption, adsorption characteristics in terms of BET surface area and pore volume determined and pore size distributions with HK and BJH method were investigated. Crystalinity structure, surface morphology and surface functional groups were observed by XRD, SEM and FTIR, respectively. They concluded that pyrolysis at a temperature of 500 ^{o}C, a holding time of 2 hour and a heating rate of 10 ^{o}C/min resulted best char characteristics for producing activated carbon with carbon dioxide activation. Under these conditions an activated carbon with a surfare area of 896 m^2/g and a micropore volume of 0.237 cm^3/g was produced.

Önal and Söylemez (2008) studied chemical activation of pistachio nut shells with different chemical reagents as potassium hydroxide, zinc chloride and potassium carbonate to obtain activated carbon. They impregnated raw shells to chemicals at a ratio of 1/1 and obtained the highest BET surface area with zinc chloride activation as 1417 m^2/g. They concluded that activated carbons were consisted of micro and mesopores according to the pore size distribution done with DFT method. Besides, they emphasized that all of the carbons were amorphous according to the XRD resuts.

Lua et al. (2004) carried out physical activation of pistachio nut shells with carbon dioxide. They investigated carbonization temperature, carbonization time, heating rate and nitrogen flow rate during pyrolysis to optimize the conditions before the activation of chars. After carbonization, they activated char at 900 ^{o}C to produce activated carbon. Characterization of products were done by nitrogen adsorption, helium pycnometer, thermo gravimetric analyser and scanning electron microscope to determine adsorption properties, solid densities, proximate analysis and surface morphologies of the products. They stated that pyrolysis at a temperature of 500 ^{o}C, a nitrogen flow rate of 150 cm^3/min, a heating rate of 10 ^{o}C/min and a holding time of 2 h gives the highest BET surface area after activation. They also emphasized that low heating rates are suitable for development of a microporous structure and too long holding time has an adverse effect to the attainment of a higher surface area values. They advised pistachio nut shells as a suitable precursor for production and development of activated carbons for both gas and liquid phase applications.

Schröder et al. (2007) published a study on generating activated carbon from different agricultural wastes. They produced activated carbon from rice straw, wheat straw, wheat straw pellets, olive stones, pistachio shells, walnut shells, bleech wood and hardcoal. Raw materials were pretreated with sodium hydroxide washing and then pyrolyzed under nitrogen atmosphere at temperatures between 500 and 600 ^{o}C. Then, they activated the chars obtained from pyrolysis experiments physically in the presence of steam at temperatures between 800 and 900 ^{o}C. A comparison of BET surface areas was carried out among the precursors by nitrogen adsorption studies. Pistachio nut shells had the highest BET values achieving 1300 m^2/g. Also, they emphasized that the production of activated carbon from pistachio nut shells might be scaled-up in the future and the necessity of the further study on this material.

Lua and Yang (2004) in another study investigated the vacuum pyrolysis followed by carbon dioxide activation. During the pyrolysis of

pistachio nut shells in the reactor, 10 °C/min heating rate was maintained until the selected temperature was attained and hold 2 h at that temperature. They selected a temperature interval from 350 to 1000 °C during pyrolysis to investigate the temperature effect on pore characteristics. After cooling down the chars they heated them again to 900 °C and at this temperature by replacing nitrogen flow by carbon dioxide they activated the chars for 30 min. Characterization of final products were done with nitrogen adsorption and SEM. BET surface area and micropore volume with the surface morphology were largely changeable depending on the pyrolysis temperature. They concluded that pistachio-nut shells can be a promising raw material for the activated carbon production but effects of pyrolysis temperature on pore characteristics should be considered carefully.

Yang and Lua (2003; a) attempted to establish a relationship between preparation and process parameters to obtain optimum conditions for activated carbon production from pistachio nut shells. They produced activated carbon by chemical activation with potassium hydroxide and investigated the effects of impregnation ratio, activation temperature and holding time on the characteristics of activated carbons. Besides, they used two different methods; impregnation of raw shells with potassium hydroxide and impregnation of chars obtained from carbonization step with potassium hydroxide. After the analyses of data obtained from the experiments, they stated the best conditions as follows; an impregnation ratio of 0.5 (potassium hydroxide/shells), an activation temperature of 800 °C and a holding time of 3 h. Also, they concluded that impregnation of char with potassium hydroxide resulted in production of an activated carbon in granular form, on the other hand, impregnation of shells directly with potassium hydroxide produced powdered activated carbon.

A study of Yang and Lua (2003; b) two different physical activation methods with carbon dioxide was performed after the pyrolysis of the pistachio-nut shells under nitrogen atmosphere and at 500 °C. In

the first method, they supplied carbon dioxide gas to the reactor only at the carbonization temperature. Apart from the first method, they also supplied carbon dioxide during the heat increase from 500 ^{o}C to the activation temperature. They investigated effects of CO_2 flow rate, heating rate, activation temperature and activation holding time during the experiments. They obtained maximum BET surface area as 1064 m^2/g at an activation temperature of 800 ^{o}C, dwell time 2.5 h, CO_2 flow rate 100 cm^3/min and a heating rate of 10 ^{o}C/min by supplying a continuous CO_2 flow to the reactor at the heating step of chars after pyrolysis. Furthermore, observations of microstructures with SEM and functional groups with FTIR were done and they concluded that, a decrease in oxygen groups, aromatization of the structure and pore development had occurred during carbonization and activation processes.

A comprehensive study was carried out by Wu et al. (2005) to compare chemically activated carbon produced with potassium hydroxide and physically activated carbons produced with steam from pistachio nut shells. After the carbonization of pistachio-nut shells under nitrogen atmosphere at 500 ^{o}C with a heating rate of 5 ^{o}C/min, they did steam activation at 830 ^{o}C. Also, by impregnating chars with potassium hydroxide in four different ratios (KOH/char = 0.5, 1, 2 and 3), they performed the chemical activation of chars at 780 ^{o}C. BET surface area values of activated carbons were found between 731 and 1687 m^2/g by N_2 adsorption. They stated that the highest value of BET surface area was obtained with potassium hydroxide activation with an impregnation ratio of 3. Then they carried out adsorption experiments to determine equilibrium and kinetics. For this purpose, adsorption of methylene blue, basic brown 1, acid blue 74, 2,4-dichlorophenol, 4-chlorophenol and phenol from water at 30 ^{o}C was done and it was showed that adsorption of organics depends not only on BET surface area of adsorbent but also affected by relative size between adsorbate molecules and pores.

In another study of Lua and Yang (2005) , pistachio nut shell based activated carbon was produced with zinc chloride activation and

effects of activation conditions both under the nitrogen atmosphere and under vacuum were investigated. To optimize process conditions, they observed the influences of impregnation ratio, activation temperature and activation holding time. For this purpose, they impregnated raw shells with $ZnCl_2$ at different ratios from 0.2 to 1.6 ($ZnCl_2$ / shells) and heated under nitrogen atmosphere at a rate of 10 ^oC/min to the final activation temperature. They studied at a temperature interval from 350 to 800 ^oC. At the end of the analysis the textural properties of porous carbons produced, the optimum conditions for prepearing microporous activated carbons from pistachio nut shells with $ZnCl_2$ was stated. An activation temperature of 400 ^oC, an activation holding time of 1 h and an impregnation ratio of 0.75 was the optimum point. Also, activation under vacuum resulted in better pore development. And, the highest BET surface area was attained at an impregnation ratio of 1.5, an activation temperature of 500 ^oC and a heating rate of 2 h as 2257 m^2/g

In another investigation, Yang and Lua (2006) produced chemically activated carbon with zinc chloride. For this purpose they impregnated pistachio nut shells with a ratio of 0.75 ($ZnCl_2$ /shells) and then activated both under the nitrogen atmosphere and in the vacuum for 2 h. For both methods, the temperature range between was 350 to 800 ^oC. They used a combination of methods including nitrogen adsorption, thermogravimetry, pycnometry, FTIR, SEM and XRD for the characterization of the products. Results showed that under vacuum, porosity development was slightly better than under nitrogen atmosphere. There was an apparent evidence that the lower temperatures were useful for the development of a porous texture with zinc chloride activation. This was explained as too high temperatures causing shrinkage of the carbon structure due to the volatiles evolved from the structure. XRD results showed that mostly amorphous structure occurred in the activated carbons, but at the elevated temperatures crystalline carbon structures began to form. FTIR provided a basis for an understanding of the structural changes occurred during impregnation

and activation. Aromatization of the carbon skeleton occurred and aromatic rings degraded according to the observations in the functional groups.

Apaydın-Varol et al. (2007) investigated slow pyrolysis of pistachio nut shell. A relationship between product yield distribution and temperature was attempted to be established. They conducted their experiments at atmospheric pressure and at 300, 400, 500, 550 and 700 ^{o}C with a heating rate of 7 ^{o}C/min. According to the results, they maximized char yield at 300 ^{o}C and bio-oil at a temperature nearly 550 ^{o}C. Yield of the char was decreased 28% to 23% with increasing temperature from 300 to 700 ^{o}C. The characterization of char with FTIR, SEM and bio-oil with FTIR, GC-MS, column chromotography was performed. Also, they calculated calorific value of char and bio-oil using Du Long's Formula with data obtained from the elemental analysis. In conclusion, they stated that both bio-oil and char obtained from the pyrolysis of pistachio nut shell had higher calorific value than the parent biomass, that's why they can be ultilized as alternative fuel or chemical feedstocks. Besides, they emphasized high carbon content of char and surface morphology changes that resulted in slight porosity on the surface.

Attia et al. (2003) prepeared activated carbon from pistachio-nut shells by phosphoric acid activation. They used 50 wt. % phosphoric acid in impregnation step and investigated the acid soaking time as 24 and 72 h. The selected activation temperature and activation holding time during research was 500 ^{o}C and 2h, respectively. Long impregnation period resulted in higher BET surface area value as 1456 m^2/g. After producing activated carbons, they carried out adsorption studies of two types dyes (methylene blue and rhodamine B) and two types of phenolics (phenol and p-nitrophenol) in batch experiments and calculated adsorption capacities of these molecules from aqueous solutions.

Kaghazchi et al. (2010) produced activated carbon from a mixture of pistachio-nut shell and licorice by chemical activation method with zinc chloride and phosphoric acid. They investigated effects of impregnation ratio, activation temprerature, activation holding time and mixing of raw materials on the final activated carbon characteristics. They heated biomass mixtures relativeley low heating rate as 2.5 ^{o}C/min during experiments. Besides they used Taguchi method in the design of experiments and determined optimum conditions to produce activated carbon. After production of activated carbons they characterized them with N_2 adsorption, SEM analysis, iodine adsorption and determined BET surface areas, iodine numbers and surface functional groups. The highest BET surface area was obtained in the case of zinc chloride activation as 1492 m^2/g. The optimum condition was stated in the case of licorice amount in the mixture was 70% with an impregnation ratio 2/1, holding time 1 h and activation temperature 600 ^{o}C.

CHAPTER III

EXPERIMENTAL WORK

3.1 PREPARATION OF RAW MATERIAL

All the experiments were carried out with the pistachio-nut shells obtained from the Gaziantep, Turkey in large amounts (about 2 kg). The shells were used on as-received basis and no physical or chemical pretreatments like drying, washing with chemicals, that would cause structural changes to the material were carried out before the experiments.

The shells were ground for size reduction and sieved mechanically. Particles having sizes between 10 and 18 mesh (or 1-2 mm) were used throughout the experiments. All the ground and sieved samples were kept at the room temperature in a sealed box.

The proximate analyses of the shells were performed according to the ASTM standards (E871, E872 and D1102) and moisture, volatile and ash contents of the shells as determined are given in Table 3.1.

Table 3.1 Proximate Analyses of Pistachio-Nut Shells

Ash Content	0.94 %
Moisture Content	7.40 %
Volatile Matter Content	77.44 %
Fixed Carbon Content	14.22 %

Elemental analysis (carbon, hydrogen, nitrogen and sulphur contents) determined by using an elemental analyzer (CHNS-932, LECO Corporation) is given in Table 3.2.

Table 3.2 Elemental Composition of Pistachio-Nut Shells

Carbon	46.3 % (wt.)
Hydrogen	6.21 (wt.)
Nitrogen	0.201 %(wt.)
Sulphur	Not detectable

3.2 PROPERTIES OF ACTIVATION AGENTS

An ortho-phosphoric acid produced by J.T. Baker with an 85 wt.% H_3PO_4 was used in experiments by diluting it to 50 wt.%.

A set of experiments were carried out with potassium hydroxide to observe the effects of activation reagent on pore development. For this purpose potassium hydroxide pellets (J.T Baker) were used.

3.3 CARBONIZATION AND ACTIVATION EXPERIMENTS

To obtain activated carbon from the pistachio nut shells two different methods were followed.

In the first method, raw material was directly impregnated with phosphoric acid. Ground and sieved pistachio nut shells were treated with 50 % (wt.) phosphoric acid solution at room temperature in three different weight ratios as 1:1, 2:1 and 3:1 (H_3PO_4 : shells). Continuous mixing of the shells with the phosphoric acid solution for 24 hours was maintained by using a magnetic stirrer. After mixing, solution was allowed to dry at the room temperature for 3 days. After this period, shells were ready for the carbonization and activation which were carried out simultaneously.

On the other hand, another set of experiments were done in the following way: The shells were heated under a continuous nitrogen flow to 500 ^{o}C with a heating rate of 10^{o}C/min and held at this temperature for 1 hour. After cooling down the system, the remaining carbonized solid product or char, was taken and impregnated with phosphoric acid in the same ratios which was done in the first method, i.e., phosphoric acid:char ratio was adjusted as 1:1, 2:1 and 3:1. As it was done in the first method, chars with the phosphoric acid solution was stirred for 24 hours and then dried at the room temperature for 3 days.

Both impregnated raw material and char followed the same steps after impregnation. For this purpose samples were heated from room temperature to the predetermined activation temperatures under nitrogen atmosphere with a heating rate of 10 ^{o}C/min and held at that temperature for 1 h. All the experimental constants were summarized in Table 3.3.

Table 3.3 Experimental Variables Which Were Kept Constants During the Work

Particle Size	10-18 mesh (or 1-2 mm)
Nitrogen Flow Rate	100 cm^3/min
Heating Rate	10 ^{o}C/min
Activation Holding Time	1 h

All the carbonization and activation experiments were conducted in a horizontal furnace, "Lenton Unit C2", which was electrically heated and well insulated. By adjusting the controller of the furnace heating rate, carbonization and activation temperatures were programmed. With the help of thermocouples temperature in the furnace was checked and verified. In the furnace, a quartz tube of 90 cm in length and 30 cm in diameter, was placed to hold the sample. The overall experimental set-up is shown in Figure 3.1.

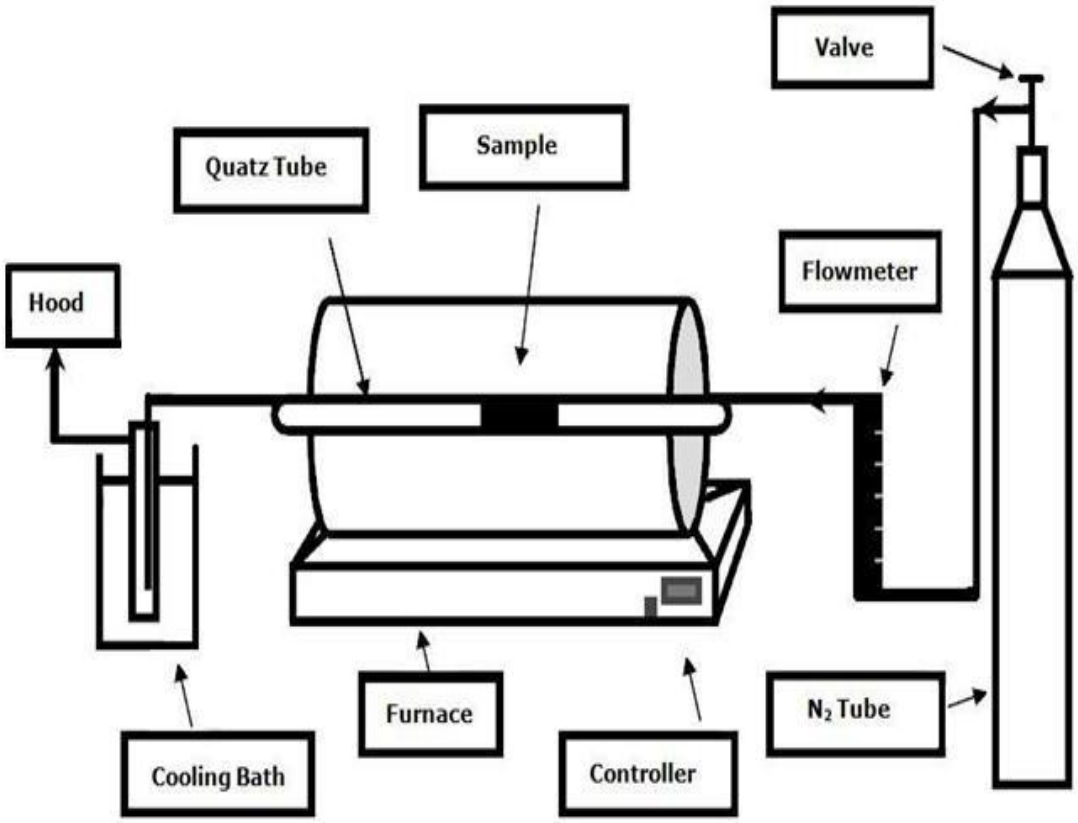

Figure 3.1 Experimental Set-up

The continuous nitrogen flow was supplied in the tube after an adjustment of volumetric flowrate by a flowmeter. The sample was put in the middle of the quartz tube to have a uniform temperature distribution. An oval quartz boat and a quartz rod were designed and adopted for the set-up for placing the sample in the reaction zone. The outlet gases were trapped in a cooling bath and the non-condensable gases were purged from the system. Trapped condensables and outlet gasses were not collected for further characterization of these products, only solid products obtained from the processes were characterized. During the study the term "product" refers to final solid product or activated carbon.

The products after heat treatment were allowed to cool down to room temperature and then washed with hot distilled water to remove

the excess chemicals. The pH was checked until it was stabilized and came closer to a neutral value. After filtering and drying the washed products in an oven at 100 ^{o}C for moisture removal, they were ready for the characterization tests. They were kept in sealed boxes and coded according to experimental conditions. The product codes are given in Table 3.4.

All the procedures applied during the production of activated carbons are also shown in the Figure 3.2 in the form of a flowchart.

Table 3.4 Experimental Variables and Sample Codes for Phosphoric Acid Activated Carbons

	Impregnation Ratio	**Temperature**	**Sample Code**
Raw Material Activation Method	1/1 (w/w) (H_3PO_4/shells)	300 ^{o}C	AAR-1-300
		500 ^{o}C	AAR-1-500
		700 ^{o}C	AAR-1-700
		900 ^{o}C	AAR-1-900
	2/1 (w/w) (H_3PO_4/shells)	300 ^{o}C	AAR-2-300
		500 ^{o}C	AAR-2-500
		700 ^{o}C	AAR-2-700
		900 ^{o}C	AAR-2-900
	3/1 (w/w) (H_3PO_4/char)	300 ^{o}C	AAR-3-300
		500 ^{o}C	AAR-3-500
		700 ^{o}C	AAR-3-700
		900 ^{o}C	AAR-3-900
Char Activation Method	1/1 (w/w) (H_3PO_4/char)	300 ^{o}C	AAC-1-300
		500 ^{o}C	AAC-1-500
		700 ^{o}C	AAC-1-700
		900 ^{o}C	AAC-1-900
	2/1 (w/w) (H_3PO_4/char)	300 ^{o}C	AAC-2-300
		500 ^{o}C	AAC-2-500
		700 ^{o}C	AAC-2-700
		900 ^{o}C	AAC-2-900
	3/1 (w/w) (H_3PO_4/char)	300 ^{o}C	AAC-3-300
		500 ^{o}C	AAC-3-500
		700 ^{o}C	AAC-3-700
		900 ^{o}C	AAC-3-900

Apart from the phosphoric acid activation, a set of experiments were conducted by activating chars with potassium hydroxide (KOH) with an impregnation ratio of 1:1 (wt. KOH: wt.char). After adding KOH pellets into the char, deionized water was added and the mixture was allowed to mix for 1 day and dried at the room temperature for 3 days, as it was done at the phosphoric acid activation experiments. Carbonization, activation, washing and drying steps after impregnation step were the same as for the char activation experiments with phosphoric acid.

Table 3.5 Experimental Variables and Sample Codes for Potassium Hydroxide Activated Carbons

	Impregnation Ratio	**Temperature**	**Sample Code**
Char Activation Method	1/1 (g char/g KOH)	300 °C	ABC-1-300
	1/1 (g char/g KOH)	500 °C	ABC-1-500
	1/1 (g char/g KOH)	700 °C	ABC-1-700
	1/1 (g char/g KOH)	900 °C	ABC-1-900

Thermal gravimetric analysis (TGA) were performed to identify the thermal behavior of raw pistachio shells, phosphoric acid impregnated shells and phosphoric acid impregnated chars. In TGA analysis, Shimadzu DTG-60H simultaneous DTA-TG apparatus in METU Chemical Engineering Department was used. TGA experiments were conducted at the same

experimental conditions with respect to carbonization and activation temperature, N_2 flow rate and heating rate.

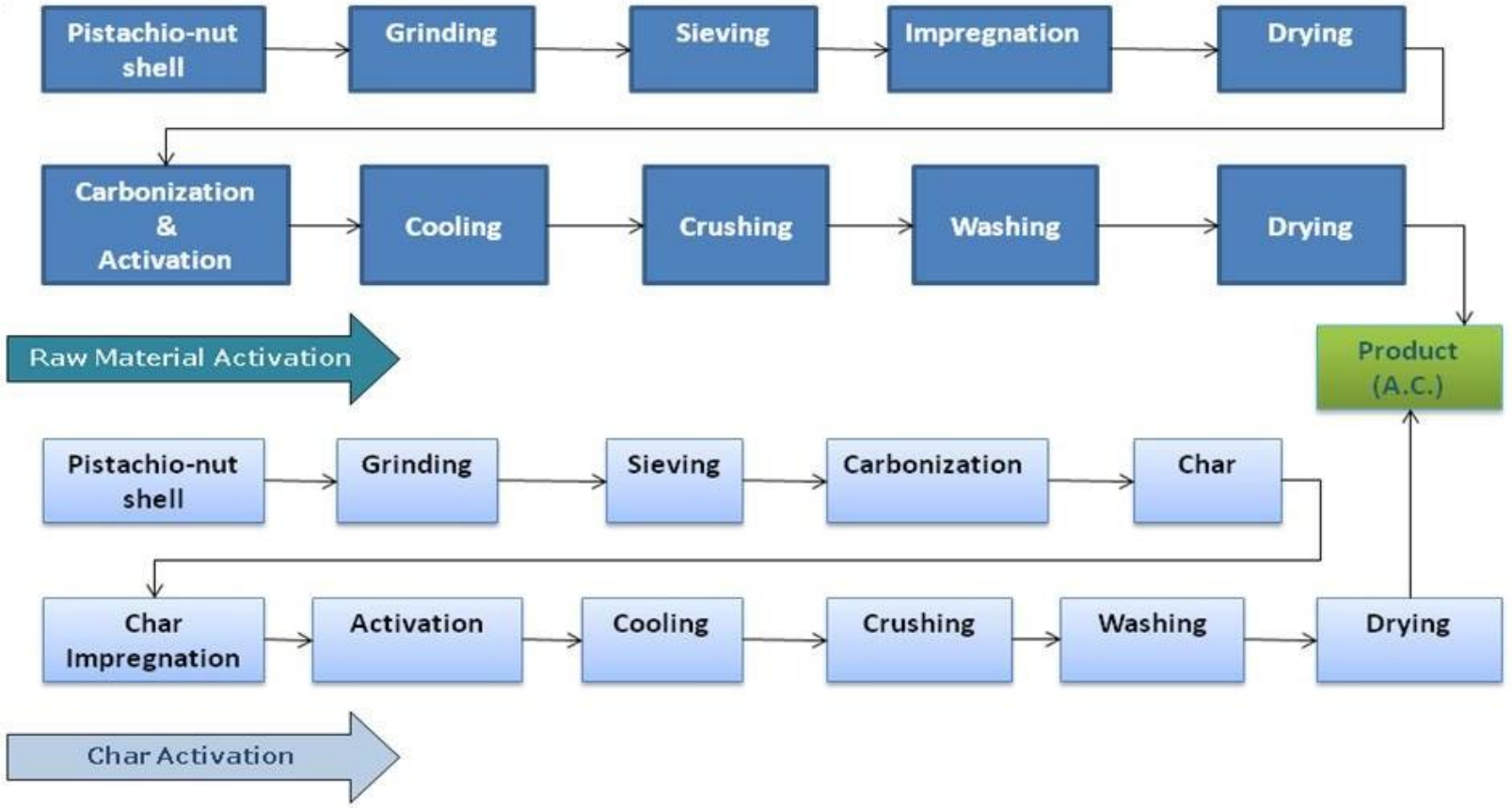

Figure 3.2 Procedures Followed During Raw Material Activation and Char Activation Experiments

3.4 CHARACTERIZATION OF THE PRODUCTS

Characterization of surface area and pore size distribution of the activated carbons were determined by nitrogen gas adsorption at -195.6 ^{o}C (77 K).

For this purpose, a commercial volumetric gas adsorption apparatus "Autosorb-6" manufactured by Quantachrome Corporation, located in METU Central Laboratory, was used.

Prior to nitrogen adsorption, samples were prepared on the degassing unit of the device for removal of water from the surface of the carbon. All the products were outgassed at 120 ^{o}C for 4 h, which would not result any structural changes on the samples. Photograph of the gas adsorption apparatus with the degassing unit is given in Figure 3.3

Figure 3.3 Surface Area and Pore Size Analyzer (Right) and Degassing Unit (Left)

Surface area and pore size analyzer, **"**Autosorb-6", has six analysis ports that have their own dewars and pressure sensor. This feature of device enables independent and concurrent analysis. The data accumulated through the adsorption process were available by the help of the software program of the device which allows applying comprehensive methods used in the pore analysis.

True density determination of the selected samples was done by a commercial pycnometer, "Ultrapycnometer 1000" which was manufactured by Quantachrome Corporation and located in METU Central Laboratory (Figure 3.4). The operating principle of this non-destructive device is based on Archimedes' principle of fluid displacement and gas expansion (Boyle's Law). Since there is a requirement of a fluid that can penetrate the finest pores of activated carbon, helium meets this condition with its small atomic size. Also, inertness of helium makes it preferable in the pycnometry method. Since true density is the ratio of the mass to the volume occupied by that mass, volume measured by pycnometer is the basis of true density calculations. But it should be taken into account that neither helium nor any other fluid is able to fill the all the pore volume of activated carbons in reality. Hence, the term of "true density" should be treated with this consideration.

Figure 3.4 Helium Pycnometer

To observe surface morphology of the selected activated carbons, raw material and phosphoric acid impregnated raw material scanning electron microscopy studies were done. By using "Quanta 400F Field Emission SEM" in METU Central Laboratory, microscopic structural changes were observed. Prior to the microscopy, samples were crushed and mixed with ethyl alcohol and this suspension was kept in ultrasonic water bath for 15 minutes for homogeneity of samples. After filtering the suspensions, the samples were dried at 105 ^{o}C and then they were coated with Au-Pd under vacuum.

Ash content of each produced activated carbon was determined, because lower ash content is desirable in activated carbons. For this purpose, each sample was heated at 120 ^{o}C in an oven to remove moisture and then the samples were ignited at 650 ^{o}C until achieving a constant weight and finally samples were cooled down and ash contents were calculated from the weight of the remaining ash.

Since pH of the activated carbons affects the adsorption performance, slurry pH values of each activated carbon sample were determined. This was done by adding 0.1 g activated carbon sample to 10 mL of deionized water and recording the pH of the slurry after 7 days at the room temperature.

Methylene blue numbers (MBN) of phosphoric acid activated carbons were determined to have an idea about decolorizing properties of activated carbons produced. To prepare stock solution of 213.9 mg/L, 0.25 g of Merck grade methylene blue trihydrate ($C_{16}H_{18}ClN_3S.3H_2O$) was mixed with 1 L of deionized water. Then 0.1 g of each produced activated carbon was added to 50 mL of methylene blue solution and mixed in water bath shaker at 120 rpm at the room temperature (nearly 25 ^{o}C) for 96 hours. After the attainment of equilibrium, solutions were filtered. Measurements of methylene blue concentration were done by a UV-Visible spectrophotometer (Hitachi UV-3200) at a wavelength of 600 nm. By assuming the area of methylene blue molecule as 1.62 nm^2

(Akgün,2005), surface areas of activated carbons which were occupied by methylene blue was calculated.

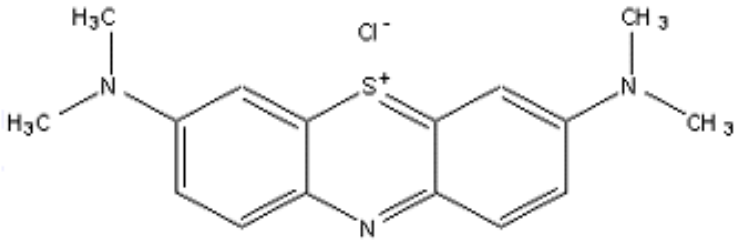

Figure 3.5 Chemical Structure of Methylene Blue

CHAPTER IV

RESULTS AND DISCUSSION

In this study, activated carbon production from pistachio-nut shells was investigated by the chemical activation method. Phosphoric acid and potassium hydroxide were used as activation agents and effects of impregnation ratio, activation temperature and activation method on the final activated carbon characteristics were explored.

4.1. THERMOGRAVIMETRIC ANALYSIS

The shape of TGA thermograms basically depends on the thermal behavior of the biomass which is related with chemical composition and chemical bonding of the structure. It should be considered that TGA can be used as a primary data for activated carbon production.

Figure 4.1 shows the effect of temperature on the residual weight percent of the raw pistachio nut shells. The thermogram of pistachio-nut shell shows that the thermal composition of material starts to be noticeable after about 150 ^{o}C. Weight loss observed prior to 150 ^{o}C corresponds to moisture content of raw material and was found as 6.95 %. After 150 ^{o}C, the main carbonization reactions started to dominate.

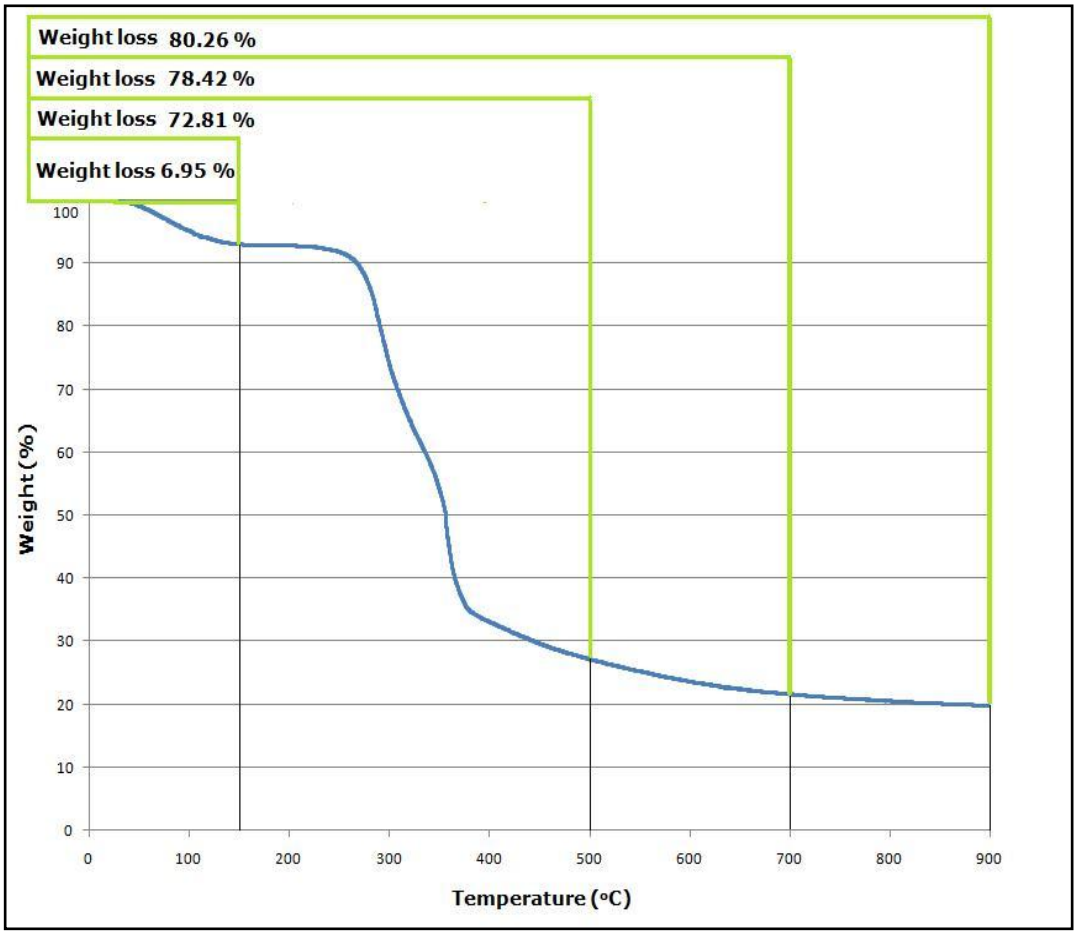

Figure 4.1 TGA Curve of Pistachio-nut Shells

The main constituents of lignocellulosic biomass degrade over a wide range of temperature. It is stated in the literature that hemicellulose degradation starts nearly at 200-260 °C and cellulose degradation occurs at around 240-350 °C. Since lignin is more thermostable than cellulose and hemicellulose, a temperature range of 280 to 800 °C was expressed for cellulose decomposition. But all of these temperature intervals are not the same for every lignocellulosic material. Also, inorganic constituents, minor extractives and their catalytic effects also have importance on the weight loss of biomass during pyrolysis (Gonzales et al., 2009).

Due to the decomposition of the main components of the pistachio-nut shells and removal of the gaseous volatile matter from the structure,

a significant weight loss was observed between 200 and 500 °C. At 500 °C, the shells lost 72.81 % of their weight. At approximately 700 °C, degradation of the lignocellulosic structure was nearly completed.

In the char activation experiments 500 °C was selected as pre-carbonization temperature to obtain chars. Despite the increase in temperature from 500 to 900 °C, weight loss was not as large as it had been at a temperature range from room temperature to 500 °C.

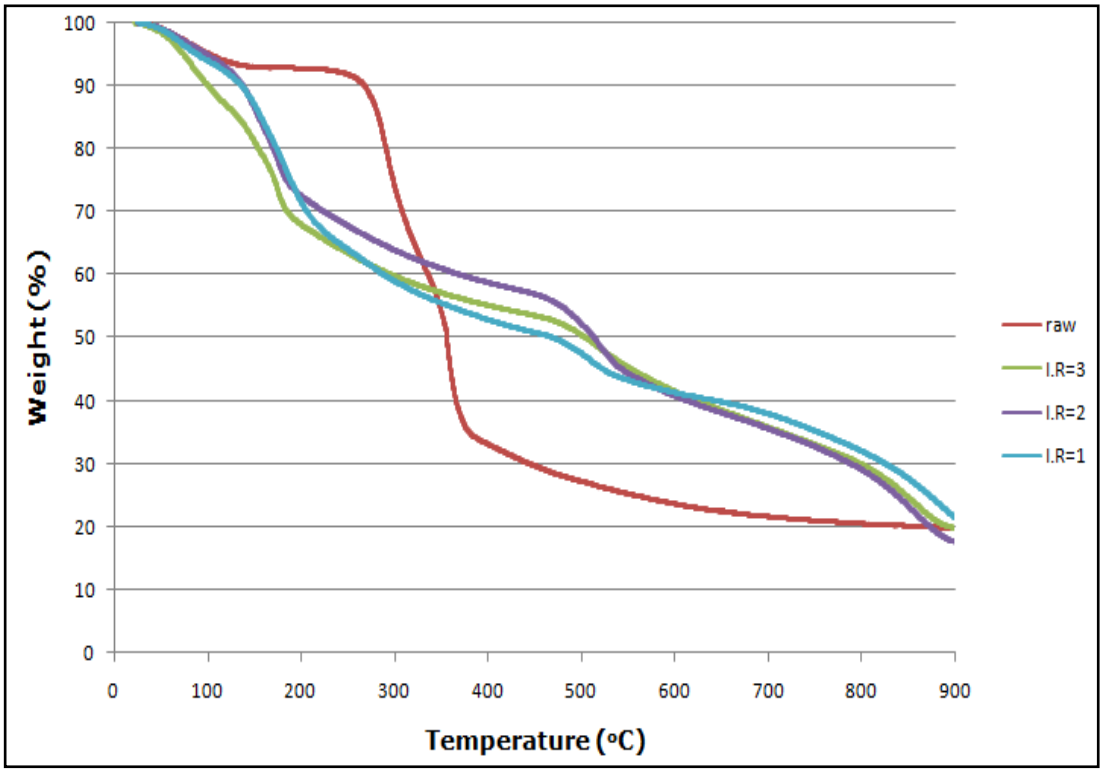

Figure 4.2 TGA Curves of Phosphoric Acid Impregnated Pistachio-nut Shells

Since it has been difficult to determine the product yields accurately from the experiments carried out with the experimental set-up described in Section 3.3., TGA analysis was used in the determination of activated carbon yields. For all the TGA experiments, the same

experimental conditions of experimental set-up such as heating rate, N_2 flow rate, temperature were maintained on the TGA device.

Yield values of raw shells and phosphoric acid impregnated shells for different temperatures and impregnation ratios are presented Table F.1, Table F.2 and Table F.3 in Appendix F. These yield values denoted the weight percentage of produced activated carbon to raw pistachio-nut shells.

It was seen from TGA curves of phosphoric acid impregnated samples (Figure 4.2) that, yield values of phosphoric acid impregnated pistachio-nut shells are higher than the yield of untreated shells and this result arose from the tar restriction behavior of phosphoric acid. Due to restriction of tar formation during pyrolysis, volatiles could not evolve so much and this caused higher yields which was an advantage of chemical activation by phosphoric acid.

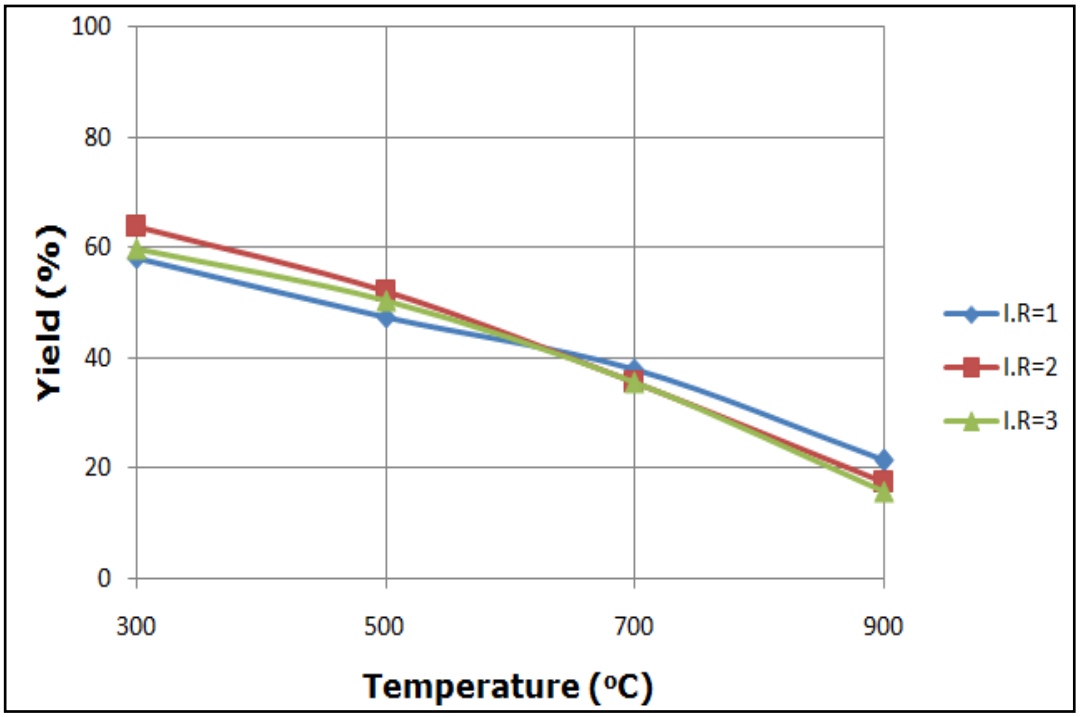

Figure 4.3 Yields of Phosphoric Acid Activated Carbons (Raw Material Activation Method)

When the effect of impregnation ratio at a given activation temperature on the product yield was investigated, it was seen that from Figure 4.3. that there was no direct relationship between the yield of activated carbon and impregnation ratio. Up to a temperature of 600 ^{o}C, slightly higher yields were attained at an impregnation ratio of 2/1 (g phosphoric acid/ g pistachio-nut shells). Above that temperature yields of shells that were impregnated at a ratio of 1/1 were slightly higher. But at all impregnation ratios, yields did not change significantly. Thus, it was clear that the main parameter affecting product yield was activation temperature which effects mass loss during process.

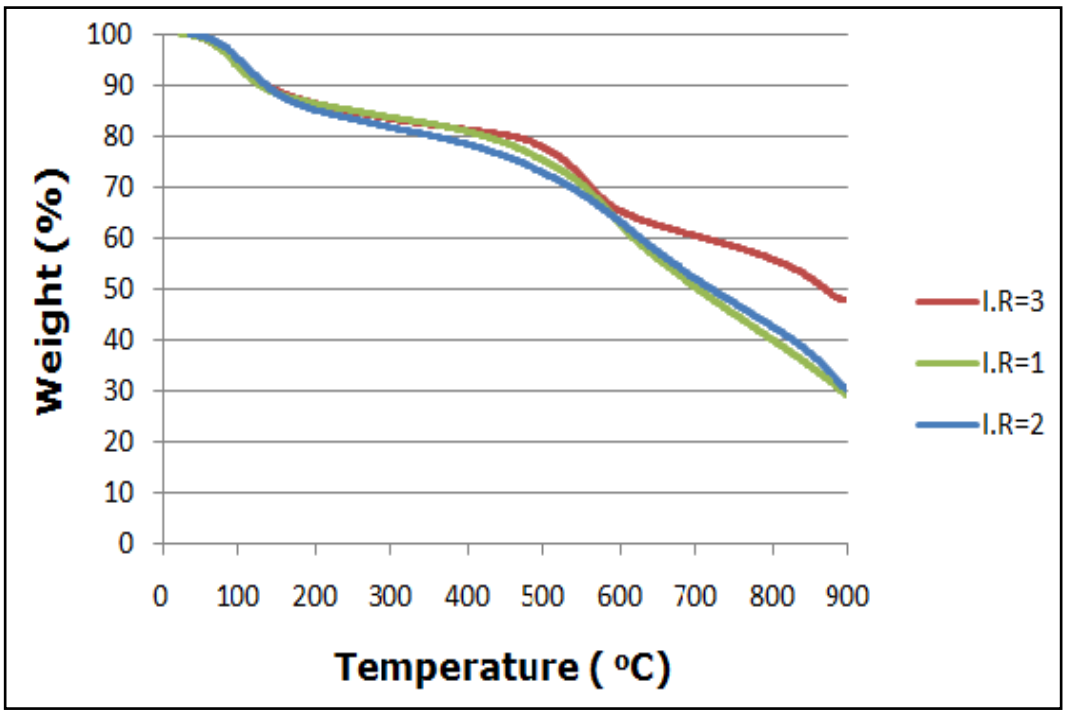

Figure 4.4 TGA Curves of Phosphoric Acid Impregnated Chars

In the char activation experiments, yield values were found to be lower than the other method since about 27 % of the raw material was converted to char and this char was exposed to an additional heat treatment after an impregnation with phosphoric acid. The yield values of

char activation experiments obtained from TGA analysis are given in Table F.4 in Appendix F. Char based yield is weight percentage of activated product to carbonized material. Raw material yield is weight percentage of activated carbon product to untreated pistachio-nut shells.

TGA curves of impregnated chars was given in Figure 4.4, and it was clearly seen that phosphoric acid changed the thermal behaviour of carbonized product as it changed the thermal behaviour of raw material. The changes in thermal behaviour can be clearly observed by investigating the curves of impregnation ratio of 1/1 (I.R=1) and impregnation ratio of 3/1 (I.R=3)

TGA curves of all acid impregnated shells and acid impregnated chars were given in Appendix F.

4.3 NITROGEN GAS ADSORPTION MEASUREMENTS

For physical characterization of the products, nitrogen adsorption was carried out and BET surface areas and pore size distributions were determined.

4.3.1 BET Surface Area Values of the Products

BET surface area values of activated carbons produced by phosphoric acid treatment of raw of pistachio-nut shells were given in Figure 4.5 and 4.6.

It was seen that activated carbon production by this reagent was an effective way to produce porous carbon with high BET surface areas.

The highest BET surface area was obtained by an impregnation ratio of 3/1 and at an activation temperature of 500 ^{o}C (Sample code: AAR-3.0-500). The BET value obtained for this activated carbon was 1640 m^2/g. If a comparison was done among BET surface area values of

activated carbons produced from pistachio-nut shells which were available in the literature, this maximum value achieved in this study seemed to one of the best results obtained up to now with this precursor.

In the literature BET surface area values of pistachio-nut shell based activated carbons, which were obtained by physical activation method, were approximately between 600 and 1300 m^2/g (Kazemipour et al. , 2007; Lua et al.,2004; Schröder et al., 2007; Yang and Lua, 2003;a,b). Considering these values chemical activation method with phosphoric acid yields better results than physical activation methods.

On the other hand, Lua and Yang (2005) prepared activated carbon from pistachio-nut shells with a surface area greater than 2500 m^2/g with zinc chloride activation. However, zinc chloride has not been preferred in chemical activation and has been replaced by phosphoric acid in recent years due to the environmental concerns (Bandosz, 2005).

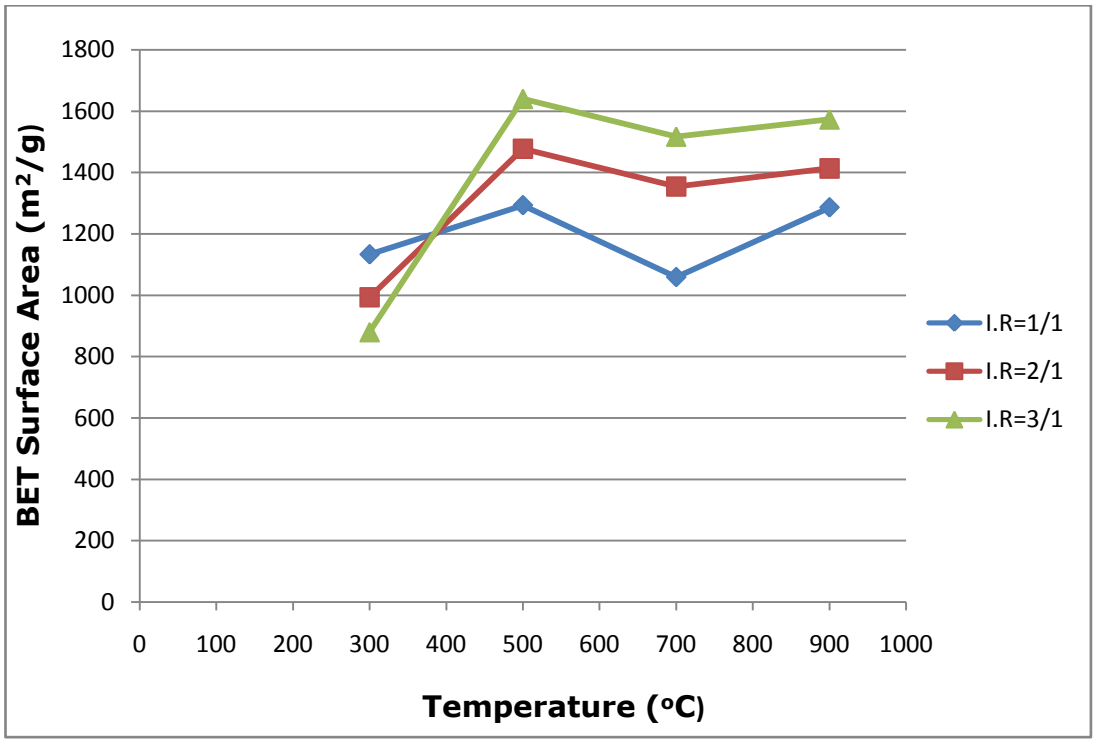

Figure 4.5 Effect of Activation Temperature on BET Surface Areas of Phosphoric Acid Activated Carbons (Raw Material Activation)

There is only one study done with pistachio-nut shells by phosphoric acid activation, and in that study Attia et al. (2003) produced activated carbons which had a maximum BET surface area of 1436 m^2/g at 500 ^oC. The main difference in their study was impregnation ratio, they used 1.44 (wt./wt.) as an impregnation value.

There was an increasing trend in BET surface area values up to 500 ^oC. After this temperature there is a decrease BET surface areas down to 700 ^oC. It can be explained that increasing temperature up to 500 ^oC caused mass loss that creates voids between carbon matrix. By increasing temperature from 500 ^oC to the 700 ^oC, existing pores in the structure were widened and thus a decrease in BET surface area values was observed. This could be because of the gasification reactions which might have destroyed some of the microporous structure by breaking down of micropores formed at lower temperatures. An interesting trend was observed between 700 and 900 ^oC, by increasing temperature BET surface area values were increased too.

The variations of BET surface areas with impregnation ratio are shown in Figure 4.6. As the impregnation ratio increased, BET surface areas increased at all temperatures except 300 ^oC. Girgis and El-Hendawy (2002) stated that at lower temperatures, impregnation ratios were hardly effective on pore development. Also, they expressed that effect of impregnation ratio can be noticed above 500 ^oC and according to Figure 4.10, after 500 ^oC, impregnation ratio effects pore development.

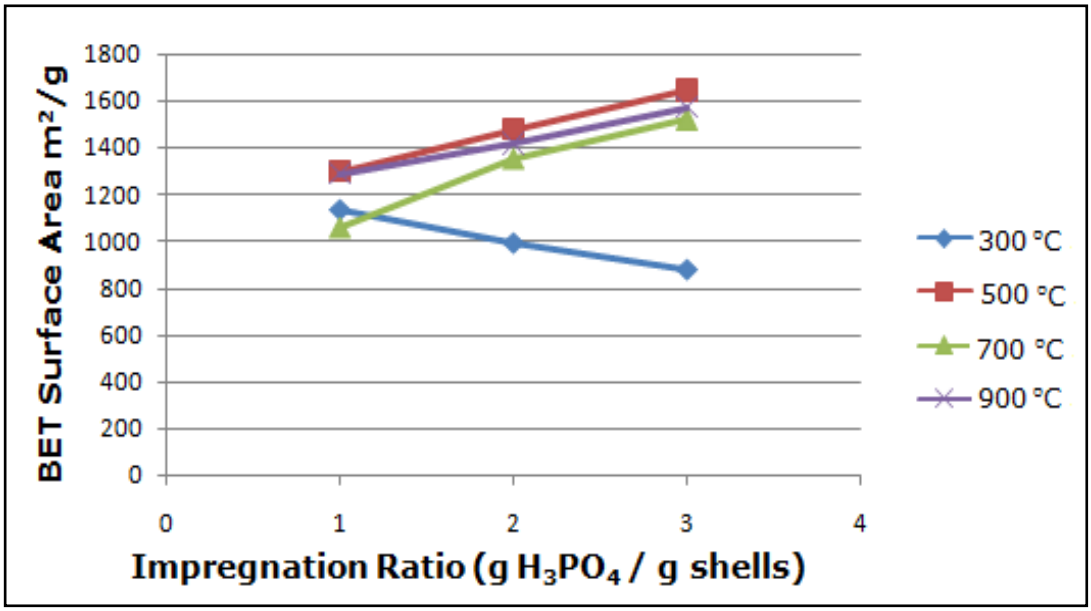

Figure 4.6 Effect of Impegnation Ratio on BET Surface Areas of Phosphoric Acid Activated Carbons (Raw Material Activation)

It is stated in the literature that increasing amount of phosphoric acid causes the action of activation agent by two ways. The first one is that as phosphoric acid amout increases, the aggressive physico-chemical effect on precursor material increases too. The second action of phosphoric acid is that it causes an increase on the porosity by preventing shrinkage or breaking down of the structure by occupying a volume inside and between the lignocellulosic structure. Following leaching process after heat treatment will leave behind free voids or pores and thus leading an increase in porosity (Girgis and El-Hendawy, 2002).

In this study, an optimum point for amount of activation agent was achieved by impregnating material with a ratio of 3/1 (g phosphoric acid / g raw material) in the raw material activation method with phosphoric acid. It is also predicted that additional phosphoric acid will still increase the BET surface area. But using too much phosphoric acid in the excess amount may cover the surface of the particle and thus inhibit the

activation process by preventing enough contact with the hot atmosphere.

The repeatability of the experiments was checked by doing raw material activation experiments twice at the same conditions. The BET surface area values of repeated experiments were given in Appendix G.

In the char activation experiments with phosphoric acid lower BET surface area values were obtained and these are given in Table 4.1.

Table 4.1 BET Surface Areas of Phosphoric Acid Activated Carbons (Char Activation)

Activated Carbon	**BET Surface Area (m^2/g)**
AAC-1-300	212
AAC-1-500	126
AAC-1-700	151
AAC-1-900	163
AAC-3-300	41
AAC-3-500	61
AAC-3-700	140
AAC-3-900	353

For char activation experiments which were carried out with phosphoric acid, a regular trend with respect to temperature and impregnation ratio could not observed. Besides, the produced activated carbons were all mesoporous in nature. The highest BET surface area was obtained with this method was 353 m^2/g and this carbon was produced at an activation temperature of 900 ^oC by impregnation the char at a ratio of 3/1 (g H_3PO_4 / g char).

To compare the effects of different chemical agents in char activation method, a set of experiments were performed with potassium hydroxide and BET surface area values of products were given in Table 4.2.

Table 4.2 BET Surface Areas of Potassium Hydroxide Activated Carbons (Char Activation)

Activated Carbon	**BET Surface Area (m^2/g)**
ABC-1-300	111
ABC-1-500	533
ABC-1-700	1000
ABC-1-900	1229

The BET surface area values of KOH activated carbons produced by char activation method increased with the activation temperature. This indicated that potassium hydroxide was effective in pore development at higher temperatures.

Since potassium hydroxide acts different to that of phosphoric acid, the pore development occurred differently from expected. Before the char activation experiments most of the volatiles were removed by carbonization and then activation process was carried out with an additional heat treatment. Potassium hydroxide behaved as a good activator at higher temperatures with char activation method and BET surface area values exceed 1000 m^2/g. As it can be seen in Figure 4.7 the char activation method is not promising with phosphoric acid but effective with potassium hydroxide at elevated temperatures. Bandosz (2006) stated that phosphoric acid activation should be applied to lignocellulosic materials. It is also stated that coal like materials could

hardly develop a porous structure with phosphoric acid. The char obtained from pyrolysis can be considered as a coal-like material, since carbonization step of biomass resembles coalification process because the biomass decomposes in an inert atmosphere by temperature. Marsh and Rodriguez-Reinoso (2006) also concluded that potassium hydroxide starts to react with the structure of the raw material at temperatures higher then 700 °C. Considering these comments BET surface area results seems more perceptible.

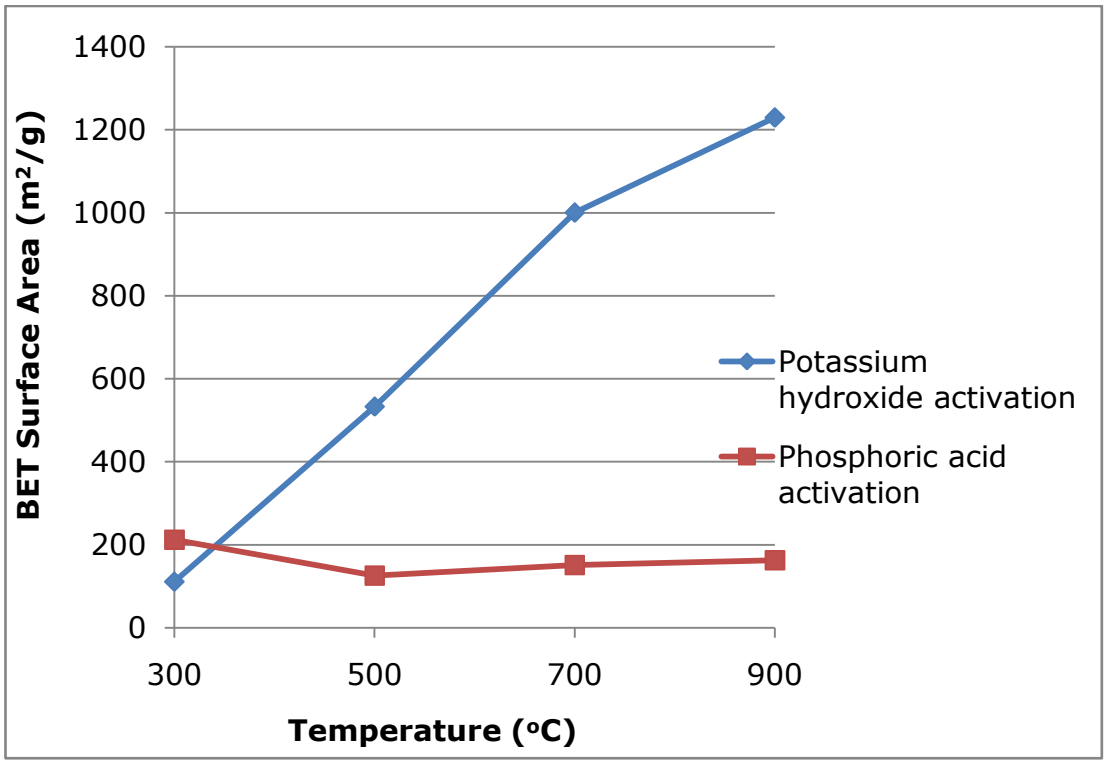

Figure 4.7 Effect of Chemical Agent on BET Surface Area [Char Activation Method with an Impregnation Ratio= 1/1 (g Activation Agent / g Char)]

Yang and Lua (2003) and Wu et al. (2005) prepared activated carbons from pistachio-nut shells by this char activation method by potassium hydroxide and achieved maximum BET surface areas values

between 1600 and 2200, approximately. The marked differences in preparation of their activated carbons were longer activation times (up to 2 h) , higher impregnation ratios (up to 4/1) and lower heating rates (down to 5 ^{o}C/min) than those in this study.

4.3.2 Nitrogen Adsorption Isotherms of the Products

Basis of constructing nitrogen adsorption isotherms is measuring the amount of adsorbed nitrogen on the activated carbon by allowing the activated carbons to come in contact with gradually increasing volumes of nitrogen and measuring the equilibrium pressures at constant temperature.

Nitrogen adsorption isotherms are used in the analysis of adsorption behavior and investigation of pore structure of a solid material and the general features of materials can be explained by the classification of these isotherm shapes.

In order to evaluate the effects of activation temperature, impregnation ratio and activation method on the pore characteristics of produced activated carbons, nitrogen adsorption isotherms of the selected products are presented in this section.

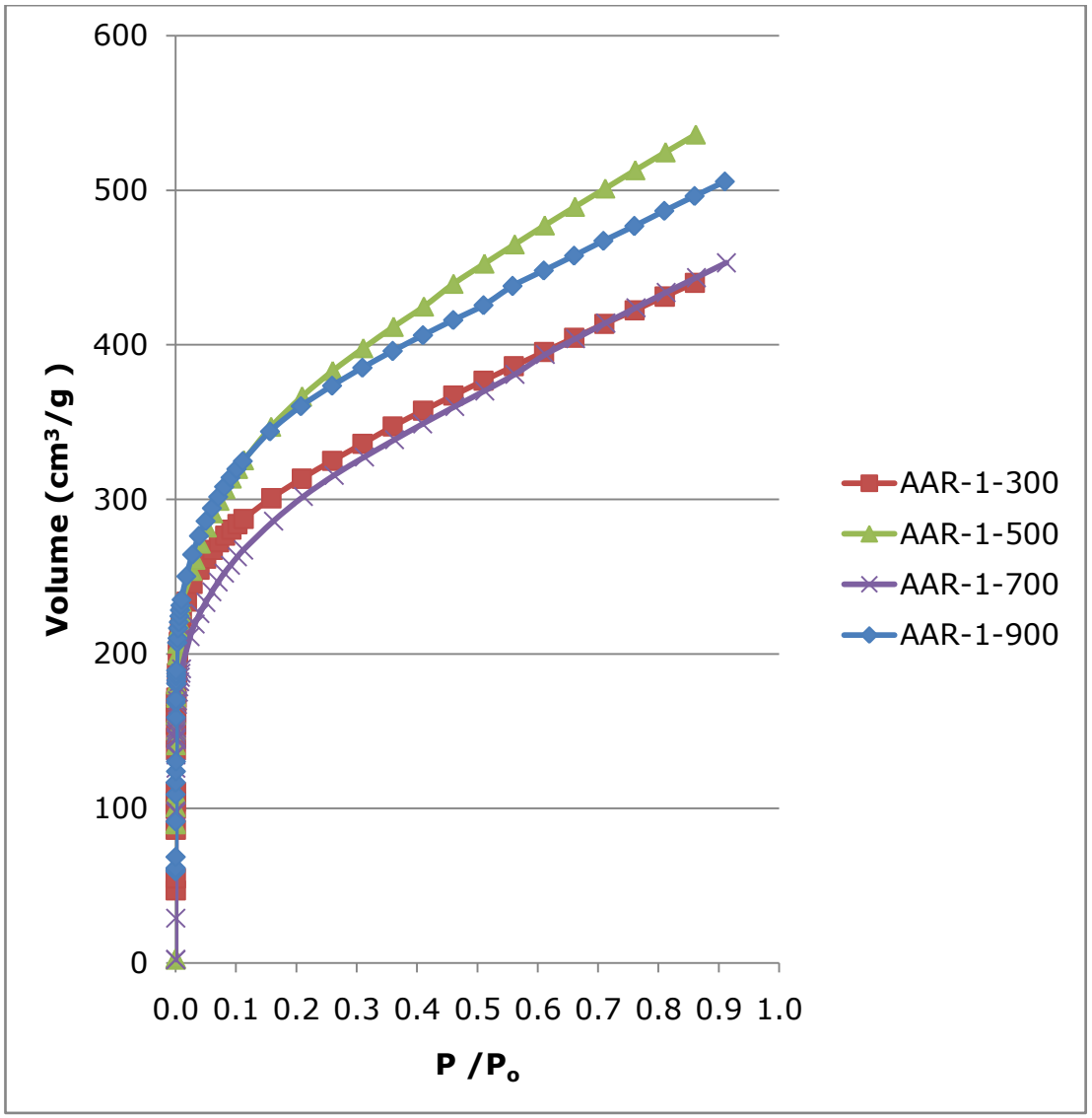

Figure 4.8 Temperature Effect on Nitrogen Adsorption Isotherms of Phosphoric Acid Activated Carbons (Raw Material Activation Method)

Figure 4.8 shows the comparison of activated carbons that were produced by the raw material activation method with phosphoric acid. In the low relative pressure region of the curves, high nitrogen uptakes were observed and the slopes of all curves decreased with increasing relative pressures.

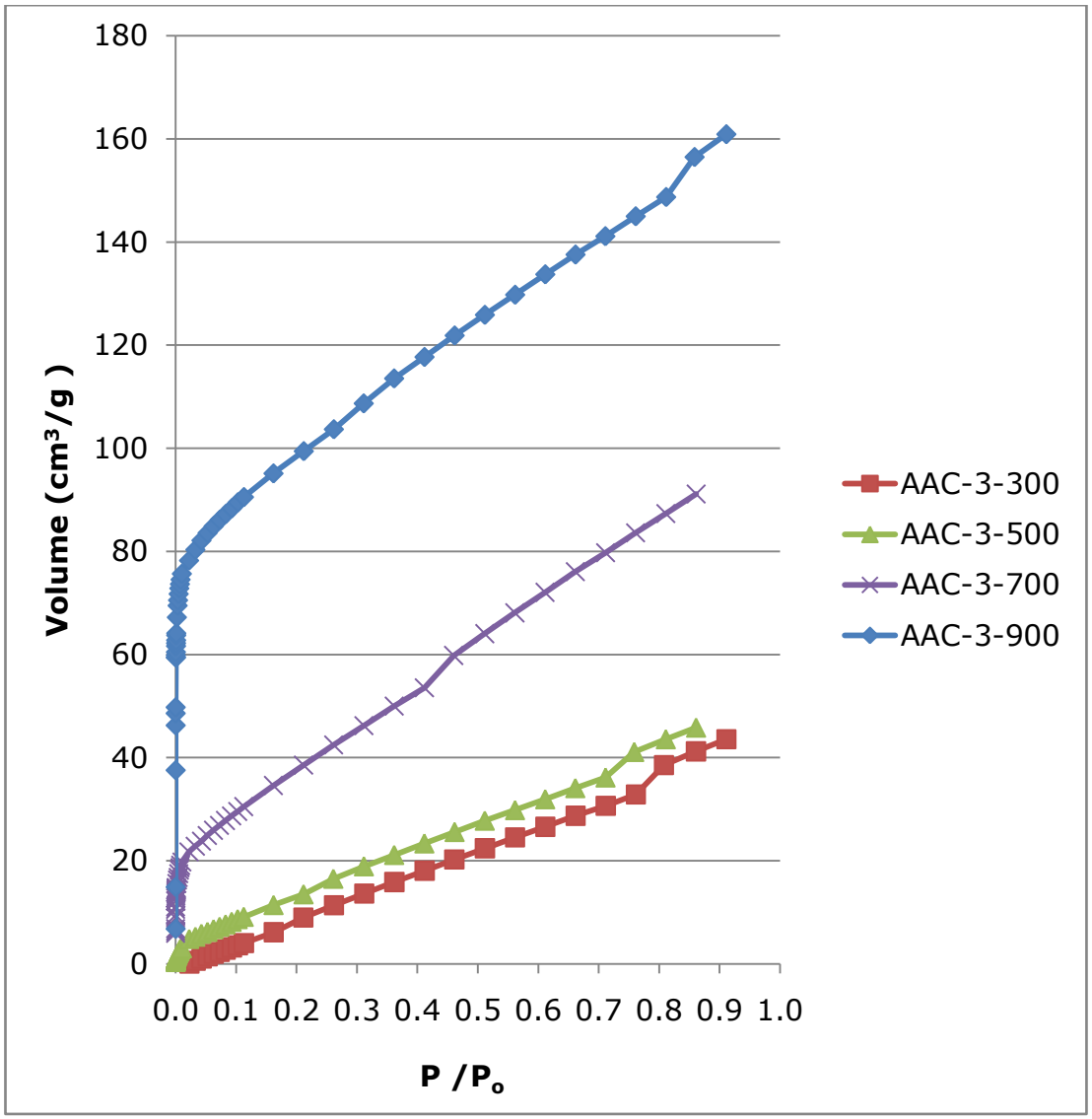

Figure 4.9 Temperature Effect on Nitrogen Adsorption Isotherms of Phosphoric Acid Activated Carbons (Char Activation Method)

As can be seen in the Figure 4.9 nitrogen adsorption isotherms of products by char activation method at different temperatures yielded relatively low adsorbed volumes that are characterized by low BET surface areas. Although isotherms showed strongly mesoporic behaviour, the sample with the highest activation temperature shows an increased amount of adsorption, together with a shift to the microporous structure.

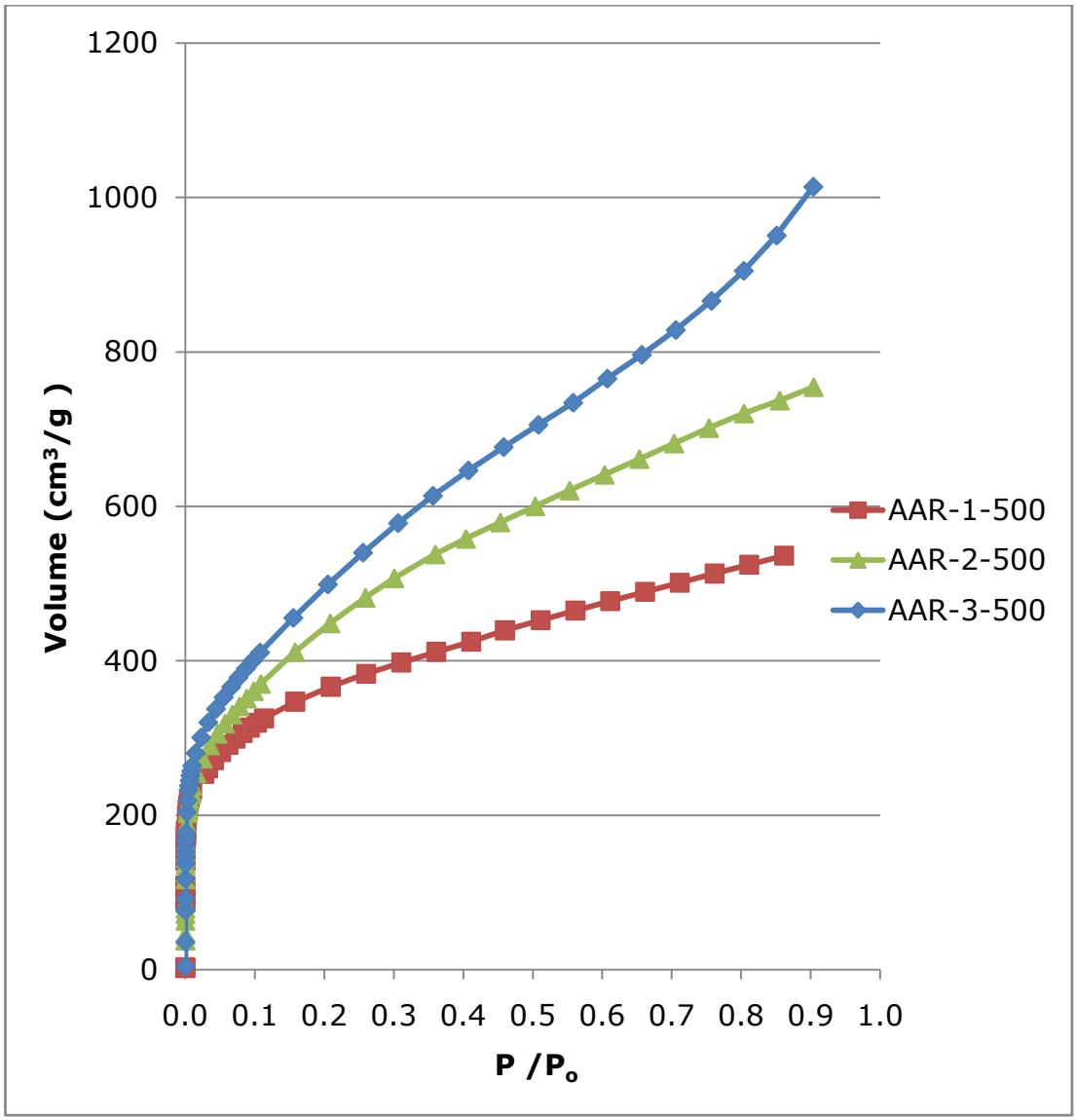

Figure 4.10 Effect of Impregnation Ratio on Nitrogen Adsorption Isotherms of Phosphoric Acid Activated Carbons (Raw Material Activation Method)

Figure 4.10 is useful in observing the effect of impregnation ratio on conventional raw material activation method with phosphoric acid. As the phosphoric acid amount was increased, the nitrogen uptake increased too. The slopes of all isotherms decreased with increasing relative pressures. Activated carbon produced with the highest impregnation ratio

(AAR-3-500) had the highest slope after a relative pressure value of 0.15, that can be considered as a qualitative interpretation of the mesopores.

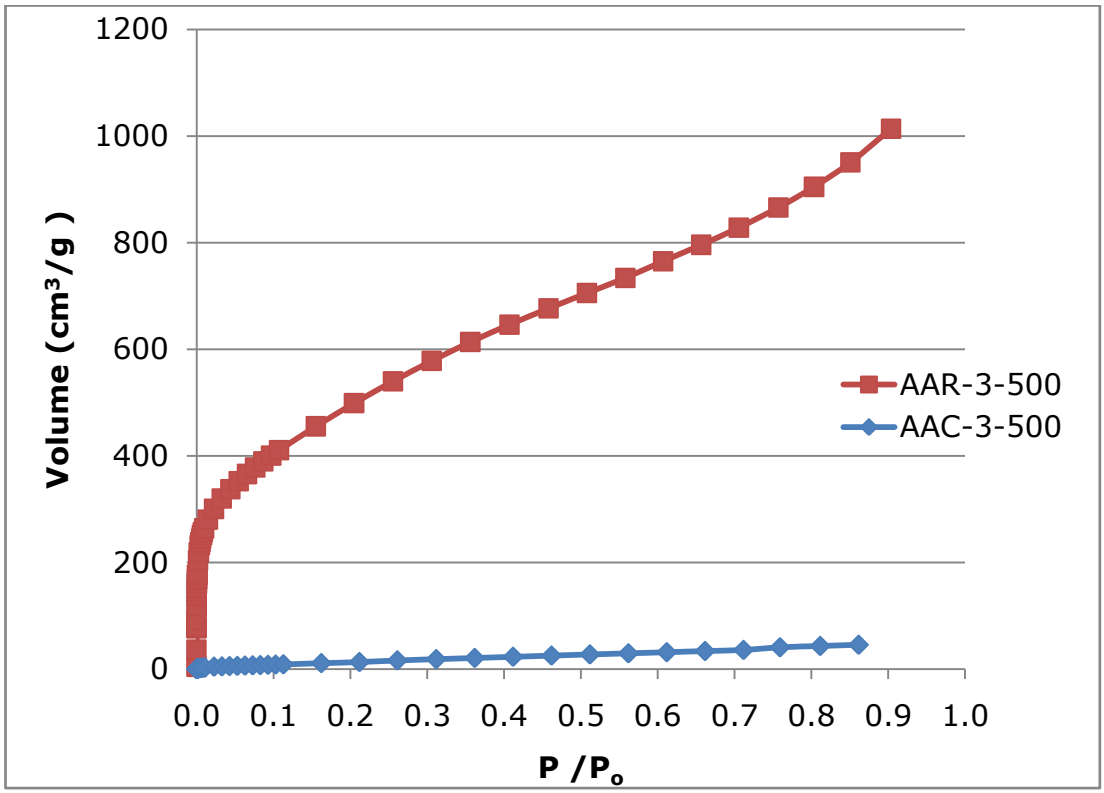

Figure 4.11 Comparison Between the Nitrogen Adsorption Isotherms of Raw Material Activation Method and Char Activation Method (Phosphoric Acid Activation)

An alternative method in producing activated carbons to chemical impregnation, namely char activation, was also tested and compared with raw material impregnation method. Nitrogen adsorption isotherms of these two methods are given in Figure 4.11. It can be observed that there is an enormous difference between the nitrogen adsorption capabilities of the activated carbons prepared by the char activation and the conventional raw material activation method. In addition, the

isotherm of activated carbon produced by raw material activation method showed a microporous trend on the other hand the char activation caused formation of larger pores.

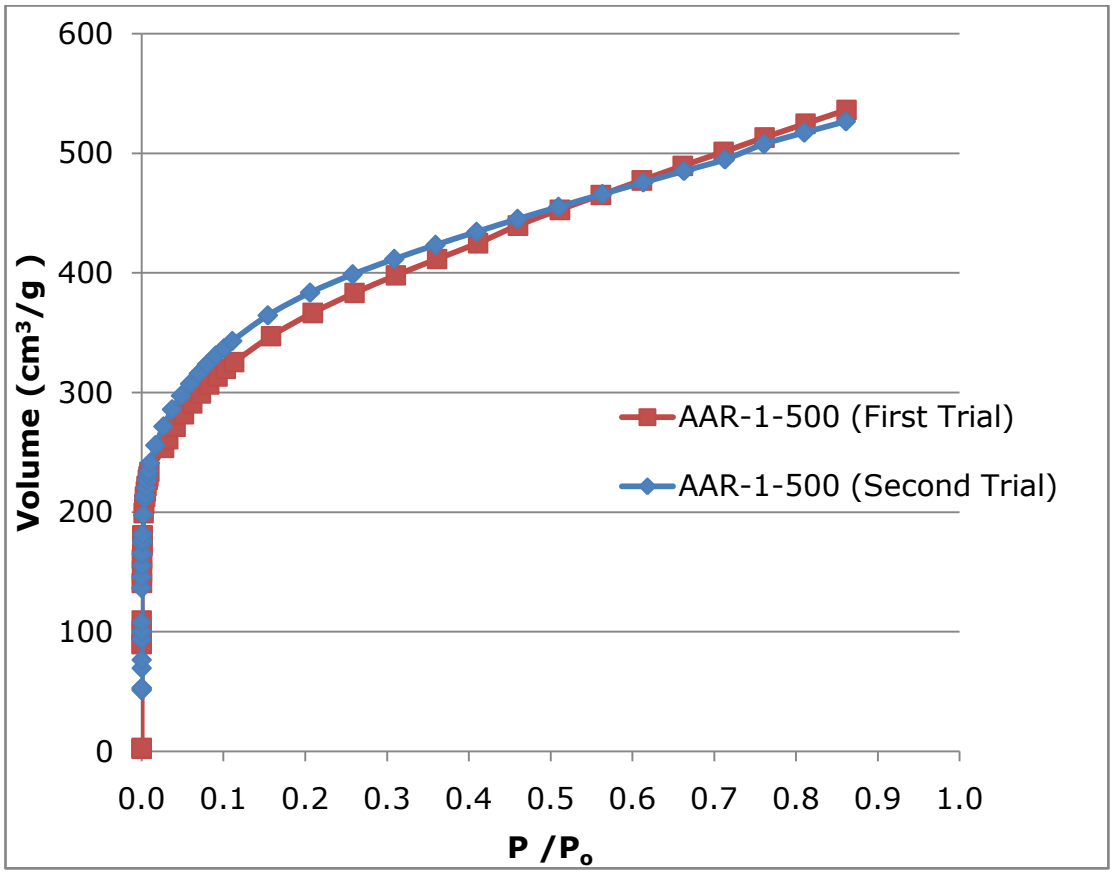

Figure 4.12 Nitrogen Adsorption Isotherms of AAR-1-500 to Test Repeatability

A randomly selected product, AAR-1-500 was used to check the repeatability of this set. In Figure 4.12 the blue line denotes the activated carbon sample produced at the first trial and the red line represents the second trial. The adsorption characteristics of these tests are very similar. Besides, the BET surface area values of these AAR-1-500 products are obtained as 1293 and 1383 m^2/g in the first and second trial, respectively.

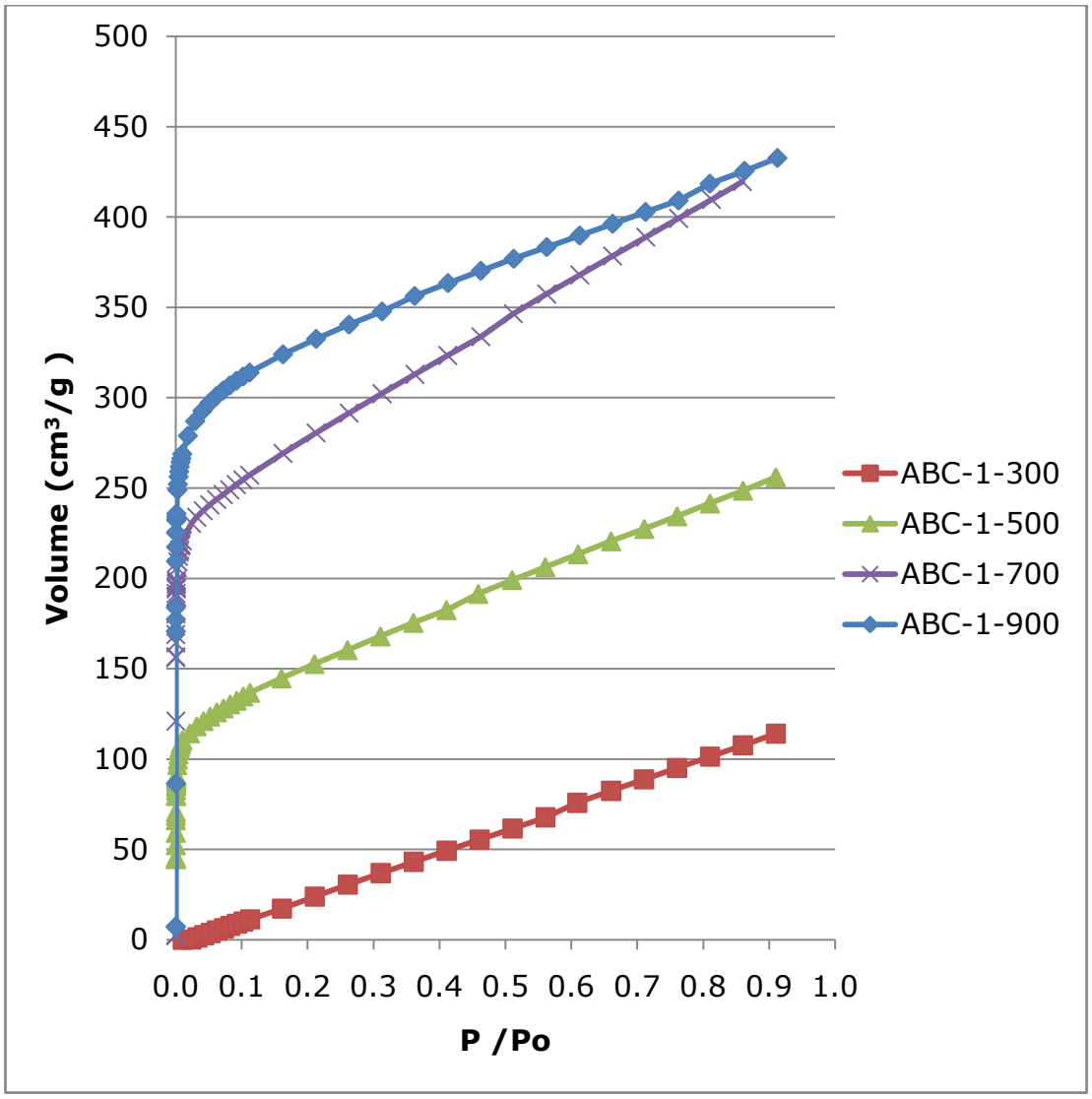

Figure 4.13 Nitrogen Adsorption Isotherms of Potassium Hydroxide Activated Carbons (Char Activation Method)

Figure 4.13 provides a basis for understanding the effect of temperature on char activation method with potassium hydroxide. The figure indicates that higher temperatures (above 500 ^{o}C) are crucial to obtain microporous activated carbon in char activation with potassium hydroxide. It would be appropriate to say that the increase in temperature resulted in higher nitrogen uptakes and a change in the structure of activated carbon from mesoporous to microporous.

4.3.3 Pore Size Distributions of the Products

Pore size distribution (PSD) is important to specify the fraction of the adsorbent surface that a molecule can access and cover. For estimation of pore size distribution quantitatively, non-local density functional theory (NLDFT) and Monte Carlo simulation method for cylindrical/slit pore shaped activated carbons was applied to the N_2 adsorption data.

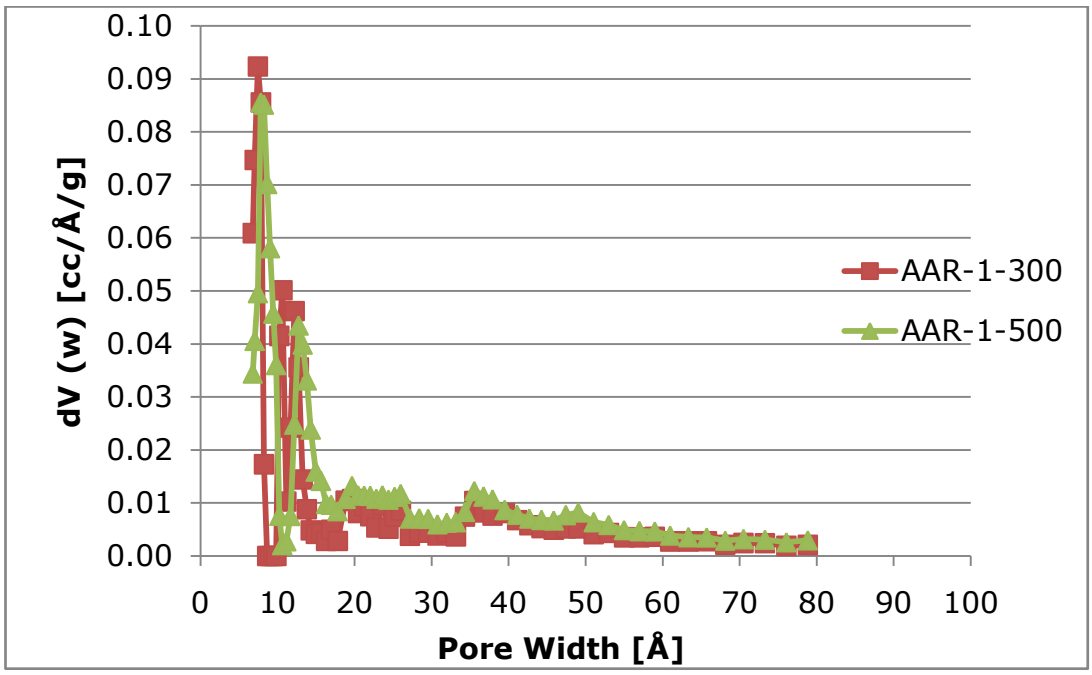

Figure 4.14 Temperature Effect on Pore Size Distributions of Phosphoric Acid Activated Carbons Between 300 and 500 °C (Raw Material Activation Method)

In order to observe the temperature effect on pore development in the phosphoric acid activation, pore size distributions were analyzed in different temperature intervals. Figure 4.14 shows the temperature range of 300 and 500 °C.

Upon increasing the activation temperature from 300 to 500 °C, the region below 20 Å acquired a different appearance, the narrow peak

near 7 Å shifting to a slightly higher pore width value and widening. New micropores appeared to have formed, and the peaks of the existing ones widened due to increasing the temperature from 300 to 500 °C.

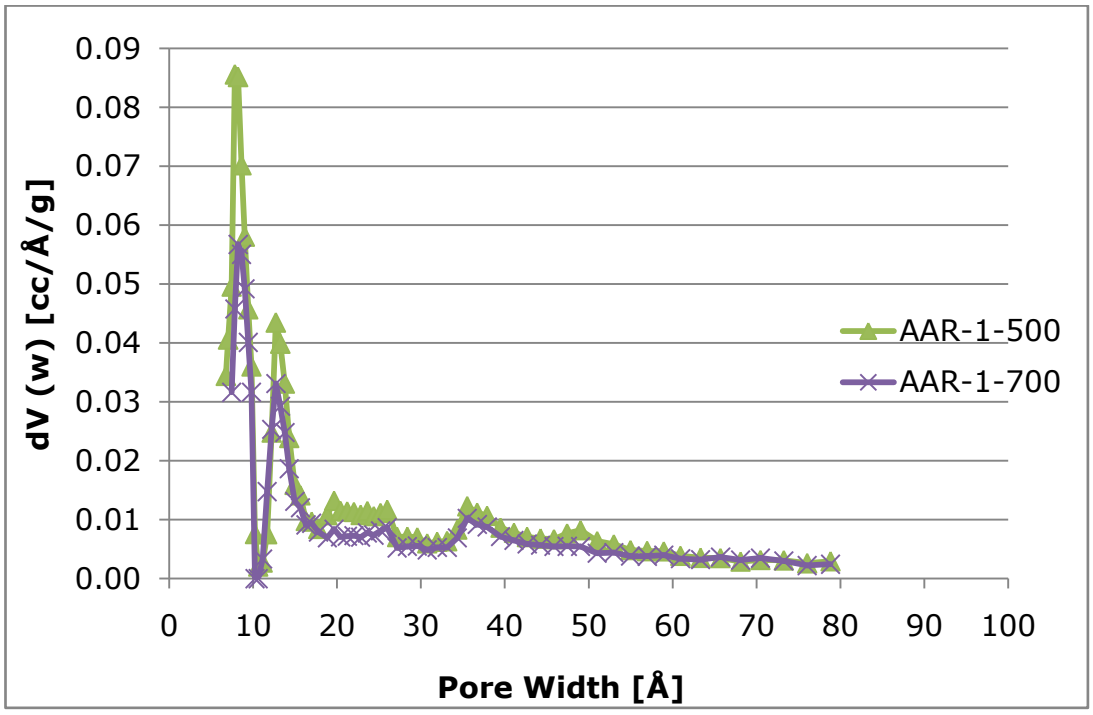

Figure 4.15 Temperature Effect on Pore Size Distributions of Phosphoric Acid Activated Carbons Between 500 and 700 °C (Raw Material Activation Method)

Figure 4.15 compares the differences in pore size distributions between 500 and 700 °C activation temperatures. Pore widths below 20 Å remained the same at 700°C, but the amount of pores are significantly less than that of 500°C.

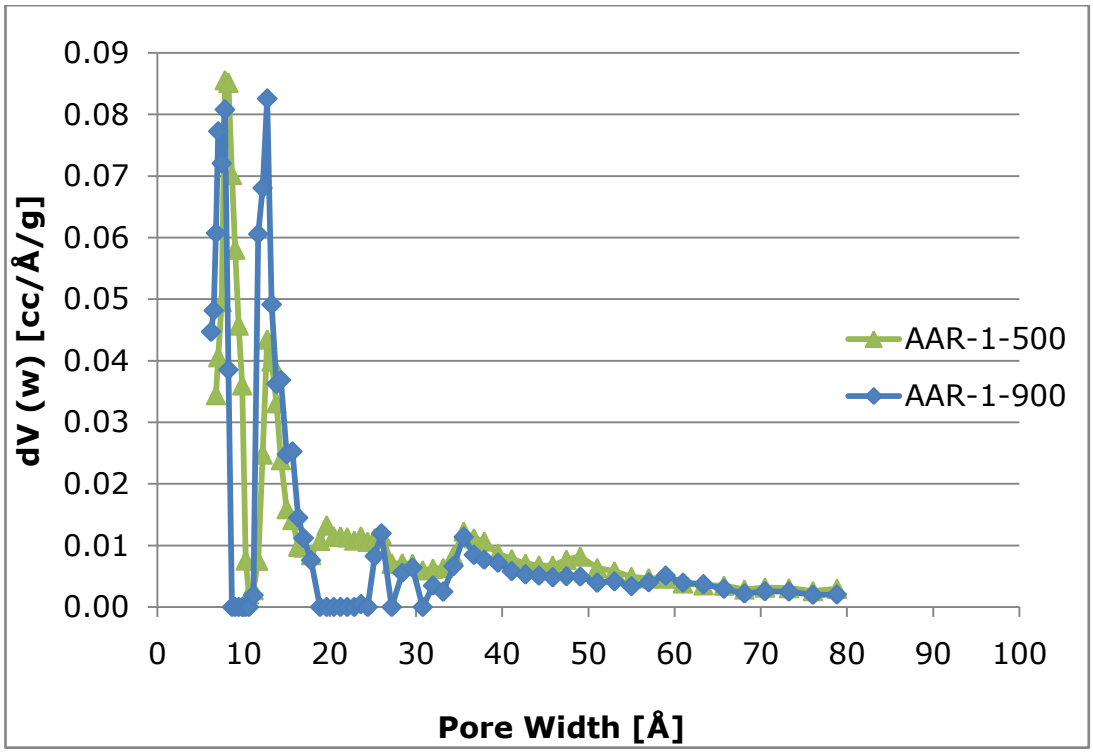

Figure 4.16 Temperature Effect on Pore Size Distributions of Phosphoric Acid Activated Carbons Between 500 and 900 °C (Raw Material Activation Method)

Contrary to the previous case, the amount of micropores seems to have increased in 900°C activation temperature compared to 500°C, while the pore widths remain roughly the same. It can also be observed that there are almost no pores between 20-25 Å for product AAR-1-900.

The pore size distributions of AAR-1 series were also given in Figure 4.17.

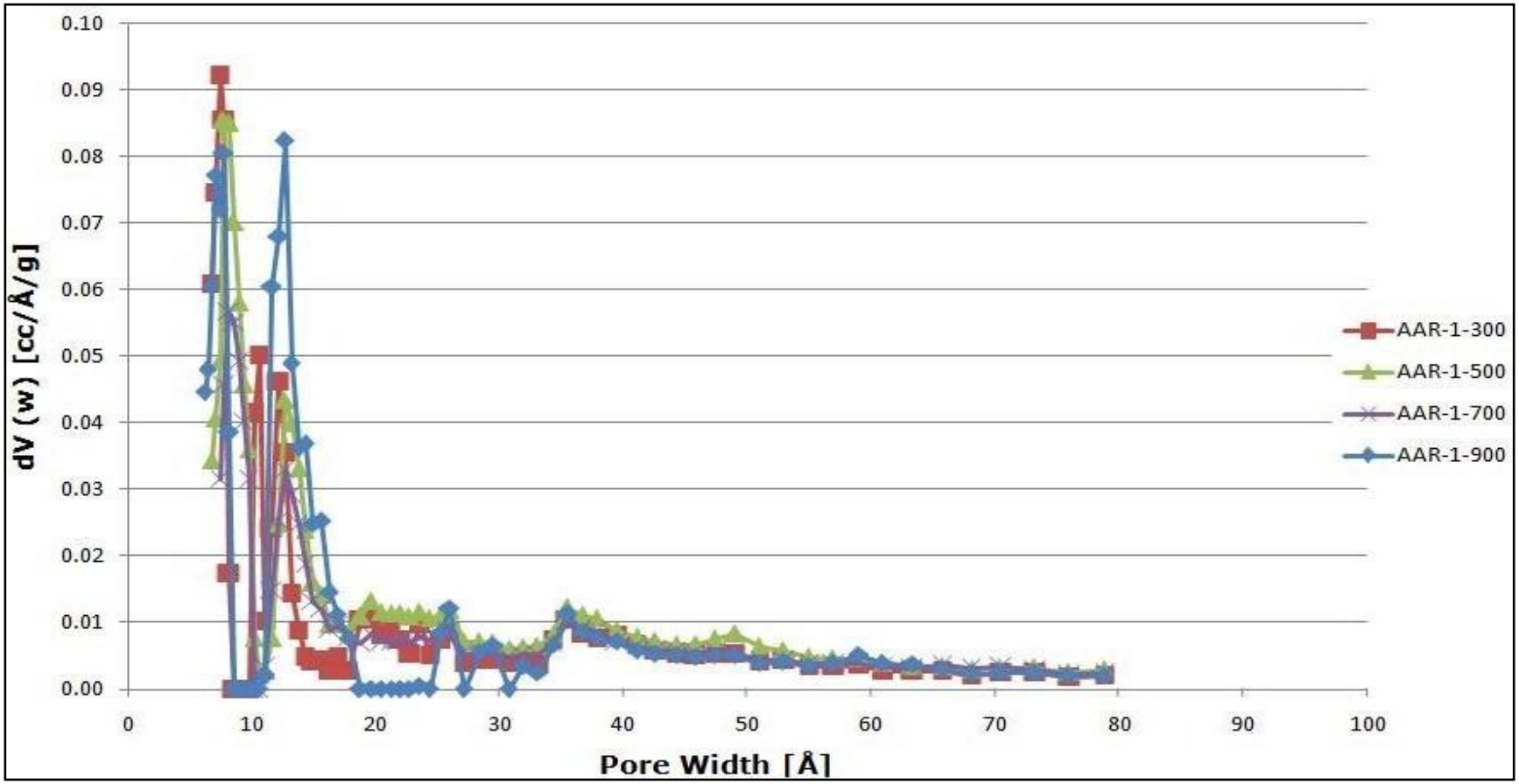

Figure 4.17 Temperature Effect on Pore Size Distributions of Phosphoric Acid Activated Carbons

(Raw Material Activation Method)

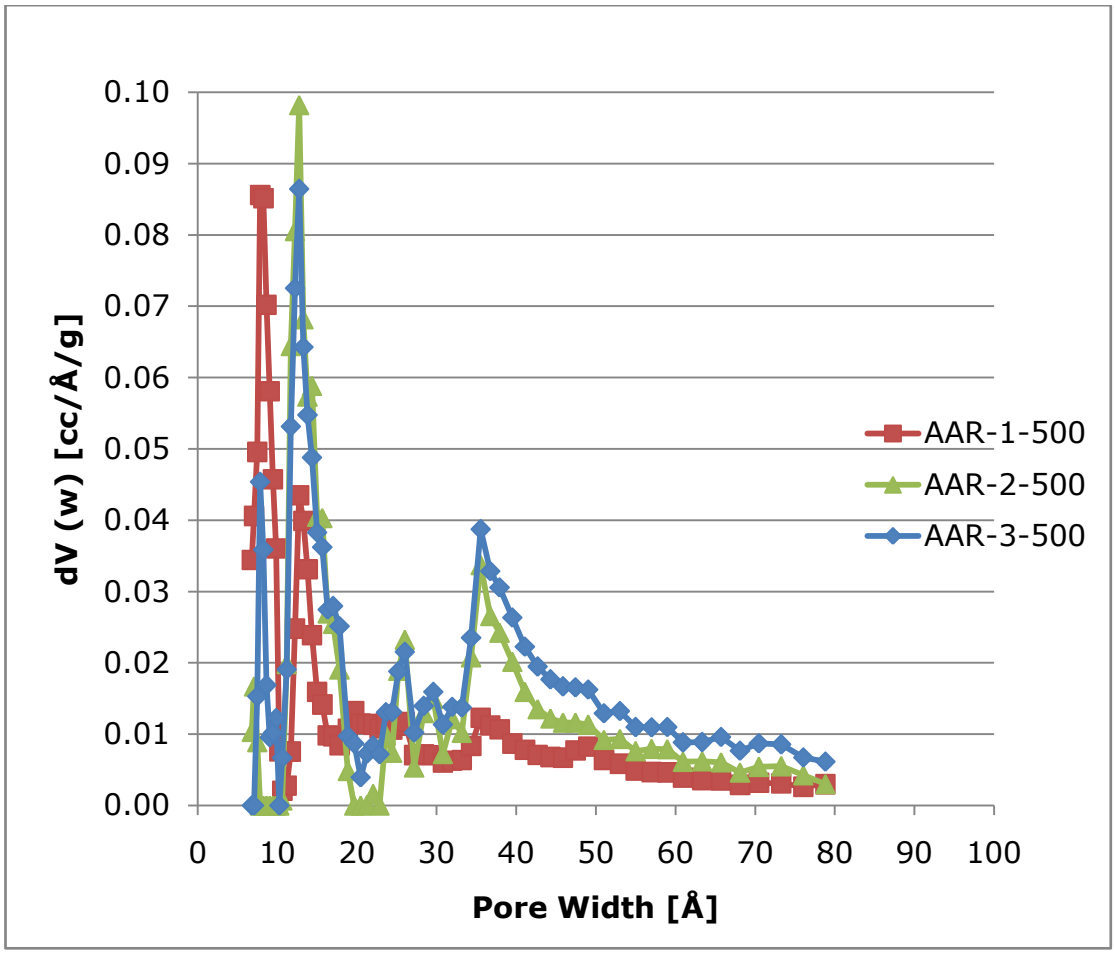

Figure 4.18 Effect of Impregnation Ratio on Pore Size Distributions of Phosphoric Acid Activated Carbons (Raw Material Activation Method)

Figure 4.18 shows the effect of impregnation ratio on pore development. Pore size distribution curves indicate distributions with similar shapes but different maxima occurrence and this seems to be related with the amount of phosphoric acid. As the ratio of phosphoric acid to shells increased, the intensities of two peaks changed in the micropore region. On the other hand formation of mesopores by phosphoric acid amount is noticeable.

While the temperature and impregnation ratio have received a great deal of attention in previous studies, there has been no information about the activation of carbonized product obtained from pyrolysis

process. The activation of char had been overlooked, as the pyrolysis process aimed for the liquid or tarry substances to produce synthetic fuel or chemical feedstocks, the remaining char as a side product had no alternative way of use generally.

When the pore size distributions of products obtained with char activation method using phosphoric acid are investigated (Figure 4.19), pore development can hardly be seen. These products showed a mesoporous nature at lower temperatures. In the case of increasing temperature the pore widths shifted to lower values but their differential pore widths were still at low values except in 900 ^{o}C.

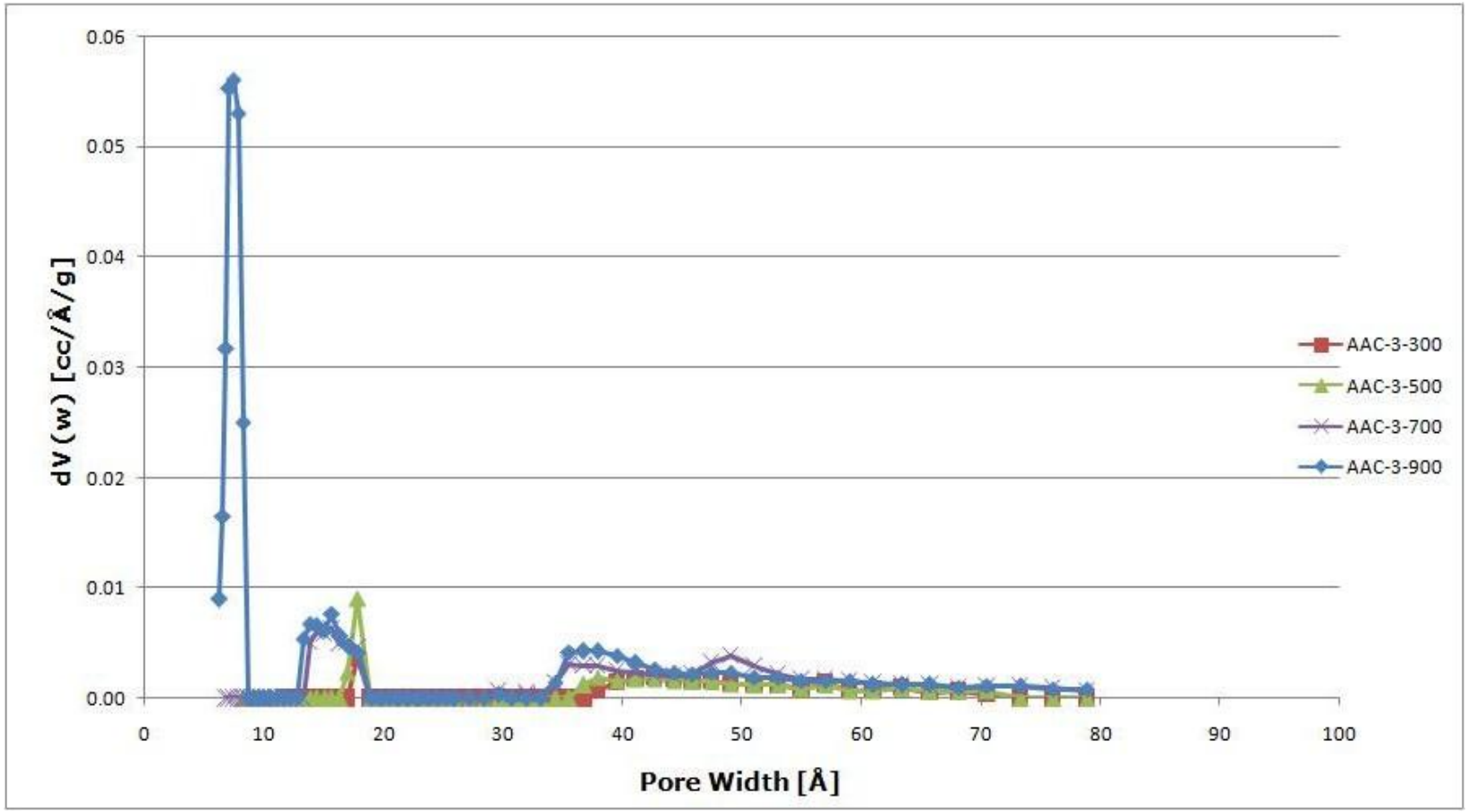

Figure 4.19 Temperature Effect on Pore Size Distributions of Phosphoric Acid Activated Carbons (Char Activation Method)

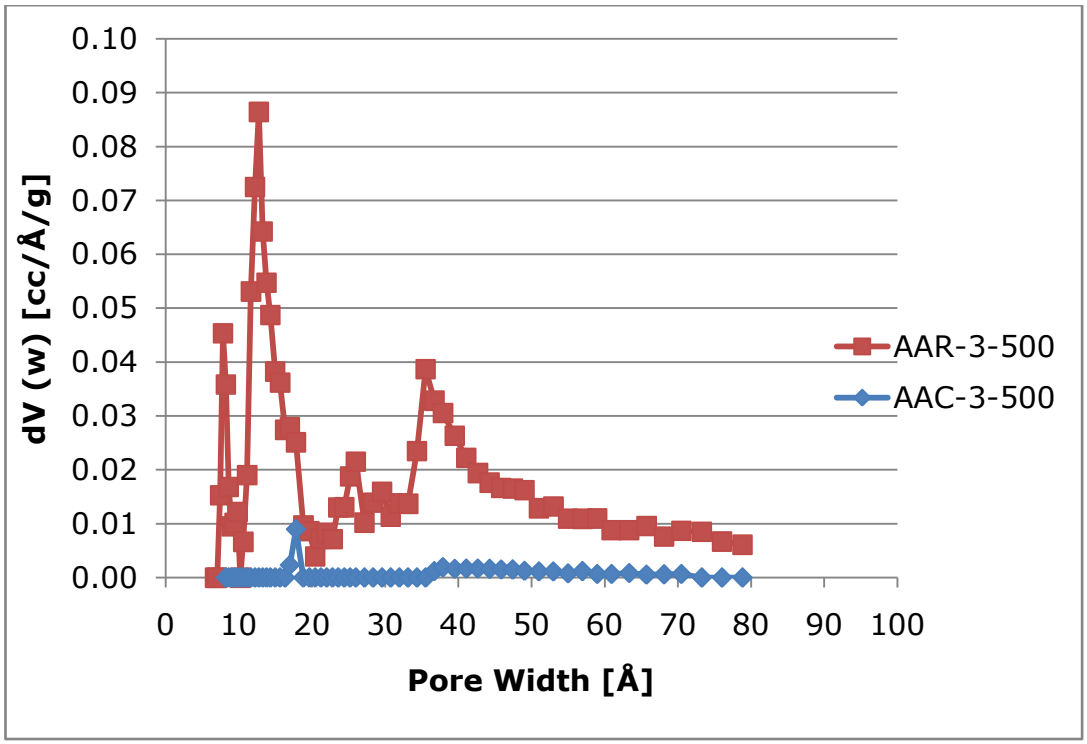

Figure 4.20 Pore Size Distributions of Raw Material Activation Method and Char Activation Method (Phosphoric Acid Activation)

Figure 4.20 aims to explain the differences between the raw material activation and char activation methods of phosphoric acid treatment. Upon examining the distribution graph, different maxima in the micro and mesopore regions with a multimodal distribution can be observed. In the case of raw material activation method, micropores were developed dramatically, together with some mesopores. On the other hand it does not look feasible to produce highly porous activated carbons by the char activation process when phosphoric acid is used as an activation agent. It can be said that raw material activation method with phosphoric acid is much more favorable in formation of microporosity and mesoporosity than char activation method.

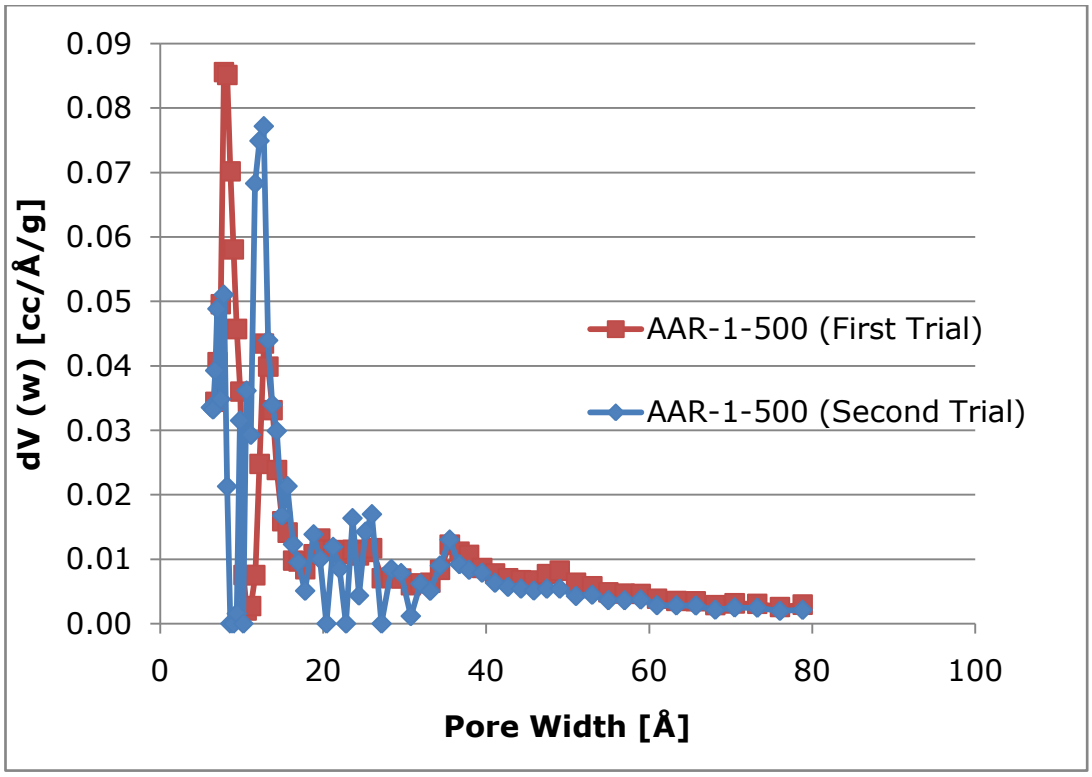

Figure 4.21 Pore Size Distributions of AAR-1-500 to Test Repeatability

Figure 4.21 shows the pore distributions of the repeated experiments of a randomly selected activated carbon (AAR-1-500). As can be seen from the distributions of pore sizes, some deviations in the amount and size of pores in micro and mesopore regions occurs. It is inevitable that some deviations may occur due to random errors in both preparation and characterization steps. Still it can be said that the results are close to each other.

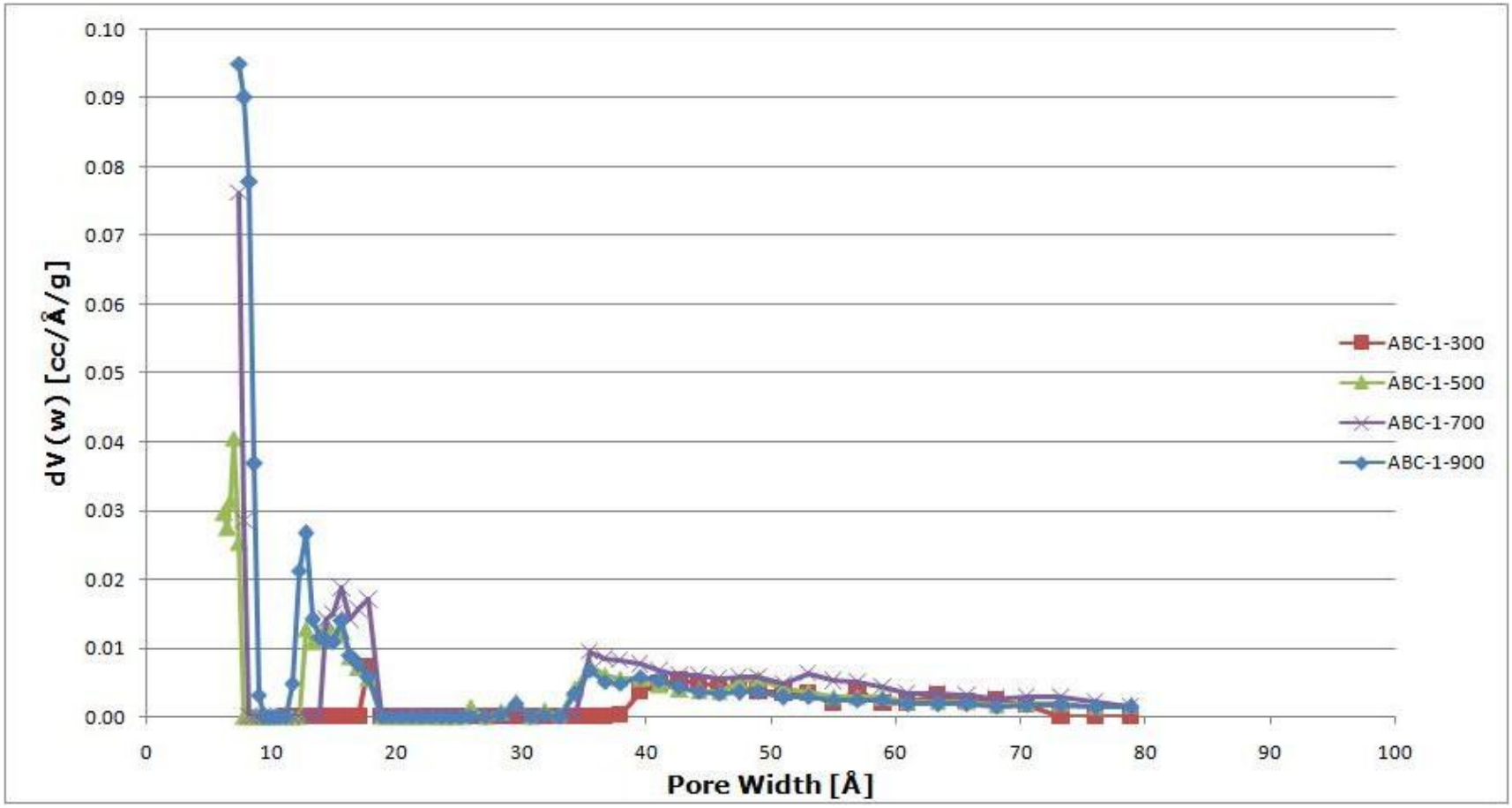

Figure 4.22 Temperature Effect on Pore Size Distributions of Potassium Hydroxide Activated Carbons (Char Activation Method)

As can be seen from Figure 4.22, char activation with potassium hydroxide resulted in different pore structures than those obtained with phosphoric acid activation. The pore size distribution curves indicate that temperature is an important parameter in producing activated carbons by char activation method with potassium hydroxide. At 300 ^{o}C the structure was mainly mesoporous but smaller pores were formed and the structure started to become microporous by increasing temperature. At 900 ^{o}C, a remarkable amount of microporous structure was observed.

4.2 CHEMICAL ANALYSIS OF PRODUCTS

The elemental analysis of the selected products and ash content and slurry pH of all products were determined and results were given in the following parts of the chapter.

4.2.1 Ash Content of the Products

The ash content is a measure of mineral content such as silica, aluminum, calcium, magnesium and iron which stay in the carbon network after the production processes. The ash content of activated carbon primarily depends on precursor material and these mineral matters are desired to be as low as possible to obtain an activated carbon of high quality. It is known that mineral content of activated carbon causes undesirable effects such as decreasing the activity and regeneration efficiency of activated carbon.

When activated carbon was incinerated, remaining ash was calculated and the results of phosphoric acid activated carbons are given in Figures 4.23-4.25 for impregnation ratios of 1/1, 2/1 and 3/1, respectively. The ash contents of products generally increased with activation temperature. On the other hand, there was no direct relationship between the ash content and both impregnation ratio and

activation method. It was seen that ash content of phosphoric acid activated carbons varied from about 0.7 to 11 %.

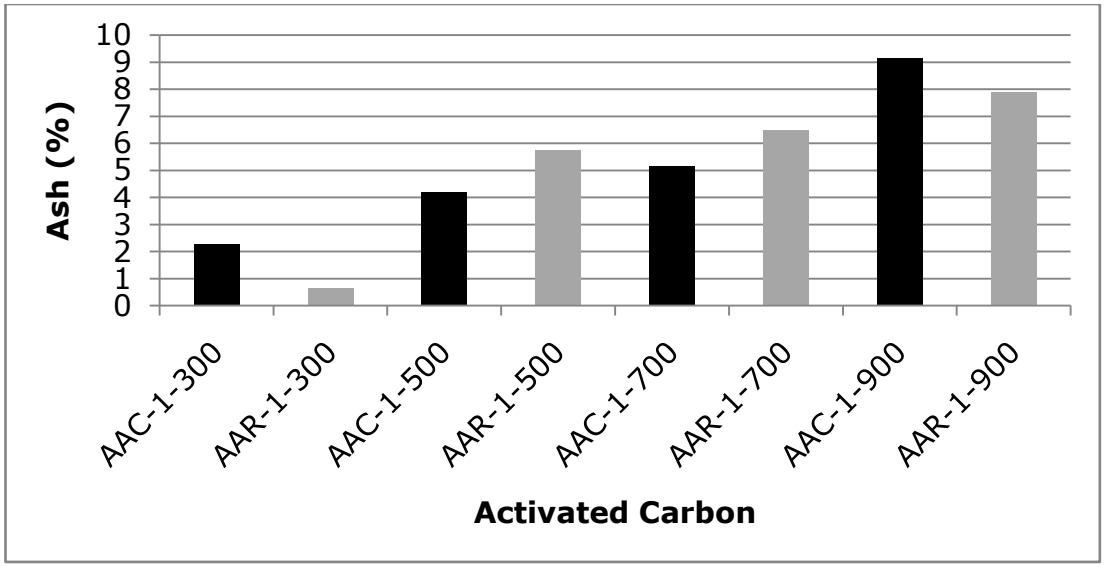

Figure 4.23 Ash Contents of the Phosphoric Acid Activated Carbons (Impregnation Ratio=1/1)

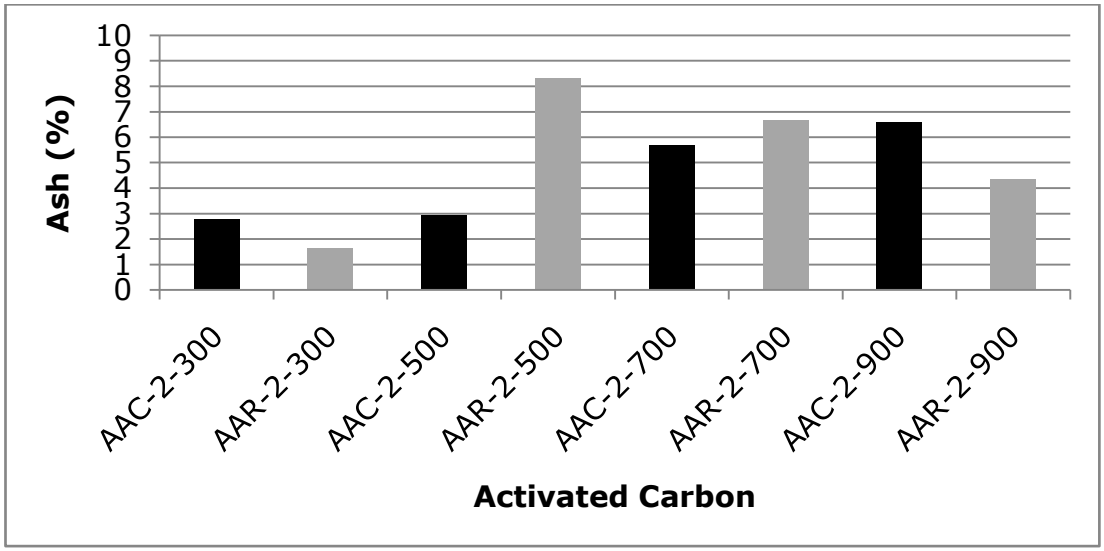

Figure 4.24 Ash Contents of the Phosphoric Acid Activated Carbons (Impregnation Ratio=2/1)

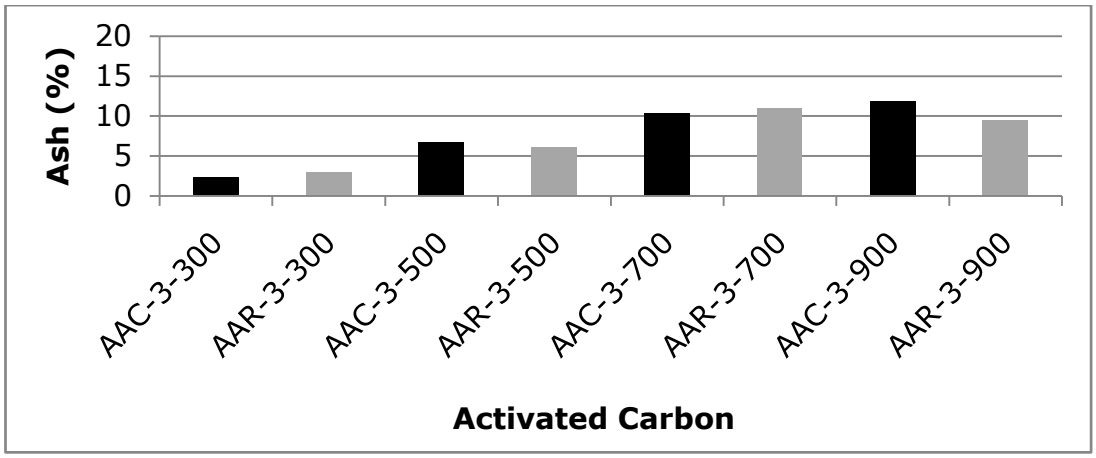

Figure 4.25 Ash Contents of the Phosphoric Acid Activated Carbons (Impregnation Ratio=3/1)

When the ash contents of potassium hydroxide activated carbons and phosphoric acid activated carbons, using char activation method, were compared, it was seen that potassium hydroxide produced activated carbons includes low inorganics. This comparison can be seen from From Figure 4.26. The ash contents of potassium hydroxide activated carbons were between 0.6 and 1.1 %.

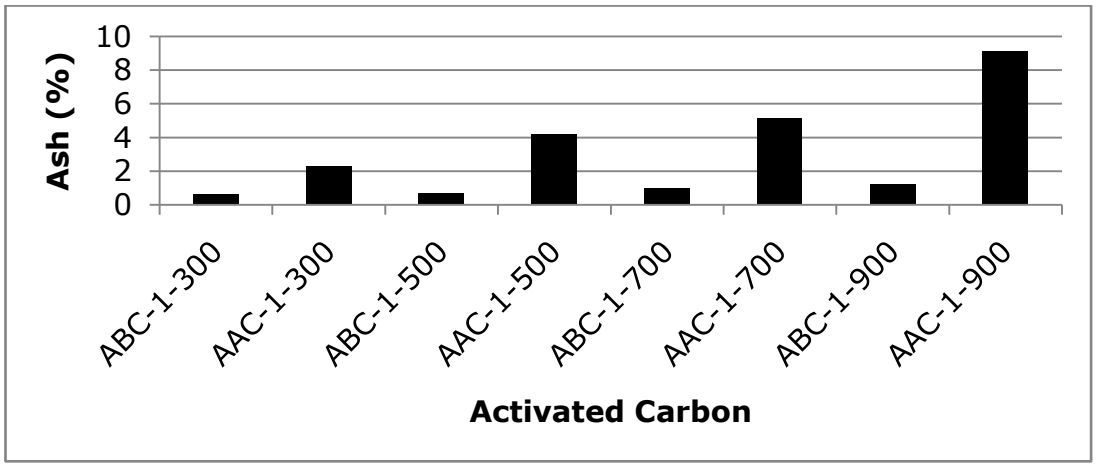

Figure 4.26 Ash Content of the Potassium Hydroxide and Phosphoric Acid Activated Carbons (Char Activation Method)

As a consequence, ash content of an activated carbon depends on the conditions employed and reagent used on preparation step. As Newcombe and Dixon (2006) stated that amount of ash of activated carbons can range from 1% to 20% and the ash content of the all produced activated carbons are between these values. The values of ash contents of the activated carbons are also given in Appendix E.

4.2.2 Elemental Analysis of the Products

Elemental analysis of selected activated carbons was performed to compare the elemental composition of the products with the precursor pistachio nut shells.

For comparison, elemental composition of raw pistachio-nut shells with the selected produced activated carbons was given in Table 4.3.

Table 4.3 Elemental Compositions of Activated Carbons

Activated Carbon	C (%)	H (%)	N (%)
AAR-1-500	65.44	3.85	0.16
AAR-2-500	74.82	3.18	0.13
AAR-3-500	74.95	3.35	0.15
AAC-1-500	75.76	3.33	0.20
AAC-2-500	71.54	2.73	0.32
AAC-3-500	73.52	3.09	0.20

Elemental analysis data reported in Table 4.3 indicated that the highest carbon content product among the selected products is AAC-1-500 with 75.76 % C. Prior to experiments, carbon content of raw pistachio-nut shells was determined as 46 %. There was a considerable increase in carbon content after carbonization and activation processes.

Adsorption process is considered to occur because of the effects of dense London dispersion forces and these forces are equal between all carbon atoms at the graphelene layers that compose the structure of activated carbon. Adsorbate molecules could stick on the surface of activated carbon more strongly when they were covered by more carbon atoms. And this phenomenon can explain the necessity of higher carbon content in the activated carbon structure.

Although carbon content is a very important parameter, it is not the only element that effects the adsorptive properties of activated carbon. There are heteroatoms bounded in the carbon matrix and those heteroatoms mainly arise from the elemental composition of the precursor material. The heteroatoms bounded as surface functional groups effects the polar character of activated carbon. Due to impregnation of raw material with chemical agents and nitrogen chemisorption in carbonization stage that takes place under nitrogen atmosphere and removal of volatiles from the structure, elemental composition of activated carbon differs.

Other then carbon, hydrogen, nitrogen amount of the selected products were also given in Table 4.3.

4.2.3 Slurry pH Values of Products

Slurry pH is an indicator of nature of the surface functional groups of activated carbon because, they give an idea about the presence and absence of oxygen or hydrogen containing functional groups. Also pH of

the solution influences the adsorption process by changing behaviour of the adsorbate-adsorbent interactions significantly.

As it was shown in Figure 4.27 all the activated carbons produced with phosphoric acid had slurry pH in the range of 3.14-3.55. This phosphoric acid treatment caused oxygen containing functional groups that made activated carbons acidic in nature.

On the other hand, slurry pH of the potassium hydroxide activated carbons was found between 7.20 and 8.36 as it can be seen in Figure 4.8. Potassium hydroxide activation made these products slightly basic. The amount and nature of the basic surface functional groups of products caused differences in pH values.

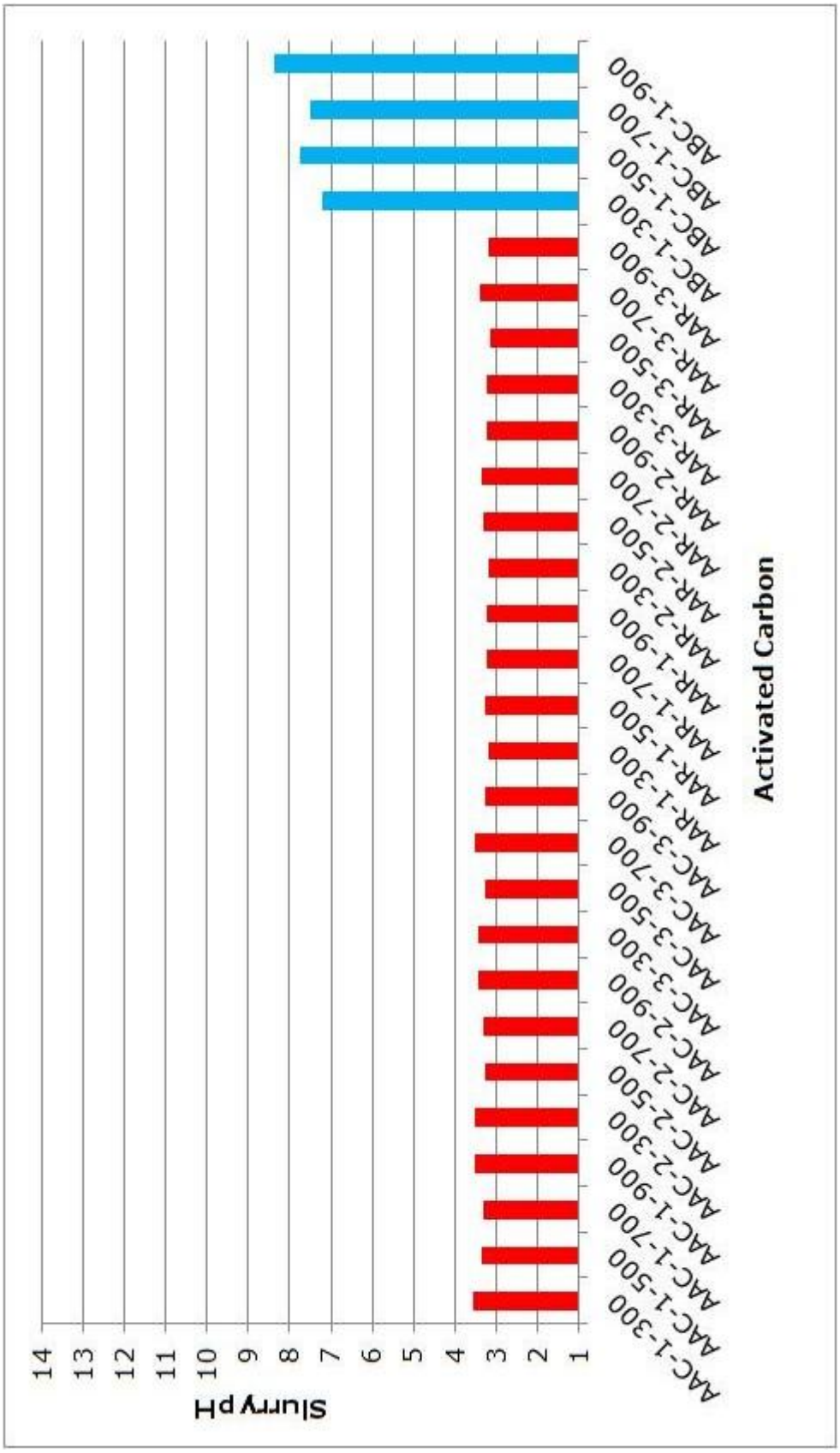

Figure 4.27 Slurry pH Values of Activated Carbons

4.4 TRUE DENSITY MEASUREMENTS

True density of an adsorbent can be defined as the ratio of the mass of the sorbent to the volume of sorbent excluding pores. To determine the true densities of selected activated carbons produced in this study, helium displacement method was used. Helium pycnometry results are given in Table 4.4.

Table 4.4 True Densities of Selected Activated Carbons

Sample Code	True Density (g/ml)
AAR-1-500	1.5225
AAR-2-500	1.7002
AAR-3-500	1.7895
AAC-1-500	1.5170
AAC-2-500	1.5752
AAC-3-500	1.5935

As it can be seen in table, the density values were found between 1.5170 and 1.7895. By increasing the impregnation ratio, true density values increased in both of methods and at the higher impregnation ratios raw material activation method produced denser activated carbons than the products of char activation method.

4.5 SCANNING ELECTRON MICROSCOPY

Scanning electron microscopy (SEM) was used to observe the morphology of raw pistachio-nut shells, carbonized pistachio-nut shells, impregnated pistachio nut shells, activated carbon produced by phosphoric acid activation and activated carbon produced by potassium hydroxide activation.

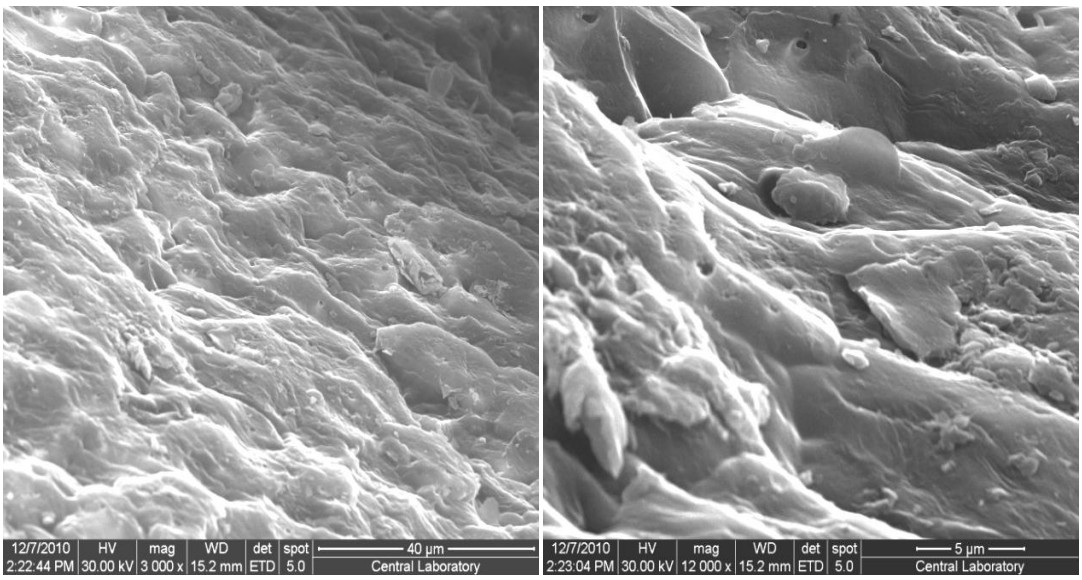

Figure 4.28 SEM Micrographs of Raw Pistachio-nut Shells

(3000 x, 12000 x)

In Figure 4.28, SEM micrographs of raw pistachio-nut shells can be seen. The surface of the shells were heteregeneous, rough and non-porous before any physical or chemical treatment. The micrographs of raw material can be beneficial to observe the structural changes occurred after impregnation, carbonization and activation processes.

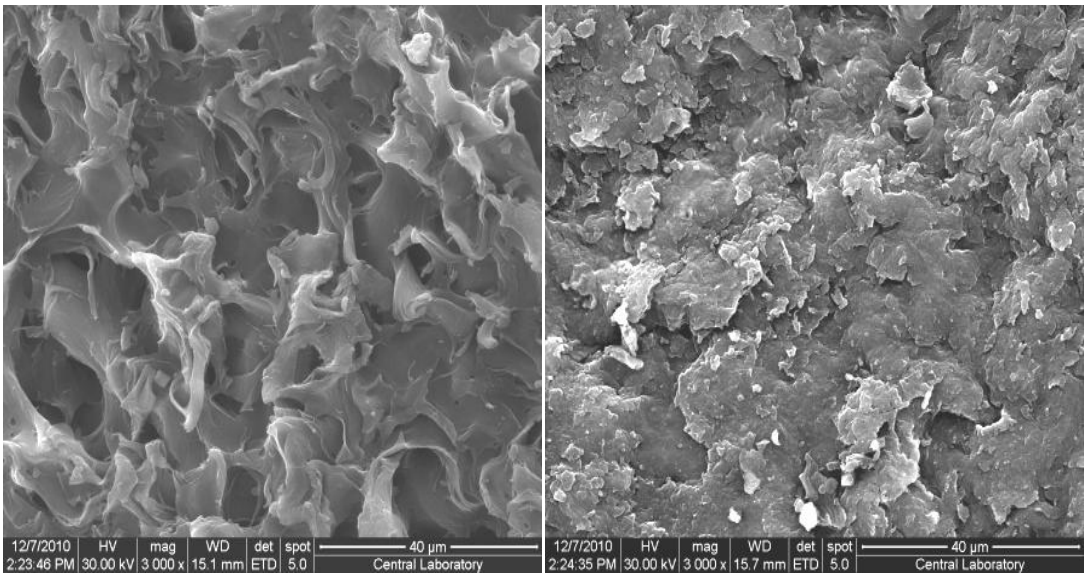

Figure 4.29 SEM Micrographs of Carbonized Pistachio-nut Shells (3000 x)

Due to using carbonized product as an intermediate in the char activation experiments, the structural changes in the surface morphology of char was observed. After carbonization at 500 ^{o}C, formation or waves and pits occurred on the surface of material. As it is clearly seen from Figure 4.29, porosity formation was initiated and undulating surfaces appeared because of the removal of the tarry substances from the lignocellulosic structure.

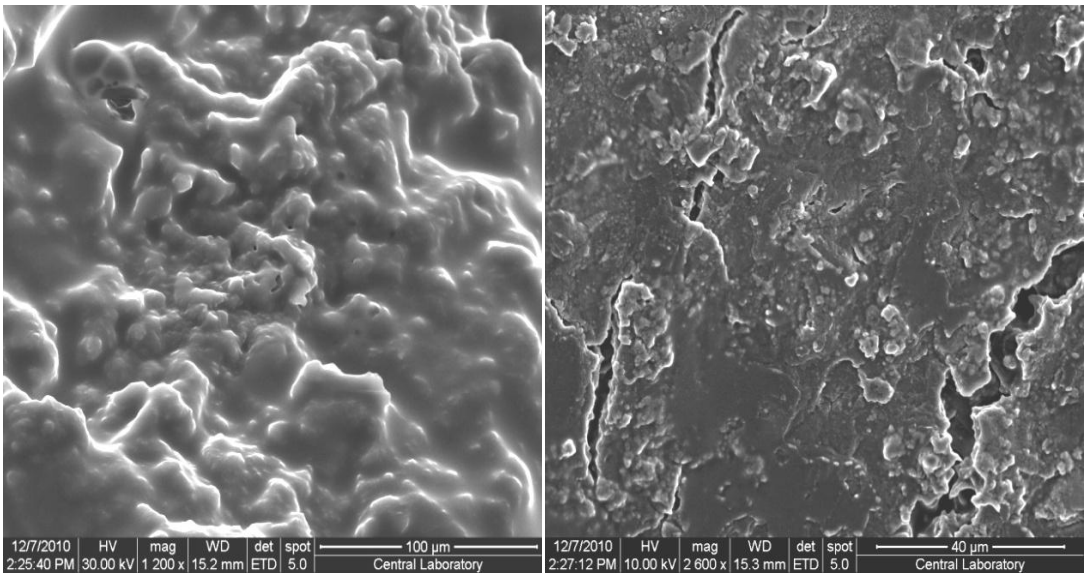

Figure 4.30 SEM Micrographs of Phosphoric Acid Impregnated Pistachio-nut Shells (3000 x)

The phosphoric acid impregnated pistachio-nut shells had micrographs that did not show any porous texture. But, it was seen that coating of the shells with phosphoric acid caused some structural changes. After phosphoric acid treatment, surface morphology changed such as swelling of the rough surface of the shells. The micrographs of phosphoric acid impregnated shells can be seen in Figure 4.30.

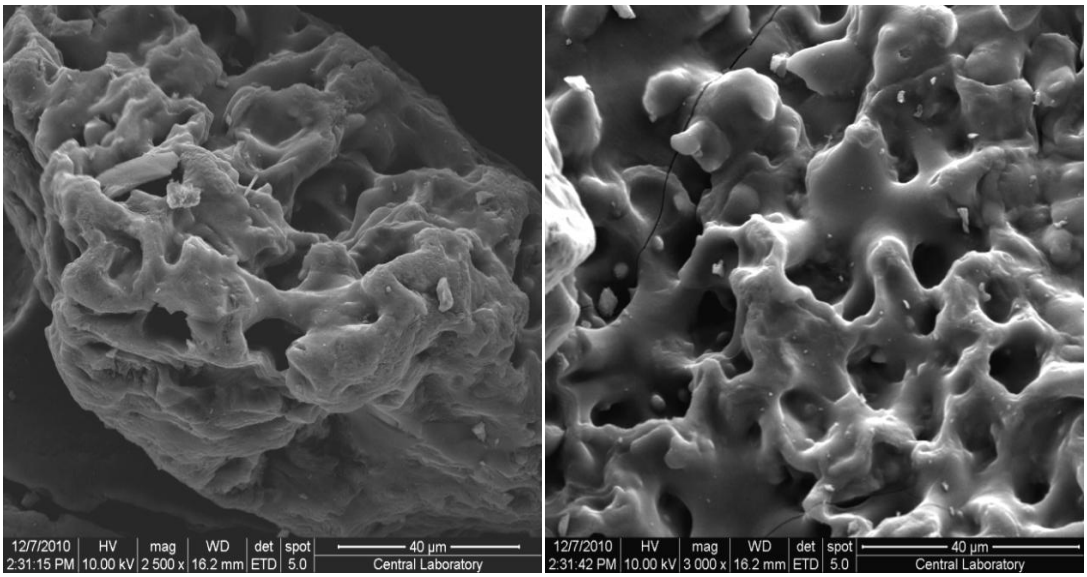

Figure 4.31 SEM Micrographs of Activated Carbon Produced by Phosphoric Acid Activation (2500 x, 3000 x)

The micrographs of activated carbon sample (AAR-3.0-500) produced in this research is given in Figure 4.31 This product achieved highest BET surface area value among the other products (1640 m^2/g) and it was expected to see a highly porous texture in the micrographs of this activated carbon. The micrographs showed a heterogeneous and irregular texture with an eroded surface. Comparing these micrographs with the raw pistachio-nut shells' micrographs proved the formation of channels and pores on the material by phosphoric acid activation. Undoubtedly, these pores or cavities occured by the thermal degradation the phosphoric acid coated on the surface during carbonization and activation by leaving voids or pores. This porous texture of produced activated carbon is essential for taking in adsorbate molecules in adsorption processes.

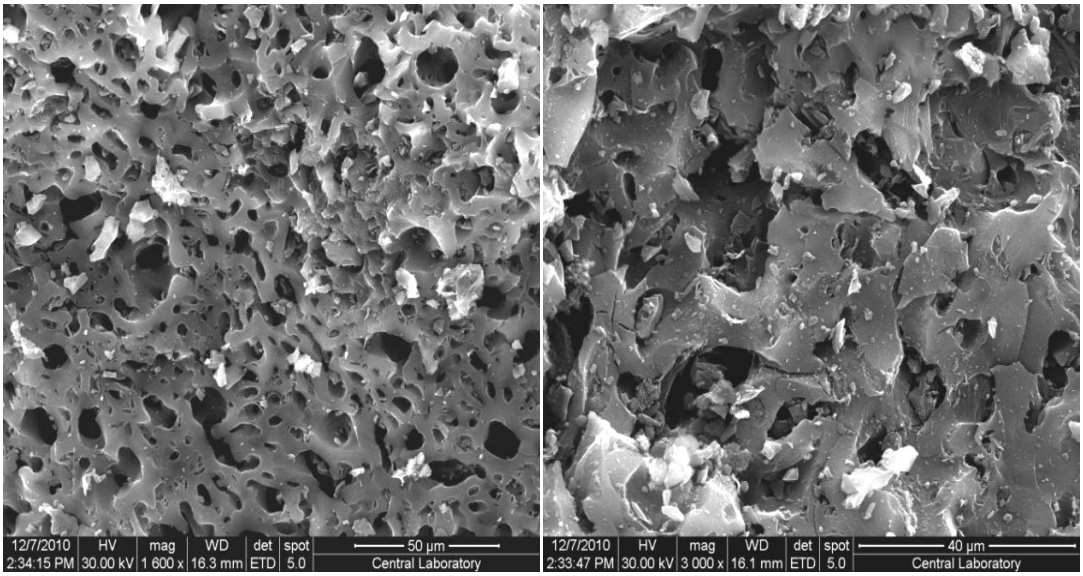

Figure 4.32 SEM Micrographs of Activated Carbon Produced by Potassium Hydroxide Activation (1600 x, 3000 x)

A sponge-like porous surface morphology was seen in the micrographs of the activated carbon produced by potassium hydroxide activation which is given in Figure 4.32. These micrographs belong to the activated carbon produced by char activation method with potassium hydroxide (ABC-1.0-900) with a BET surface area of 1229 m^2/g. If a comparison among the micrographs of raw pistachio-nut shells and potassium hydroxide activated carbons is done, pore formation could be seen obviously as it was seen in the micrographs of phosphoric acid activated carbon.

4.6 METHYLENE BLUE NUMBER

Methylene blue number can be used as an indicator of the adsorptive capacity of activated carbons. Methylene blue numbers of activated carbons indicate the ability of adsorbent to adsorb on super micropores and mesopores (Akgün, 2005).

Table 4.5 Properties of Dehydrated Methylene Blue (Raposo et al., 2009)

Molecular weight	320 g /mol
Molecular width	14.3 Å
Molecular depth	6.1 Å
Molecular thickness	4 Å
Molecular volume	241.9 cm^3/ mol
Molecular diameter	0.8 nm

Since surface area covered by methylene blue (S_{MB}) is used to estimate surface area of super micropores and mesopores, the ratio of S_{MB} to BET surface area (S_{BET}) represents the ratio of surface area of super micropores and mesopores to total surface area. When this ratio is higher, activated carbon is more preferable in adsoption of larger molecules or when this ratio is smaller, adsorption of smaller molecules should be preferred (Akgün,2005).

Results of methylene blue adsorption is summarized in Table 4.6 and detailed calculations and experimental data are given in Appendix D.

Activated carbons produced from raw material activation with phosphoric acid had methylene blue numbers (MBN's) varying between 61.5 and 97.4. Since methylene blue is assumed to be adsorbed on pores whose diameters were greater than 1.5 nm (Attia et al., 2003), in the case of known surface area covered by methylene blue, the surface area of super micropores and mesopores could be estimated. Surface areas of these pores of produced activated carbons were between 187.6 and 297.1 m^2/g. The ratio of surface area covered by methylene blue to total surface area indicates that how much methylene blue can adsorbed on the surface of an adsorbent. For activated carbon product AAR-3-500,

this ratio indicates that approximately 18% of the total surface area was covered with methylene blue.

Table 4.6 Results of Methylene Blue Adsorption Experiments

Activated Carbon	MB	SMB	SMB/SBET
AAR-1-300	82.1	250.3	0.221
AAR-1-500	95.8	292.2	0.226
AAR-1-700	76.9	234.5	0.221
AAR-1-900	97.3	296.7	0.231
AAR-2-300	96.5	294.4	0.296
AAR-2-500	96.7	295.0	0.200
AAR-2-700	96.4	293.9	0.217
AAR-2-900	97.4	297.0	0.210
AAR-3-300	61.5	187.6	0.213
AAR-3-500	97.4	297.1	0.181
AAR-3-700	97.1	296.2	0.195
AAR-3-900	96.7	294.8	0.187

Also, the ratio of surface area covered by methylene blue to total surface area (BET surface area) gives a preliminary information about the suitable adsorbate molecule size that should be used in the adsorption on the activated carbon. Higher S_{MB}/S_{BET} ratios make activated activated carbon more preferable in the adsorption of large molecules because this high ratio indicates the amount of the pores greater than 1.5 nm is more than pores smaller than this size. On the other hand, smaller S_{MB}/S_{BET}

ratios of activated carbons are more suitable in the adsorption of small molecules.

The photographs of methylene blue solutions before and after adsorption with an activated carbon is given in Figure 4.33.

Figure 4.33 Methylene Blue Solutions Before and After Adsorption

(with product AAR-3-500)

CHAPTER V

CONCLUSIONS

Results of this study indicate that pistachio-nut shells can be used as a raw material in the activated carbon production. N_2 adsorption data was used for qualitative interpretation of pore structure and for quantitative analysis of BET surface area and pore size distributions. Promising results were achieved with BET surface areas exceeding 1000 m^2/g by chemical activation method.

Phosphoric acid and potassium hydroxide were used as activating agents in the experiments and phosphoric acid activation was applied in the form of two different methods.

When raw material was impregnated with phosphoric acid before carbonization and activation processes, a well-developed porosity was formed. Also, high activated carbon yields were obtained by conventional raw material activation method with phosphoric acid. Conversely, in the case of impregnation of carbonized shells followed with an activation process, low activated carbon yields, mesoporous structure and hence lower BET values were obtained.

In the case of char activation method with potassium hydroxide a well-developed microporosity formed only at higher temperatures while there was a reduction in lower BET surface areas at lower activation temperatures.

Pore size distributions of produced activated carbons supported the BET surface area values in emphasizing the effects of temperature,

impregnation ratio, activation agent and activation method on pore formation.

When the temperature effect was examined in phosphoric acid activation of raw material, it was seen that higher BET surface areas were obtained at 500 ^{o}C. Also increases in amount of phosphoric acid, caused BET surface areas to increase above 500 ^{o}C and highest BET surface area was obtained as 1640 m^2/g with an impregnation ratio of 3/1 (g H_3PO_4/ g shells).

From the thermogravimetric analysis, it is concluded that higher yields above 50 % can be achieved by phosphoric acid activation of pistachio-nut shells with raw material activation methods. But lower activation temperatures seem to be favorable for production of activated carbon with higher yields.

Chemical analysis of products yielded main chemical properties of activated carbons with respect to production conditions. Elemental analysis gave the carbon content of pistachio-nut shells after carbonization and activation processes. Amount of inorganic constituents of activated carbons were found to be higher than that of the raw material in phosphoric acid activation. On the other hand ash contents of the potassium hydroxide activated carbons were found to be lower than those of phosphoric acid activated carbons, which can be attributed to the effects of chemical agents. Another significant difference was the one observed in the slurry pH values of activated carbons. While phosphoric acid activated carbons were acidic, potassium hydroxide activated carbons were slightly basic in nature.

It was concluded from this study that the properties of the final activated carbon are strongly influenced by both process conditions and production method in the preparation step.

CHAPTER VI

RECOMMENDATIONS

This systematic study was made to utilize a waste biomass, pistachio-nut shells, which is found in Turkey large amounts. Two different processes with various process parameters were tested to obtain activated carbon by chemical activation and then the products were subjected to detailed characterization. Since activated carbon can be produced from a wide variety of materials, it is cost effective. Besides, production of activated carbon from waste materials is enviromentally conscious. In the light of these reasons stated, more research should be carried out with different precursors and different experimental parameters to optimize the process conditions. It is recommended to perform the experiments with different raw materials and experimental parameters such as heating rate, activation holding time and so forth.

It is also crucial to investigate kinetics of carbonization and activation processes because it is still an uncertain issue. For this purpose, analysing tarry and gaseous products evolved from the structure of biomass can be beneficial to enlighten the kinetics of activated carbon production process.

In this thesis, activated carbons were prepared by chemical activation using phosphoric acid and potassium hydroxide. Other chemical reagents such as potassium carbonate, sulfuric acid and sodium hydroxide should be tried on the pistachio-nut shells.

In the literature different activation procedures have been employed. For example, a combined physical and chemical activation or two step chemical activation or microwave activation might be tried with pistachio-nut shells and the consequences could be observed.

There are several techniques to characterize materials and it is recommended to characterize activated carbons by analysis methods such as XRD, FTIR, XPS and Raman spectroscopy.

Investigations on the surface modifications of activated carbons produced will be beneficial in finding new application fields for activated carbons.

It is known that some pretreatments cause a decrease in ash content. For example washing of raw material with hydrochloric acid before carbonization reduces ash content of the activated carbon. To improve the quality of activated carbons, ash reduction should be optimized.

At the washing step of production of activated carbon, a leaching process is done to remove excess chemicals from the structure. Considering this part of the process, recovery efficiency of the chemical activating agent should be aimed at.

A detailed cost analysis of overall activated carbon process should be done to minimize operating costs.

Since adsorption is related with the adsorbent-adsorbate interactions, the future efforts should be made to determine the performances of different adsorbates on the produced activated carbons for investigation of liquid phase and gaseous phase adsorption behaviours and kinetics of adsorption.

REFERENCES

- Abdallah, W., "Production and Characterization of Activated Carbon from Sulphonated Styrene Divinylbenzene Copolymer", MSc. Thesis in Chemical Engineering, Middle East Technical University, Ankara, Turkey, 2004.

- Akgün, A.M., "Sorption of Cadmium and Lead on Activated Carbons Produced from Resins and Agricultural Wastes", MSc. Thesis in Chemical Engineering, Middle East Technical University, Ankara, Turkey, 2005.

- Akikol, İ., "Heavy Metal Removal from Water with The Activated Carbons Developed with Different Activation Methods", MSc. Thesis in Chemical Engineering, Yıldız Technical University, İstanbul, Turkey, 2005.

- Apaydın-Varol. E., Pütün, E., Pütün, A.E., "Slow Pyrolysis of Pistachio Shell", *Fuel*, Vol.86, pp. 1892–1899, 2007.

- Apaydın-Varol. E., "Thermal Conversion of Different Biomass Samples and Characterisation of The Products", Ph.D. Thesis in Chemical Engineering, Anadolu University, Eskişehir, Turkey, 2007.

- Attia, A. A., Girgis, B. S., Khedr, S. A. "Capacity of Activated Carbon Derived from Pistachio Shells by H_3PO_4 in the Removal of Dyes and Phenolics", *J. Chem. Technol. Biot*., Vol. 78, pp. 611–619, 2003.

- Ariyadejwanich, P., Tanthapanichakoona, W., Nakagawab, K., Mukaib, S.R., Tamon, H., "Preparation and Characterization of Mesoporous Activated Carbon from Waste Tires", *Carbon*, Vol. 41, pp. 157–164, 2003.

- Allen, S.J., Whitten, L., "The Production and Characterisation of Activated Carbons: A Review", *Dev. Chem. Eng. Mineral Process*., Vol. 6, pp. 231-261, 1998.

- Balcı, S., "Kinetics of Activated Carbon Production from Almond Shell, Hazelnut Shell and Beech Wood and Characterization of Products", Ph.D. Thesis in Chemical Engineering, Middle East Technical University, Ankara, Turkey, 1992.

- Bektaş, İ., "Liquifaction of Pistachio Shells and Analyzing the Products", M.S Thesis in Chemical Engineering, Yıldız Technical University, Ankara, Turkey, 2006.

- Bansal, R.C. and Goyal,M., "Activated Carbon Adsorption", CRC Press, USA, 2006.

- Bandosz, T.J., "Activated Carbon Surfaces in Enviromental Remediation",Academic Press, New York, USA, 2006.

- Barrett, E. P., Joyner, L. G., Halenda, P. P., "The Determination of Pore Volume and Pore Area Distributions in Porous Substances. I. Computations from Nitrogen Isotherms", *J. Am. Chem. Soc.*, Vol. 73, pp. 373-380, 1951.

- Baçaoui , A., Yaacoubi , Dahbi , A., Bennouna , C. , Luu , R. P. T., Maldonado-Hodar, F.J., Rivera-Utrilla, J., , Moreno-Castilla, C., "Optimization of Conditions for the Preparation of Activated

Carbons from Olive-Waste Cakes", *Carbon* , Vol. 39, pp. 425–432, 2001.

- Baquero, M.C., Giraldo, L., Moreno, J.C. , Suarez-Garcia, F., Martinez-Alonso, A., Tascon, J.M.D, "Activated Carbons by Pyrolysis of Coffee Bean Husks in Presence of Phosphoric Acid", *J. Anal. Appl. Pyrol.*, Vol. 70, pp. 779-784, 2003.

- Brunauer, S., Demming, L. S, Demming, W. S., Teller, E., "On a Theory of the Van Der Waals Adsorption of Gasses" , *J. Am. Chem. Soc.,* Vol. 62, pp. 1723–1732, 1938.

- Brunauer, S., Emmet, P. H., Teller, E., "Adsorption of Gases in Multimolecular Layers, *J. Am. Chem. Soc.,* Vol. 60, pp. 309-19, 1938.

- Bouchelta, C., Medjram, M. S., Bertrand , O., Bellat, J.P., "Preparation and Characterization of Activated Carbon from Date Stones by Physical Activation with Steam", *J. Anal. Appl. Pyrol.* , Vol. 82, pp. 70–77, 2008.

- Budinova , T., Ekinci, E. ,Yardim F., Grimm, A., Björnbom , E. , Minkova , V., Goranova, M., "Characterization and Application of Activated Carbon Produced by H_3PO_4 and Water Vapor Activation", *Fuel Process. Technol*., Vol. 87 , pp. 899–905, 2006.

- Bottani, E.,J., Tascon, J.M.D., " Adsorption by Carbons", Elsevier Ltd., 2008.

- Çetinkaya, E., "Flue Gas Desulfurisation on Activated Carbon Derived From Olive Stone", MSc. Thesis in Energy Science and Technology, İstanbul Technical University, İstanbul, Turkey, 2009.

- Chang, C.F., Chang, C.Y.,Tsai, W.T., "Effects of Burn-off and Activation Temperature on Preparation of Activated Carbon from Corn Cob Agrowaste by CO_2 and Steam*", J. Colloid and Interf. Sci*., Vol. 232, pp. 45–49 , 2000.

- Crittenden, B., Thomas, W.J., "Adsorption Technology and Design", Elsevier Ltd., 1998.

- Condon, J.B., "Surface Area and Porosity Determinations by Physisorption Measurements and Theory", Elsevier, 2006.

- Çuhadar, Ç., "Production and Characterization of Activated Carbon from Hazelnut Shell and Hazelnut Husk", MSc. Thesis in Chemical Engineering, Middle East Technical University, Ankara, Turkey, 2004.

- Do,D.D., "Adsorption Analysis: Equilibria and Kinetics", Imperial Collage Press, London, England, 1998.

- El-Hendawy, A.N.A, "An Insight into the KOH Activation Mechanism Through the Production of Microporous Activated Carbon for the Removal of Pb^{2+} Cations", *Appl. Surf. Sci.* , Vol. 255, pp. 3723–3730, 2009.

- Franklin, R. E., "Crystallite Growth in Graphitizing and Non-graphitizing Carbons", *Proc. Roy. Soc*., A 209, pp. 196-218, 1951.

- Fierro, V., Muniz G., Basta, A.H., El-Saied, H., Celzard, A., "Rice Straw as Precursor of Activated Carbons: Activation with Ortho-phosphoric Acid", *J. Hazard. Mater.,* Vol. 181, pp. 27–34, 2010.

- Food and Agricultural Organization of United Nations (FAO), http://www.fao.org, (Last Visited on 04.10.2010)

- Girgis, B. S., El-Hendawy, A.N.A., "Porosity Development in Activated Carbons Obtained from Date Pits Under Chemical Activation with Phosphoric Acid", *Micropor. Mesopor. Mat*. , Vol. 52, pp. 105–117, 2002.

- Girgis, B.S., Smith, E., Louis, M. M., El-Hendawy, A.N.A., "Pilot Production of Activated Carbon from Cotton Stalks Using H_3PO_4", *J. Anal. Appl. Pyrol.*, Vol. 86, pp. 180–184, 2009.

- Gonzalez, J.F., Roman,S., Gonzalez-Garcia,C.M., Nabais, J.M.V., Ortiz, A.L., "Porosity Development in Activated Carbons Prepared from Walnut Shells by Carbon Dioxide or Steam Activation", *Ind. Eng. Chem. Res*., Vol. 48, pp. 7474–7481, 2009.

- Gregg, S. J. and Sign, K.S.W., "Adsorption, Surface and Porosity", 2nd Edn, New York Academic Press, New York, USA, 1982.

- Gonzalez, J.F., Roman, S., Encinar, J.M., Martinez, G., "Pyrolyis of Various Biomass Residues and Char Utilization for the Production of Activated Carbons", *J. Anal. Appl. Pyrol*, Vol. 85, pp. 134-141, 2009.

- Halsey, G. D., "Physical Adsorption on Non-uniform Surfaces", *J. Chem. Phys.*, Vol. 16, pp.931, 1948.

- Hassler, J.W.,"Purification with Activated Carbon", Chemical Publishing Co. Inc., Newyork, USA, 1974.

- Hayashi, J., Horikawa, T., Takeda, I., Muroyama, K., Ani, F.N.," Preparing Activated Carbon from Various Nutshells by Chemical Activation with K_2CO_3", *Carbon*, Vol. 40, pp. 2381–2386, 2002.

- Hazourli, S., Ziati, M. , Hazourli, A., "Characterization of Activated Carbon Prepared from Lignocellulosic Natural Residue: Example of Date Stones", *Physics Procedia* , Vol. 2, pp. 1039–1043, 2009.

- Hon, D.N.S., Shiraishi, N., "Wood and Cellulosic Chemistry",Marcel Dekker Inc. , 2001.

- Inglezakis, V. J., Poulopoulos, S. G., "Adsorption, Ion Exchange and Catalysis: Design of Operations and Environmental Applications", Elsevier, 2006.

- IUPAC (International Union of Pure and Applied Chemistry) Physical Chemistry Division Commission on Colloid and Surface Chemistry Including Catalysis, "Reporting Physisorption Data for Gas/Solid Systems with Special Referance to Determination of Surface Area and Porosity", Pure Appl. Chem., Vol. 57, No. 4, pp. 603—619, 1985.

- Jagtoyen M., Derbyshire F., "Activated Carbons from Yellow Poplar and White Oak by H_3PO_4 Activation,", *Carbon*, Vol. 36, pp. 1085-1097, 1998.

- Jibril ,B., Houache, O., Al-Maamari, R., Al-Rashidi, B., "Effects of H_3PO_4 and KOH in Carbonization of Lignocellulosic Material", *J. Anal. Appl. Pyrol.* , Vol. 83, pp. 151–156, 2008.

- Kaghazchi, T., Kolur, N.A., Soleimani, M., "Licorice Residue and Pistachio-nut Shell Mixture: A Promising Precursor for Activated Carbon", *J. Ind. Eng. Chem*., Vol. 16 pp. 368–374, 2010.

- Karamanlıoğlu, M., " Xylan-Based Biodegradable and Wheat Gluten-Based Antimicrobial Film Production", MSc. Thesis in

Biotechnology, Middle East Technical University, Ankara, Turkey, 2008.

- Kazemipour, M. , Ansari, M. , Tajrobehkar, S., Majdzadeh, M., Kermani, H.R., "Removal of Lead, Cadmium, Zinc, and Copper from Industrial Wastewater by Carbon Developed from Walnut, Hazelnut, Almond, Pistachio Shell, and Apricot Stone", *J. Hazard. Mater.* , Vol. 150, pp. 322–327, 2008.

- Kirk Othmer, "Kirk-Othmer Encyclopedia of Chemical Technology", Vol. 4, John Wiley and Sons Inc., 2001.

- Klass, D.L., "Biomass for Renewable Energy, Fuels, and Chemicals" Elsevier Inc. , 1998.

- Kruk, M, , Jaronieca, A, Choma, J., "Comparative Analysis Of Simple and Advanced Sorption Methods for Assessment of Microporosity in Activated Carbons", *Carbon* ,Vol. 36, No. 10, pp. 1447–1458, 1998.

- Lee, J., "Biological Conversion of Lignocellulosic Biomass to Ethanol", *J. Biotechnol.,* Vol. 56, pp. 1–24, 1997.

- Lillo-Rodenas, M.A., Juan-Juan, J., Cazorla-Amoros, D., Linares-Solano, A., "About Reactions Occurring During Chemical Activation with Hydroxides", *Carbon* ,Vol. 42, pp.1371–1375, 2004.

- Lim, W.C., Srinivasakannan,C., Balasubramanian, N., "Activation of Palm Shells by Phosphoric Acid Impregnation for High Yielding Activated Carbon", *J. Anal. Appl Pyrol.* , Vol. 88, pp. 181–186, 2010.

- Lua, A.C., Yang, T., "Effect of Activation Temperature on the Textural and Chemical Properties of Potassium Hydroxide Activated Carbon Prepared from Pistachio-nut Shell", *J. Colloid Interf. Sci.* , Vol. 274, pp. 594–601, 2004 (a).

- Lua, A.C., Yang, T., "Effects of Vacuum Pyrolysis Conditions on the Characteristics of Activated Carbons Derived from Pistachio-nut Shells", *J. Colloid Interf. Sci.,* Vol. 276, pp. 364–372, 2004 (b).

- Lua, A.C., Yang, T., Guo, J. "Effects of Pyrolysis Conditions on the Properties of Activated Carbons Prepared from Pistachio-nut Shells", *J. Anal. Appl. Pyrol.* , Vol. 72, pp. 279–287, 2004.

- Lua, A.C., Yang, T., "Characteristics of Activated Carbon Prepared from Pistachio-nut Shell by Zinc Chloride Activation Under Nitrogen and Vacuum Conditions", *J. Colloid Interf. Sci*., Vol. 290, pp. 505–513, 2005.

- Lowell, S., Shields, J.E., Thomas, M.A., Thommes, M., "Characterization of Porous Solids and Powders: Surface Area, Pore Size and Density", Springer , The Netherlands, 2006.

- Marsh, M., Rodriguez-Reinoso, F., "Activated Carbon", Elsevier, 2006.

- McKendry, P., "Energy Production from Biomass (Part 1): Overview of Biomass", *Bioresour. Technol*., Vol. 83, pp.37-46, 2002.

- McKetta J. J., Cunningham, W. A., "Encyclopedia of Chemical Processing and Design", Vol. 6, M. Dekker Inc., New York, 1978.

- Mendez-Linan, L., Lopez-Garzon, F.J., Domingo-Garcia, M., Perez-Mendoza, M.," Carbon Adsorbents from Polycarbonate Pyrolysis

Char Residue: Hydrogen and Methane Storage Capacities", *Energ. Fuel.*, Vol. 24, pp. 3394–3400, 2010.

- Moreno-Castilla, C., Carrasco-Marin, F., Lopez-Ramon, M.V., Alvarez-Merino, M.A., "Chemical and Physical Activation of Olive-Mill Waste Water to Produce Activated Carbons", *Carbon* , Vol. 39, pp. 1415–1420, 2001.

- Molina-Sabio, M., Almansa, C., Rodriguez-Reinoso, F., "Phosphoric Acid Activated Carbon Discs for Methane Adsorption", *Carbon* , Vol. 41 , pp. 2113-2119, 2003.

- Newcombe, G. and Dixon, D. ,"Interface Science in Drinking Water Treatment", Elsevier, 2006.

- Ok, S., "Adsorption Properties of Carbon Nanoparticles", MSc. Thesis in Chemical Engineering, Middle East Technical University, Ankara, Turkey, 2005.

- Okada,K., Yamamoto, K., Kameshima, Y., Yasumori, A., "Porous Properties of Activated Carbons from Waste Newspaper Prepared by Chemical and Physical Activation", *J. Colloid Interf. Sci.* , Vol. 262, pp. 179–193, 2003.

- Onay, O., Kockar, O. M., "Slow, Fast and Flash Pyrolysis of Rapeseed", Renew. Energ., Vol.28, pp. 2417-2433, 2003.

- Önal, Y., Söylemez, İ., "Production of Activated Carbon From Pistachio-nut Shell by Chemical Activation", UKMK-8 (8^{th} National Chemical Engineering Congress) Proceedings Book, İnönü University, Malatya, Turkey, 2008

- Özmak, M., "Production of Activated Carbon From Biomass Wastes", Ph.D. Thesis in Chemical Engineering, Ankara University, Ankara, Turkey, 2010.

- Öztürk, A., "Production and Characterization of Activated Carbon from Pyrolysis of Copolymers", MSc. Thesis in Chemical Engineering, Middle East Technical University, Ankara, Turkey, 1999.

- Pütün, E., Apaydın-Varol, E., "Carbonaceous Products from Different Biomass Samples: A General Review", Carbon Materials for Today and Future Turkish-Japanese Joint Carbon Symposium, Proceedings Book, pp.46, Istanbul Technical University, 2010.

- Puziy, A.M. , Poddubnaya, O.I. , Martinez-Alonso ,A., Suarez-Garcia, F. , Tascon, J.M.D., "Synthetic Carbons Activated with Phosphoric Acid I. Surface Chemistry and Ion Binding Properties", *Carbon* , Vol. 40, pp. 1493–1505, 2002 (a).

- Puziy, A.M. , Poddubnaya, O.I. , Martinez-Alonso ,A., Suarez-Garcia, F. , Tascon, J.M.D., "Synthetic Carbons Activated with Phosphoric Acid II. Porous Structure", *Carbon* , Vol. 40, pp. 1507–1519, 2002 (b).

- Puziy, A.M. , Poddubnaya, O.I. , Martinez-Alonso ,A., Suarez-Garcia, F. , Tascon, J.M.D., "Synthetic Carbons Activated with Phosphoric Acid III.Carbons Prepared in Air", *Carbon*, Vol. 41, pp. 1181–1191, 2003.

- Raposo, F., De La Rubia, M.A., Borja,R "Methylene Blue Number as Useful Indicator to Evaluate the Adsorptive Capacity of Granular Activated Carbon in Batch Mode: Influence of Adsorbate/Adsorbent

Mass Ratio and Particle Size", *J. Hazard. Mater.* , Vol. 165, pp. 291–299, 2009.

- Ravikovitch, P.I., Neimark, A.V. "Characterization of Micro and Mesoporosity in SBA-15 Materials from Adsorption Data by the NLDFT Method", *J. Phys. Chem*. B, Vol. 105, pp. 6817-6823, 2001.

- Rouquerol, F., Rouquerol, J., Sing, K., "Adsorption by Powders and Porous Solids: Principles, Methodology and Applications", Academic Press, United Kingdom, 1999.

- Schröder, E., Thomauske, K., Weber, C., Hornung, A., Tumiatti, V., "Experiments on the Generation of Activated Carbon from Biomass", *J. Anal. Appl. Pyrol.* , Vol. 79, pp. 106–111, 2007.

- Smisek, M., Cerny, S., "Active Carbon Manufacture, Properties and Aplications", Elsevier, New York, 1970.

- Soleimani, M., Kaghazchi,T., "Adsorption of Gold Ions from Industrial Wastewater Using Activated Carbon Derived from Hard Shell of Apricot Stones – An Agricultural Waste", *Bioresource Technol.* , Vol. 99, pp. 5374–5383, 2008.

- Soleimani, M., Kaghazchi, T., "Agricultural Waste Conversion to Activated Carbon by Chemical Activation with Phosphoric Acid, *Chem. Eng. Technol*, Vol. 30, pp. 649–654, 2007.

- Suarez-Garcia, F., Martinez-Alonso, A., Tascon, J.M.D., "Pyrolysis of Apple Pulp: Chemical Activation with Phosphoric Acid", *J. Anal. Appl. Pyrol.,* Vol. 63, pp. 283–301, 2002.

- Teng, H., Wang, S.C., "Preparation of Porous Carbons from Phenol–Formaldehyde Resins with Chemical and Physical Activation", *Carbon*, Vol. 38, pp. 817–824, 2000.

- Toles, C.A., Marshall, W. E., Mitchell M. Johns, M.M., Wartelle, L.H, Andrew McAloon, A., "Acid-activated Carbons from Almond Shells: Physical, Chemical and Adsorptive Properties and Estimated Cost of Production", *Bioresource Technol.* , Vol. 71, pp. 87-92, 2000.

- Ullmann, " Ullmann's Encyclopedia of Industrial Chemistry", 6th Edition, Wiley VCH Publishers, 2002.

- Valix, M., Cheung, W.H., McKay, G., "Preparation of Activated Carbon Using Low Temperature Carbonisation and Physical Activation of High Ash Raw Bagasse for Acid Dye Adsorption, *Chemosphere* , Vol. 56 , pp. 493–501, 2004.

- Valladares, D.L., Rodriguez Reinoso, F., Zgrablich, G., "Characterization of Active Carbons: The Influence of the Method in the Determination of the Pore Size Distribution", *Carbon* , Vol. 36, pp. 1491–1499, 1998.

- Vernersson, T., Bonelli P.R., Cerrella, E.G., Cukierman, A.L., "Arundo Donax Cane as a Precursor for Activated Carbons: Preparation by Phosphoric Acid Activation", *Bioresource Technol*. , Vol. 83, pp. 95–104, 2002.

- Wigmans, T., "Industrial Aspects of Production and Use of Activated Carbons", *Carbon,* Vol. 27, pp. 13-29, 1989.

- Walker, P.L. "Chemistry and Physics of Carbon", Vol. 2, Marcel Dekker, New York, USA, 1968.

- Wu, F.C., Ru-Ling Tseng, R.L., Hu, C.C., "Comparisons of Pore Properties and Adsorption Performance of KOH-Activated and Steam-Activated Carbons", *Micropor. Mesopor. Mat.,* Vol. 80, pp. 95–106, 2005.

- Yahşi, N.U., "Production and Characterization of Activated Carbon from Apricot Stones", MSc. Thesis in Chemical Engineering, Middle East Technical University, Ankara, Turkey, 2004.

- Yaman, S., "Pyrolysis of Biomass to Produce Fuels and Chemical Feedstocks", *Energy Convers. Manage,* Vol. 45, pp. 651-671, 2004.

- Yang, R.T., "Gas Separation by Adsorption Processes", Imperial Collage Press, London, England, 1997.

- Yang, R.T., "Adsorbents, Fundamentals and Applications", John Wiley & Sons, Inc., New Jersey, USA, 2003.

- Yagmur, E., Ozmak, M., Aktas, Z., "A Novel Method for Production of Activated Carbon from Waste Tea by Chemical Activation with Microwave Energy", *Fuel* ,Vol. 87, pp. 3278–3285, 2008.

- Yang, T., Lua, A.C., "Characteristics of Activated Carbons Prepared from Pistachio-nut Shells by Potassium Hydroxide Activation", *Micropor. Mesopor. Mat.,* Vol. 63, pp. 113–124, 2003 (a).

- Yang, T., Lua, A.C., "Characteristics of Activated Carbons Prepared from Pistachio-nut Shells by Physical Activation", *J. Colloid Interf. Sci.*, Vol. 267, pp. 408–417, 2003 (b)

- Yang, T., Lua, A.C., "Textural and Chemical Properties of Zinc Chloride Activated Carbons Prepared from Pistachio-nut Shells", *Mater. Chem. Phys.,* Vol. 100, pp. 438–444, 2006.

- Yang, K., Peng, J.,Srinivasakannan, C., Zhang, L., Xia, H., Duan, X., "Preparation of High Surface Area Activated Carbon from Coconut Shells Using Microwave Heating", *Bioresource Technol.* , Vol. 101, pp. 6163–6169, 2010.

- Yeganeh, M. M., Kaghazchi, T., Soleimani, M., "Effect of Raw Materials on Properties of Activated Carbons", *Chem. Eng. Technol.*, Vol. 29, pp. 1247-1251, 2006.

- Zhang, T., Walawender, W. P., Fan, L.T. , Fan, M., Daugaard,D., Brown, R.C., "Preparation of Activated Carbon from Forest and Agricultural Residues Through CO_2 Activation", *Chem. Eng. J.* , Vol. 105, pp. 53–59, 2004.

- Zuo, S., Yang, J., Liu , J., Cai, X., "Significance of the Carbonization of Volatile Pyrolytic Products on the Properties of Activated Carbons from Phosphoric Acid Activation of Lignocellulosic Material", *Fuel Process. Technol.,* Vol. 90, pp. 994–1001, 2009.

APPENDIX A

ANALYSIS OF N_2 SORPION DATA

A.1. Determination of BET Surface Area

BET surface areas of the products can be obtained by the physical adsorption data of nitrogen molecules on the surface. (Brunauer et al., 1938).

Final form of BET equation can be expressed as;

$$\frac{P}{V[P_O - P]} = \frac{1}{VmC} + \frac{C-1}{V_mC}\frac{P}{P_O} \qquad \text{(B.1)}$$

According to the equation mentioned above,in a relative pressure range of 0.05-0.3 , a plot of P/ V (P_o-P) versus P/P_o yields a line with a slope (S) and an intercept (I) which are given as;

$$S = \frac{C-1}{V_mC} \quad \text{and} \quad I = \frac{1}{VmC} \qquad \text{(B.2)}$$

The graphical representation of BET equation is given in Figure A.1.

BET surface area can be determined using the following equation;

$$S_{BET} = \frac{\left[\left(CSA_{N_2}\,nm^2\right)\left(6.023x10^{23}(1/mol)\right)\right]}{\left[\left(22414\left(cm^3/mol - STP\right)\right)\left(10^{18}\left(nm^2/m^2\right)\right)\left((S+I)\left(g/cm^3 - STP\right)\right)\right]} \qquad \text{(B.3)}$$

where CSA_{N2} denotes cross sectional area of a nitrogen molecule and has a numerical value of 0.162 nm^2. (Walker et al.,1968)

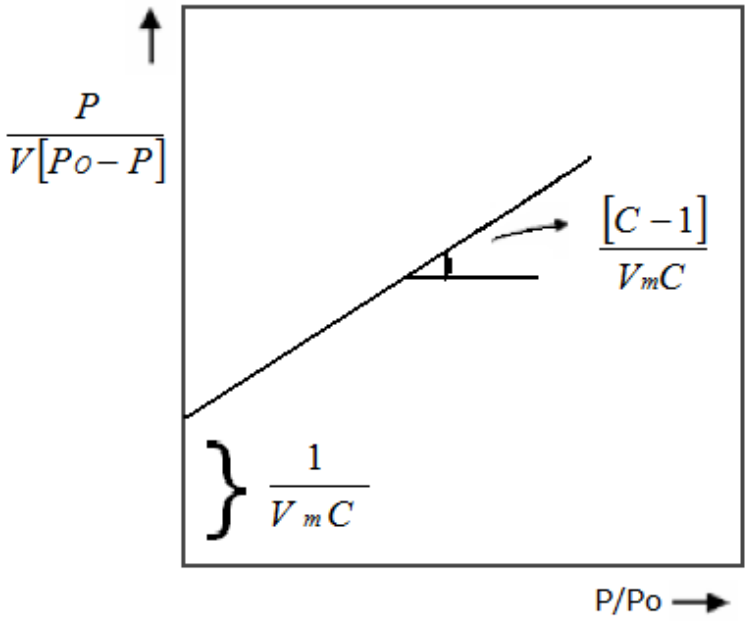

Figure A.1 Graphical Representation of BET Equation

A.2. Analysis of Mesopores

The study of the pore structure including pore size and pore size distributions generally make use of Kelvin equation which is a quantitative expression of capillary condensation. This equation takes into account both equilibrium vapor pressure of a curved structure such as that of a liquid in a pore or cappilary and the equilibrium pressure of the same fluid on a plane surface (Gregg and Sing, 1982; Lowell et al., 2006).

The Kelvin equation is stated as;

$$\ln \frac{P}{Po} = \frac{-2\gamma Vmol Cos\theta}{r_p RT} \qquad \text{(B.4)}$$

In the equation above, P and P_o denote equilibrium vapor pressure of liquid contained in a narrow pore of radius r_p and equilibrium pressure

of the same liquid at a plane surface, respectevely. γ and V_{mol} terms belong to surface tension and molar volume of the fluid and θ term represent contact (wetting) angle with which the liquid meets the pore wall.

If d_n moles of vapor in equilibrium with the bulk liquid at pressure P_o into a pore where the equilibrium pressure P is considered to be transferred, this transport process include three steps. These three steps are; evaporation from the bulk fluid, expansion of vapor from P_o to P and condensation in the pore. If these three steps are analyzed thermodynamically, undoubtedly the free energies of first and last steps will be equal to zero since these steps are equilibrium processes. But, free energy of the second step is given by;

$$dG = \left(RT\ln\left(\frac{P}{Po}\right)\right)dn \qquad \text{(B.5)}$$

When the adsorbate condenses in the pore;

$$dG = -(\gamma Cos\theta)dS \qquad \text{(B.6)}$$

where θ is the wetting angle that is taken to be zero because of the assumption of the liquid is wet completely the adsorbed layer and dS corresponds to the change in the area of film-vapor interface. If a combination of equations B.5 and B.6 is done;

$$\frac{dn}{dS} = \frac{-\gamma}{RT\ln(P/Po)} \qquad \text{(B.7)}$$

If Vp is the volume of liquid adsorbate which condenses in a pore of volume, it will be given by;

$$dVp = Vmoldn \qquad \text{(B.8)}$$

And a substitution of equation B.7 into B.8 is done, equation B.9 can be obtained as;

$$\frac{dVp}{dS} = \frac{-\gamma Vmol}{RT\ln(P/Po)} \tag{B.9}$$

Undoubtedly, the ratio of volume to area within a pore related with the geometry of the pore. In the cases of pores with a wide variety of regular geometries or pores with highly irregular shapes, mathematical expression of the volume to area ratio will be so complex and challenging. Also specific information about pore geometry may be deficient. Under these circumstances, the pore geometry is usually assumed to be cylindrical. Equation B.9 with cylindrical pore geometry assumption leads to equation B.10 or Kelvin equation, since the ratio of volume to area is r/2 for cylinders;

$$\ln\left(\frac{P}{Po}\right) = \frac{-2\gamma Vmol}{rRT} \tag{B.10}$$

For nitrogen molecule at its normal boiling point of -195.6 ^{o}C, the Kelvin equation can be rewrited as;

$$r_k = \frac{2\left(8.85\frac{erg}{cm^2}\right)\left(34.6\frac{cm^3}{mol}\right)\left(\frac{10^{8\,o}A}{cm}\right)}{\left(8.314x10^{7}\frac{erg}{Kmol}\right)(77K)(2.303)\log(P_o/P)} \tag{B.11}$$

In the equation B.8, numerical values of 8.85 erg/cm^2 and 34.6 cm^3 come from the surface tension and molar volume of liquid nitrogen at -195.6 ^{o}C. After calculation and arrangement equation B.12 can be found as;

$$r_k = \frac{4.15}{\log(P_o/P)} \tag{B.12}$$

The term r_k is the radius into which condensation takes place at the required relative pressure. It is also called Kelvin radius or critical radius.

It can't be stated as the actual pore radius since some adsorption has already occurred on the pore wall prior to condensation, leaving a center core or radius r_k. Similarly, an adsorbed film remains on the pore wall when evaporation of the center core occurs during desorption. By considering the depth of the film when condensation or evaporation occurs as t, the actual pore radius is given by;

$$r_p = r_k + t \qquad \text{(B.13)}$$

Equation B.13 is used to calculate pore radius, r_p, but the value of adsorbed film depth, t, is necessary for the calculation. By assuming that adsorbed film depth in a pore is the same as that on a plane surface at any relative pressure, one can write;

$$t = \left(\frac{W_a}{W_m}\right)\tau \qquad \text{(B.14)}$$

The terms Wa and Wm indicate the quantity adsorbed at a particular relative pressure and the weight corresponding to the BET monolayer, respectively. Basically, equation B.14 expresses that the thickness of the adsorbed film can be found by multiplying the number of layers with the thickness of one layer, τ, regardless of whether the film is in a pore or on a plane surface. By considering the area, S, and the volume filled by one mole of liquid nitrogen, V_{mol}, the value of τ can be calculated if it was spread over a surface to the depth of one molecular layer;

$$\tau = \frac{V_{mol}}{S} = \frac{\left(34.6x10^{24}\right)A^3}{\left(16.2\frac{A^2}{mol}\right)\left(6.02x10^{23}\frac{1}{mol}\right)} = 3.54Å \qquad \text{(B.15)}$$

Above a relative pressure of 0.3, when W_a/W_m versus P/P_o data is plotted for nonporous materials, it has been observed that data all approximately fit common type II curve.

The common curve is intimately characterized by Halsey (1948),

equation which for nitrogen can be stated as;

$$t = 3.54\left(\frac{5}{2.303\log\left(P_o/P\right)}\right)^{1/3} \qquad \text{(B.16)}$$

The thickness of the adsorbed layer that is calculated for a specific relative pressure from the equation B.16 and this thickness becomes thicker and thicker with successive increase in pressure. That's why, the measured amount of gas in a step includes the quantity of liquid cores formed and a quantity adsorbed by the pore walls of pores whose cores have been formed in that and early steps. A method which was developed by Barrett, Joyner and Halenda, combines these described concepts. The N_2 adsorption device used in the present study also performs BJH method with an algorithm. This implementation is done by determining $\Delta V_{gas,}$ the change in adsorbed volume between two consecutive P/Po values. Then ΔV_{gas} values can be converted to ΔV_{liq} values, change in volume in liquid state by multiplying the molar volume of liquid nitrogen at standard temperature and pressure. This conversion can be showed as;

$$\Delta V_{liq} = \frac{\Delta V_{gas}\left(cm^3/g\right)}{22414\left(cm^3/mol - STP\right)}\left(34.6\left(cm^3/mol\right)\right) = \Delta V_{gas}\left(1.54x10^{-3}\right) \qquad \text{(B.17)}$$

The actual pore volume is determined by;

$$\Delta V_{liq} = \pi r^2{}_{KAVE} + \Delta t \sum S \qquad \text{(B.18)}$$

In the equation B.18, the term r_{KAVE} corresponds to the average Kelvin radius and $\Delta t\ \Sigma S$ is the product of the increase in the film depth and film area, so;

$$V_p = \pi r^2{}_{PAVE} L \qquad \text{(B.19)}$$

where L is the pore length. If a combination of equations B.18 and B.19 is done;

$$V_p = \left(\frac{r_{PAVE}}{r_{KAVE}} \right)^2 \left[\Delta V_{liq} - \left(\Delta t \sum S \right) \left(10^{-4} \right) \right] \text{ (cm}^3\text{)} \qquad \text{(B.20)}$$

Since a cylindrical pore assumption is done, the surface area of the pore walls can be calculated by pore volume;

$$S = \frac{2V_p}{r_{PAVE}} \left(10^4 \right) \text{ (m}^2\text{)} \qquad \text{(B.21)}$$

Finally, mesopore volume and surface area can be calculated by applying the incremental pore volume and surface area values obtained from the equations B.20 and B.21;

$$V_{meso} = \left[\sum V_p \Big|_{d_p = 0.002\mu.} - \sum V_p \Big|_{d_p = 0.05\mu.} \right] \text{(cm}^3\text{/g)} \qquad \text{(B.22)}$$

$$S_{meso} = \left[\sum S \Big|_{d_p = 0.002\mu.} - \sum S \Big|_{d_p = 0.05\mu.} \right] \text{(m}^2\text{/g)} \qquad \text{(B.23)}$$

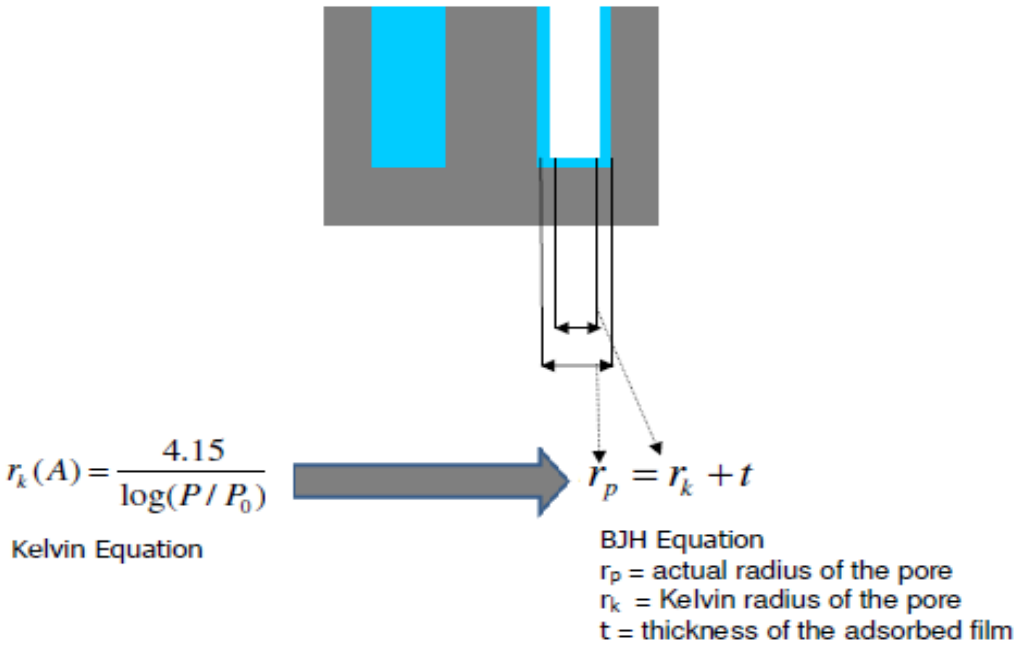

Figure A.2 Layer Approximation in BJH Method (Ok, 2005)

APPENDIX B

SCHEME OF PANEL COMPONENTS OF SURFACE ANALYZER

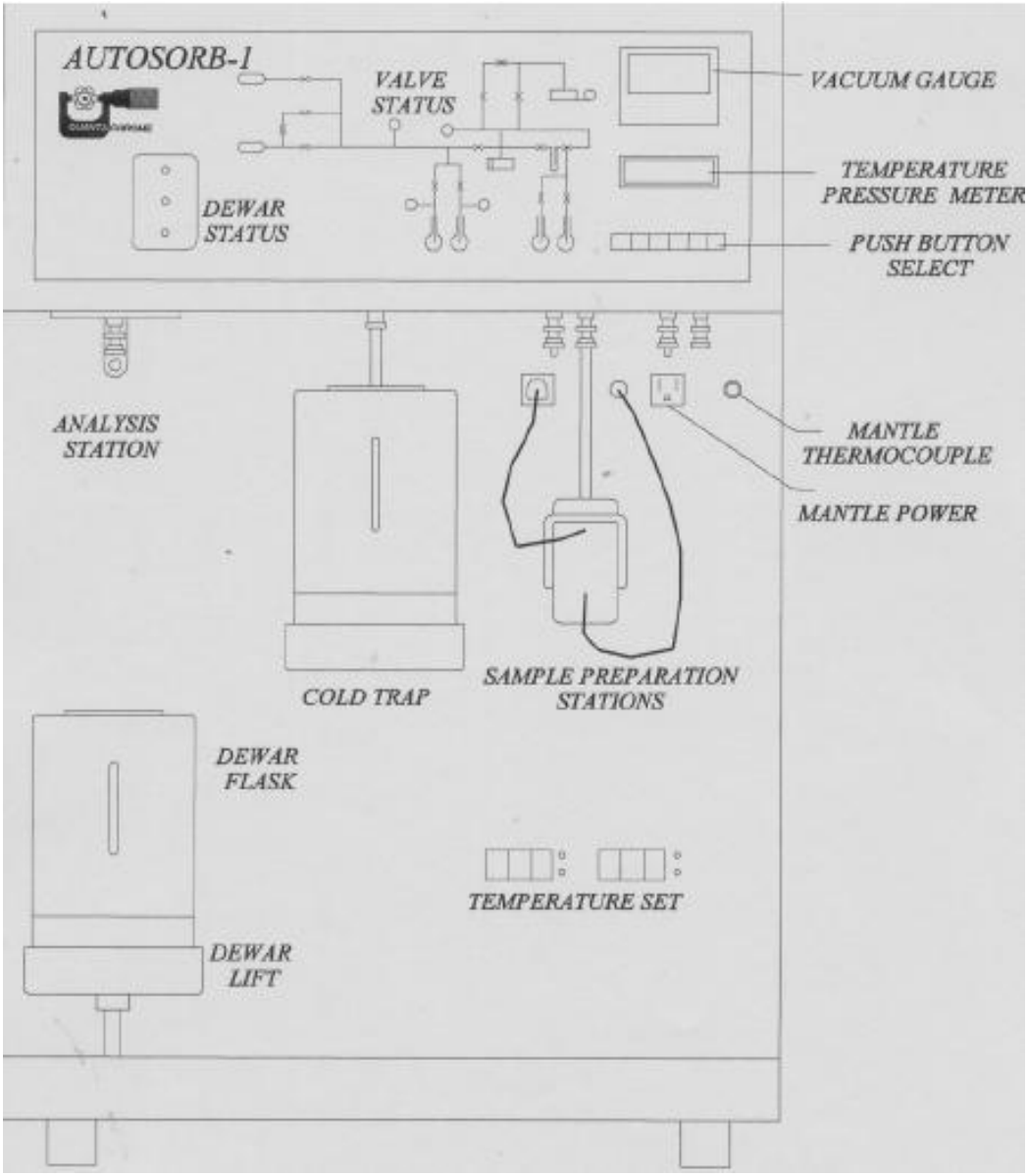

Figure B.1 Scheme of Panel Components of Surface Analyzer Device

APPENDIX C

ANALYSIS OF HELIUM PYCNOMETER DATA

C.1. Determination of True Density

In the determination of true densities of selected products helium displacement method was used. A commercial automatic helium pycnometer, "Ultrapycnometer 1000" manufactured by Quantachrome Corporation was used to measure true densities of the products

.

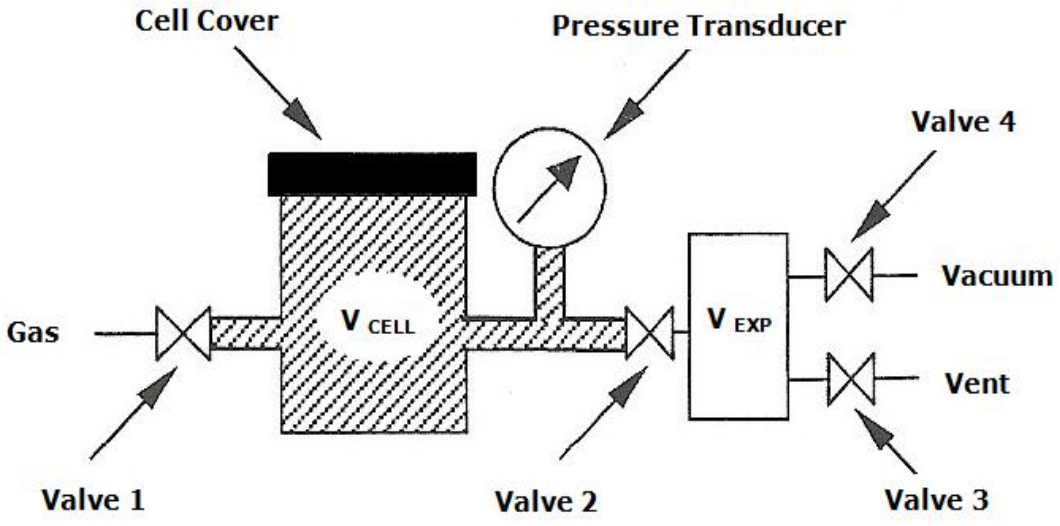

Figure C.1 Shematic Representation of Gas Expansion Pycnometer (Lowell et al., 2006)

Since true or real density is the ratio of the mass to the volume occupied, the volume of pores should be subtracted in the true density measurement. Commercial pycnometers operate by using the principle of gas expansion or Boyle's law and Archimedes' principle of fluid displacement.

In the figure, the shaded volume is the cell volume which is the volume of the sample cell. Prior to the measurement all the volumes were brought to ambient pressure, P_a, at the ambient temperature, T_a, by purging. When cell volume,V_{CELL}, was charged to a higher pressure,P_1, the mass balance equation across the cell would be written as;

$$P_1\left(V_{CELL} - V_{SAMP}\right) = n_C R T_a \qquad \text{(C.1)}$$

In the equation C.1 V_{SAMP} is the volume of powdered sample, n_c is the number of moles of gas in the sample cell and R is the gas constant.

If n_E is the number of moles of gas in the expansion volume, a mass equation for the expansion volume can be expressed as;

$$P_a V_{EXP} = n_E R T_a \qquad \text{(C.2)}$$

When the valve 2 is opened, pressure drops to P_2 and the reference volume, V_{EXP} , is transferred from the cell. Then mass balance becomes;

$$P_2\left(V_{CELL} - V_{SAMP} + V_{EXP}\right) = n_C R T_a + n_E R T_a \qquad \text{(C.3)}$$

Then a substitution of equations C.1 and C.2 into equation C.3 resulted in another equation;

$$V_{CELL} - V_{SAMP} = \frac{P_a - P_2}{P_2 - P_1} V_{EXP} \qquad \text{(C.4)}$$

After arrangements of equation C.4;

$$V_{SAMP} = V_{CELL} - \frac{V_{EXP}}{\frac{(P_1 - P_a)}{(P_2 - P_a)} - 1} \quad (C.5)$$

Because P_1, P_2 and P_a pressures are stated in equations C.1 through C.5 as absolute pressures, equation D.5 has derived so that P_a is subtracted from P_1 and P_2. Then new pressures may be redefined as gauge pressures as P_{1g} and P_{2g}.

$$P_{1g} = P_1 - P_a \quad (C.6)$$

$$P_{2g} = P_2 - P_a \quad (C.7)$$

Finally, equation C.5 may be expressed as the working equation of the helium pycnometer;

$$V_{SAMP} = V_{CELL} - \frac{V_{EXP}}{\frac{P_{1g}}{P_{2g}} - 1} \quad (C.8)$$

C.2 Sample Calculation

By using AAR-1-500 as a sample;

V_{SAMP}= 1.5587 cm^3 and m_{SAMP}= 2.3731 g

$$\rho_{SAMP} = \frac{m_{SAMP}}{V_{SAMP}} = \frac{2.3731}{1.5587} = 1.5225 \text{ g/cm}^3$$

APPENDIX D

EXPERIMENTAL DATA FOR METHYLENE BLUE NUMBER DETERMINATION

Methylene blue is a dark green powder which possesses a dark blue color in aqueous solutions. Since methylene blue is a model of viable pollution, it is widely used in the evaluation of activated carbon in liquid phase adsorption. Methylene blue number (MBN) is an indicator of performance and adsorptive capacity of activated carbon like iodine number, molasses number.

A chemical compound absorbs the light at specific wavelengths and this is related with the electronic structure of the compound. Besides, intensity of absorption of light depends on the quantity of the molecules between the light source and the dedector. By using a UV spectrometer, quantitative and qualitative information of a given compound can be obtained by measuring the amount of ultraviolet and visible light absorbed by the sample placed in the device.

Before measuring, an empirical calibration curve is done with the known concentrations of methylene blue. Data for these calibration and calibration curve is given in Table D.1 and Figure D.1, respectively.

After the adsorption of methylene blue, samples were taken and diluted to one of one hundred before the measurement by UV spectrometer. Absorbance values of UV measurements can be seen n Table D.2.

Table D.1 Data for Calibration Curve

Methylene Blue Concentration(mg/l)	Absorbance
0	0
4.28	0.088
10.7	0.237
21.4	0.555
42.8	1.16

Absorbance of blank experiment = 0.0510 (1/100 dilution)

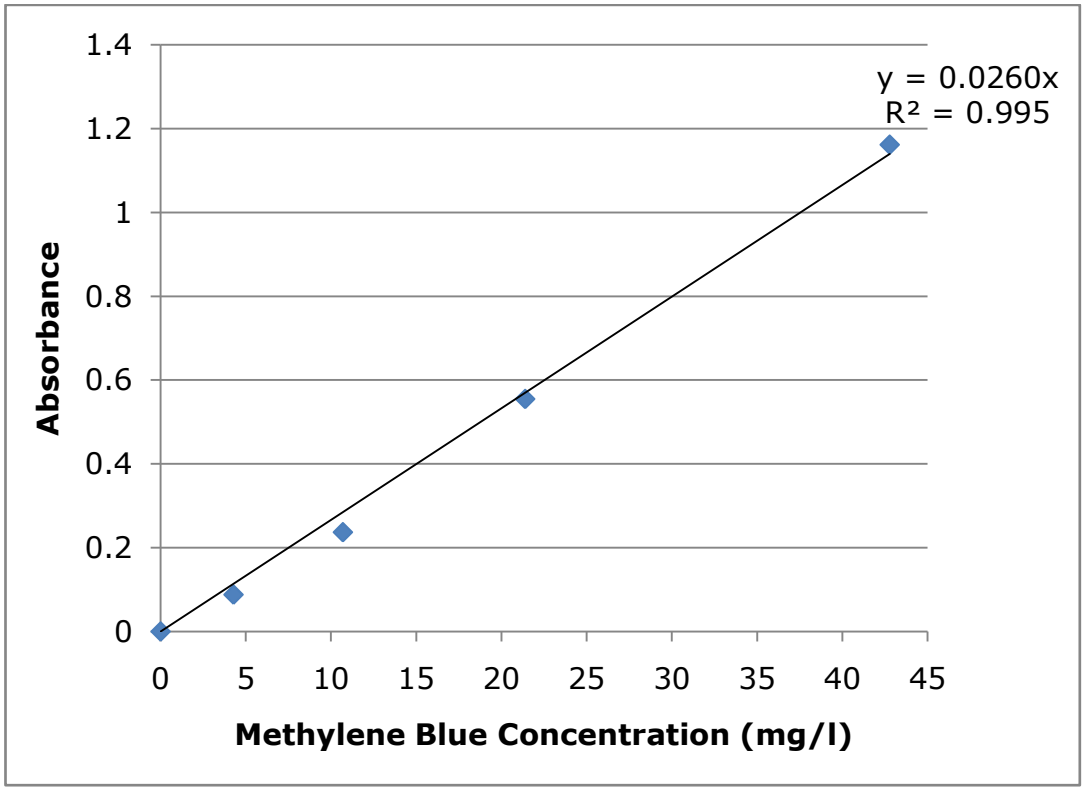

Figure D.1 Calibration Curve for Methylene Blue Number Experiments

Table D.2 Results of UV Measurements

Activated Carbon	Absorbance	Dilution
AAR-1-300	0.831	-
AAR-1-500	0.117	-
AAR-1-700	0.0110	1/100
AAR-1-900	0.0400	-
AAR-2-300	0.0790	-
AAR-2-500	0.0690	-
AAR-2-700	0.0870	-
AAR-2-900	0.0340	-
AAR-3-300	0.0190	1/100
AAR-3-500	0.0330	-
AAR-3-700	0.0480	-
AAR-3-900	0.0720	-

Sample Calculation for AAR-1-300;

Concentration of blank experiment= (0.051/ 0.026)x100= 196.154 mg/L

Final concentration of solution= 31.961 mg/L

$$\mathrm{MBN} = \frac{(\mathrm{Cblank} - \mathrm{Cfinal})\mathrm{x\ Vsol}}{\mathrm{MAC}} \qquad \text{(D.1)}$$

$$\mathrm{MBN} = \frac{(196.154 - 31.961)\mathrm{mg/L\ x\ 0.05L}}{0.1\ \mathrm{g}}$$

MBN= 82.096 mg/g

$$\mathrm{SMB} = \frac{\mathrm{MNB\ x\ MB\ Surface\ \ Area\ x\ Avagadro\ \ no}}{\mathrm{MB\ Molecular\ \ Weig\ ht}} \qquad \text{(D.2)}$$

MB Surface Area= 1.62×10^{-18} m^2/molecule

MB Molecular Weight = 319.86 g/mol

Avagadro no= 6.02×10^{23}

S_{MB}= 250.307 m^2/g

S_{MB}/S_{BET}= 250.307/1133 = 0.221

APPENDIX E

ASH CONTENT OF ACTIVATED CARBONS

Table E.1 Ash Contents of Phosphoric Acid Activated Carbons

Activated Carbon	Ash Content (%)	Activated Carbon	Ash Content (%)
AAR-1-300	0.649	AAC-1-300	2.26
AAR-1-500	5.76	AAC-1-500	4.19
AAR-1-700	6.48	AAC-1-700	5.14
AAR-1-900	7.91	AAC-1-900	9.15
AAR-2-300	1.62	AAC-2-300	2.75
AAR-2-500	8.32	AAC-2-500	2.92
AAR-2-700	6.68	AAC-2-700	5.67
AAR-2-900	4.35	AAC-2-900	6.56
AAR-3-300	2.97	AAC-3-300	2.38
AAR-3-500	6.01	AAC-3-500	6.66
AAR-3-700	11.0	AAC-3-700	10.3
AAR-3-900	9.41	AAC-3-900	11.9

Table E.2 Ash Contents of Potassium Hydroxide Activated Carbons

Activated Carbon	**Ash Content (%)**
ABC-1-300	0.646
ABC-1-500	0.702
ABC-1-700	0.974
ABC-1-900	1.20

APPENDIX F

THERMOGRAVIMETRIC ANALYSIS

Table F.1 Yield Values (%) for Samples Impregnated by Phosphoric Acid for an Impregnation Ratio of 1/1 (Raw Material Activation Method)

Temperature (°C)	**300**	**500**	**700**	**900**
Acid Impregnated Pistachio-nut Shells	58.1	47.6	37.9	21.4
Raw Pistachio-nut Shells	74.3	27.2	21.6	19.7

Table F.2 Yield Values (%) for Samples Impregnated by Phosphoric Acid for an Impregnation Ratio of 2/1 (Raw Material Activation Method)

Temperature (°C)	**300**	**500**	**700**	**900**
Acid Impregnated Pistachio-nut Shells	64.0	52.2	35.6	17.6
Raw Pistachio-nut Shells	74.3	27.2	21.6	19.7

Table F.3 Yield Values (%) for Samples Impregnated by Phosphoric Acid for an Impregnation Ratio of 3/1 (Raw Material Activation Method)

Temperature (°C)	**300**	**500**	**700**	**900**
Acid Impregnated Pistachio-nut Shells	59.8	50.4	35.8	15.7
Raw Pistachio-nut Shells	74.3	27.2	21.6	19.7

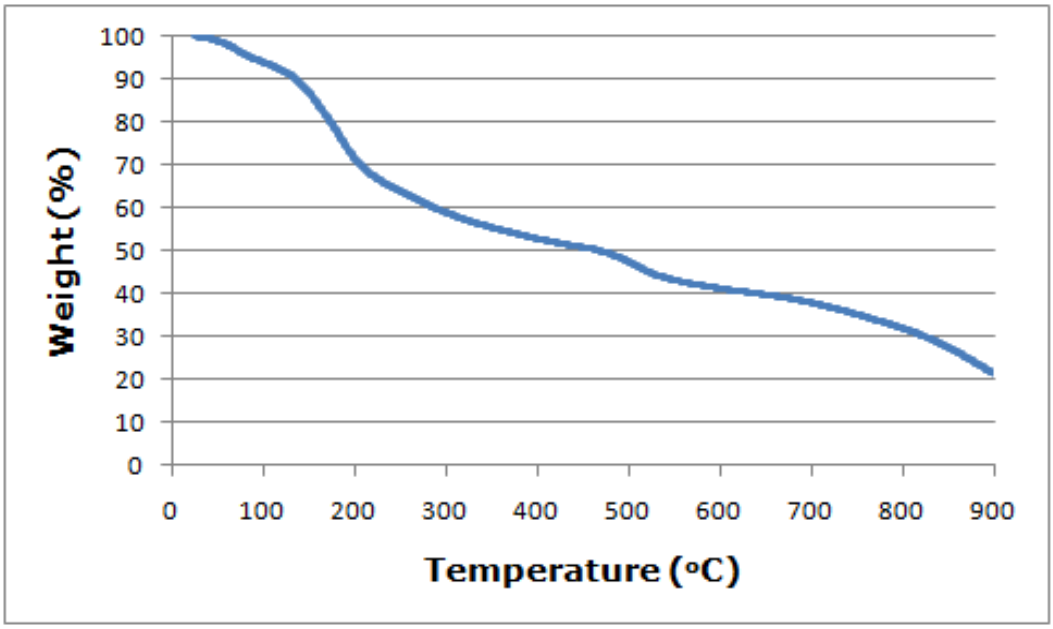

Figure F.1 TGA Result of Phosphoric Acid Impregnated Pistachio-nut Shells for T=900 °C (Impregnation Ratio= 1/1)

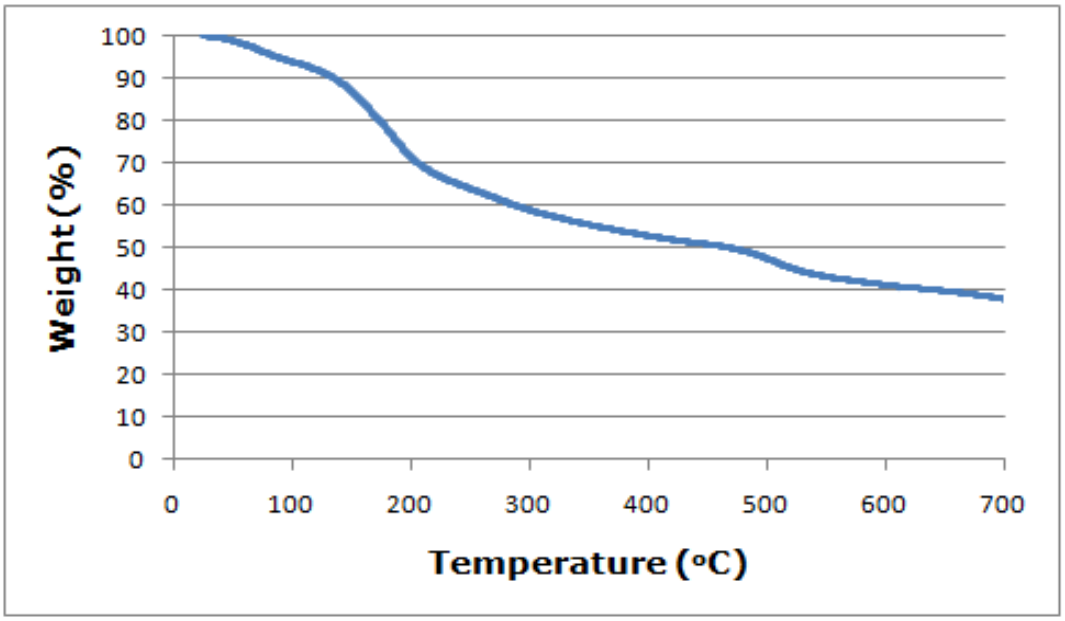

Figure F.2 TGA Result of Phosphoric Acid Impregnated Pistachio-nut Shells for T=700 °C (Impregnation Ratio= 1/1)

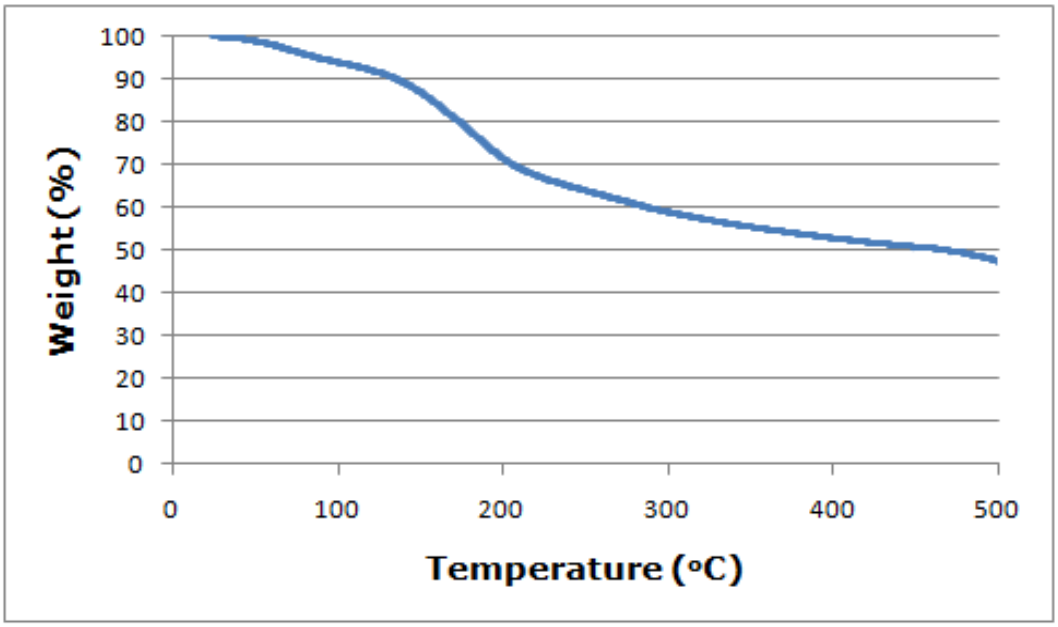

Figure F.3 TGA Result of Phosphoric Acid Impregnated Pistachio-nut Shells for T=500 °C (impregnation ratio= 1/1)

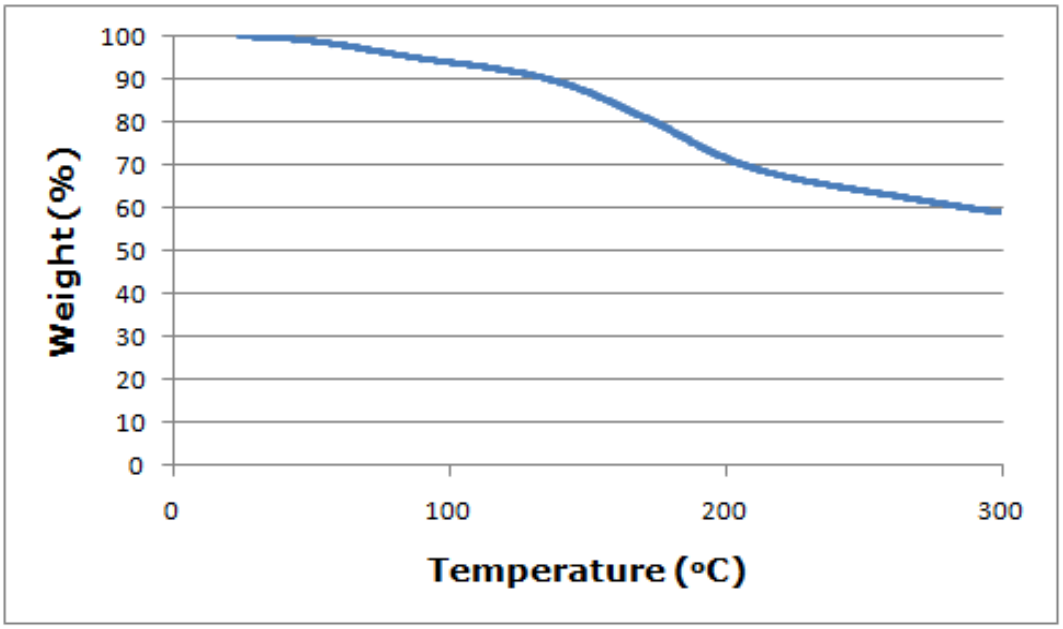

Figure F.4 TGA Result of Phosphoric Acid Impregnated Pistachio-nut Shells for T=300 °C (Impregnation Ratio= 1/1

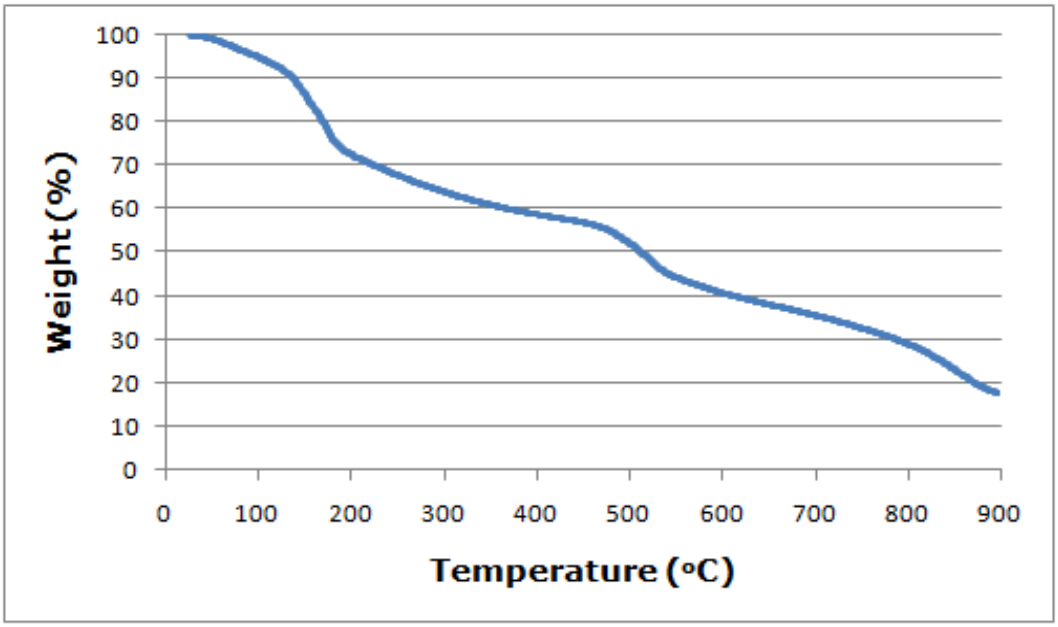

Figure F.5 TGA Result of Phosphoric Acid Impregnated Pistachio-nut Shells for T=900 °C (Impregnation Ratio= 2/1)

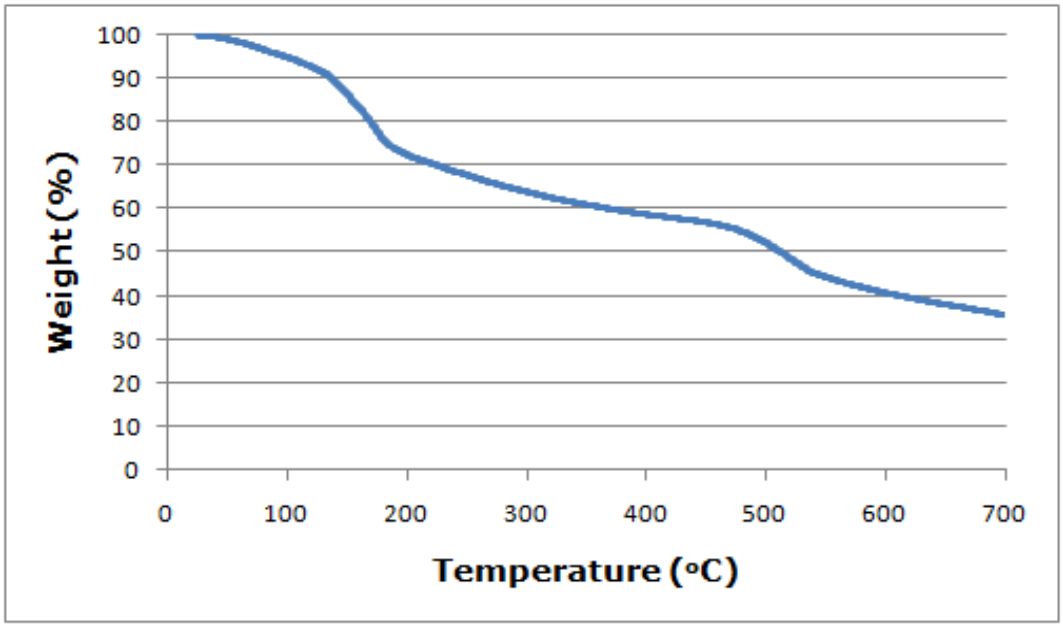

Figure F.6 TGA Result of Phosphoric Acid İmpregnated Pistachio-Nut Shells for T=700 °C (Impregnation Ratio= 2/1)

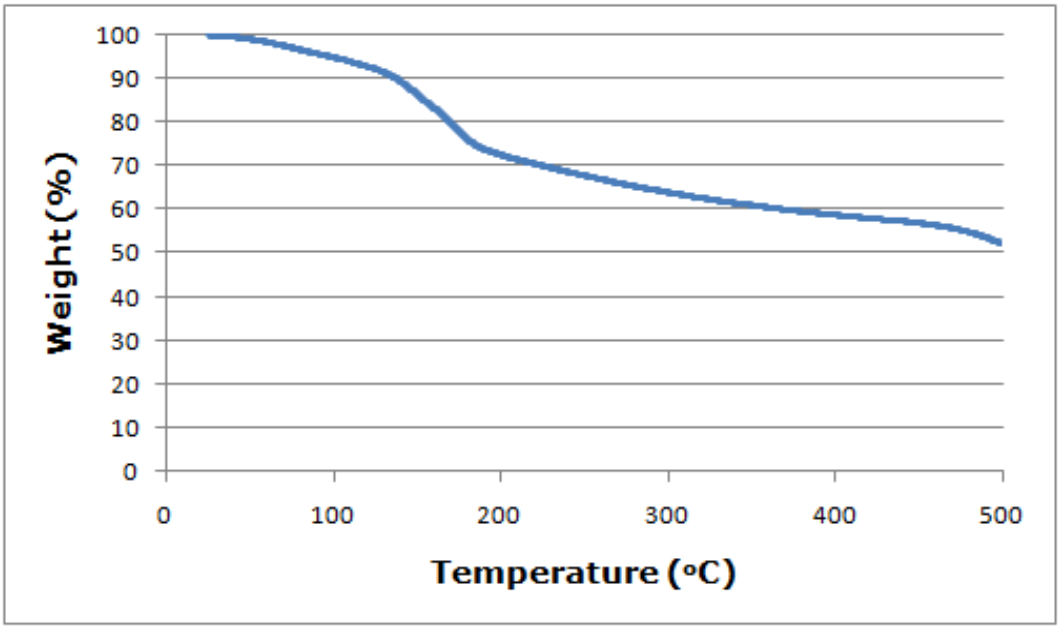

Figure F.7 TGA Result of Phosphoric Acid Impregnated Pistachio-nut shells for T=500 °C (Impregnation Ratio= 2/1)

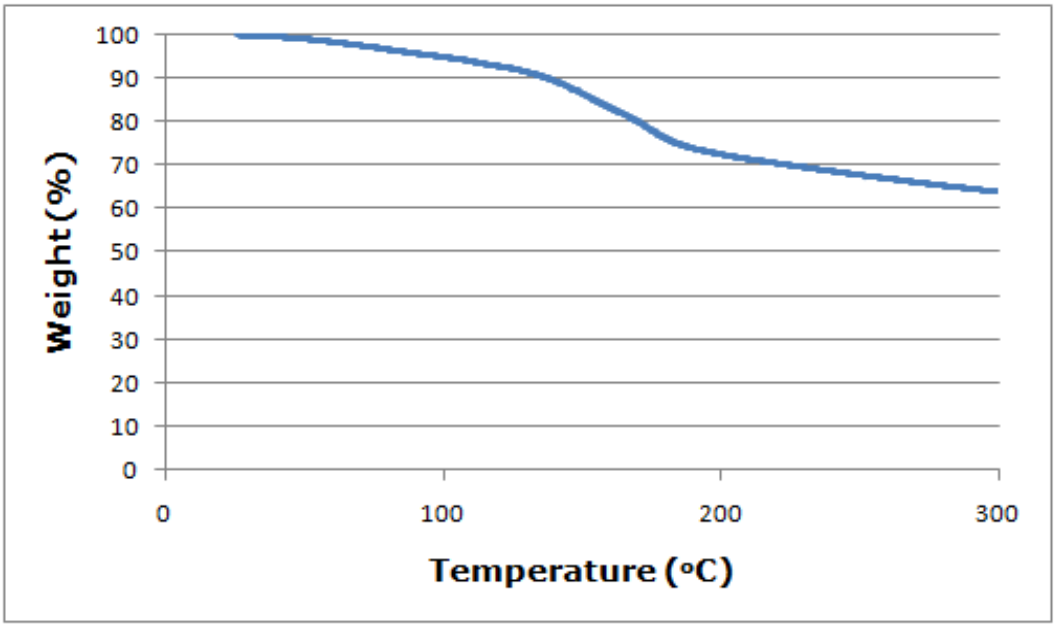

Figure F.8 TGA Result of Phosphoric Acid Impregnated Pistachio-nut Shells for T=300 °C (Impregnation Ratio= 2/1)

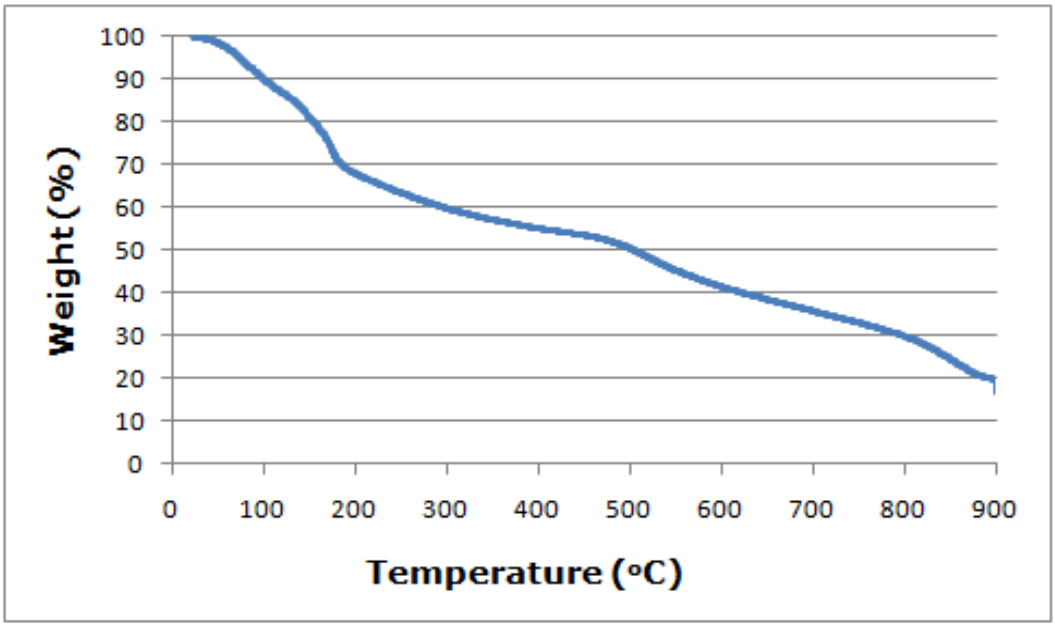

Figure F.9 TGA Result of Phosphoric Acid Impregnated Pistachio-nut Shells for T=900 °C (Impregnation Ratio= 3/1)

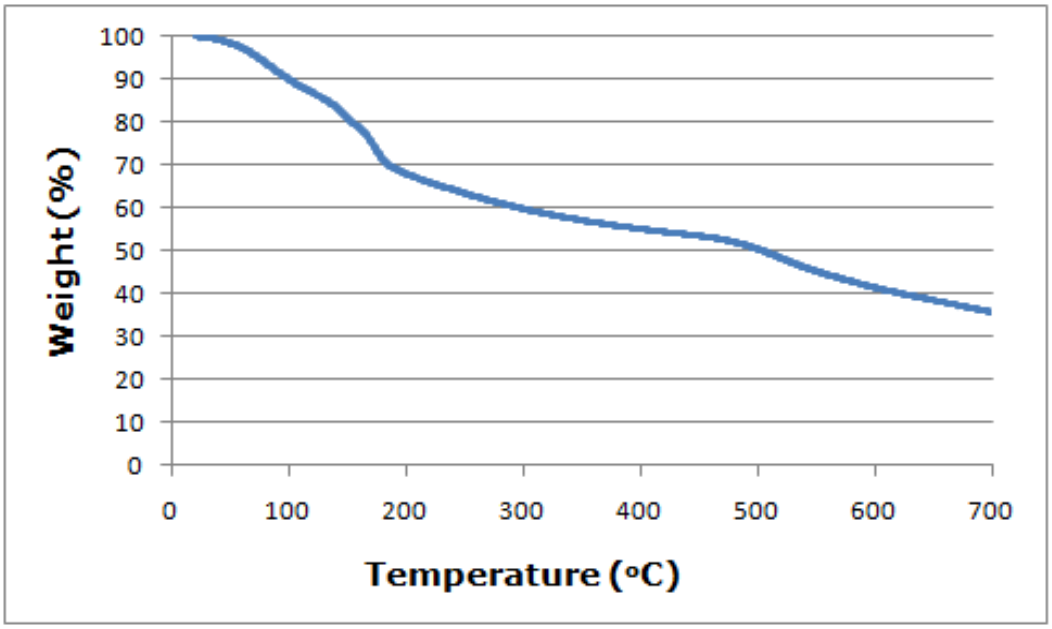

Figure F.10 TGA Result of Phosphoric Acid Impregnated Pistachio-nut Shells for T=700 °C (Impregnation Ratio= 3/1)

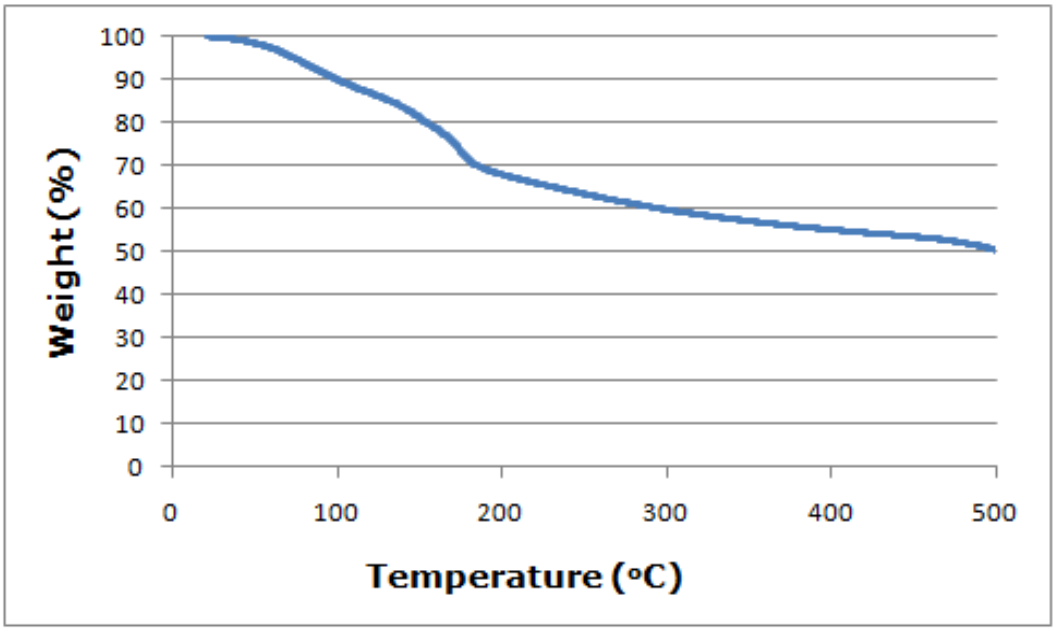

Figure F.11 TGA Result of Phosphoric Acid Impregnated Pistachio-nut Shells for T=500 °C (Impregnation Ratio= 3/1)

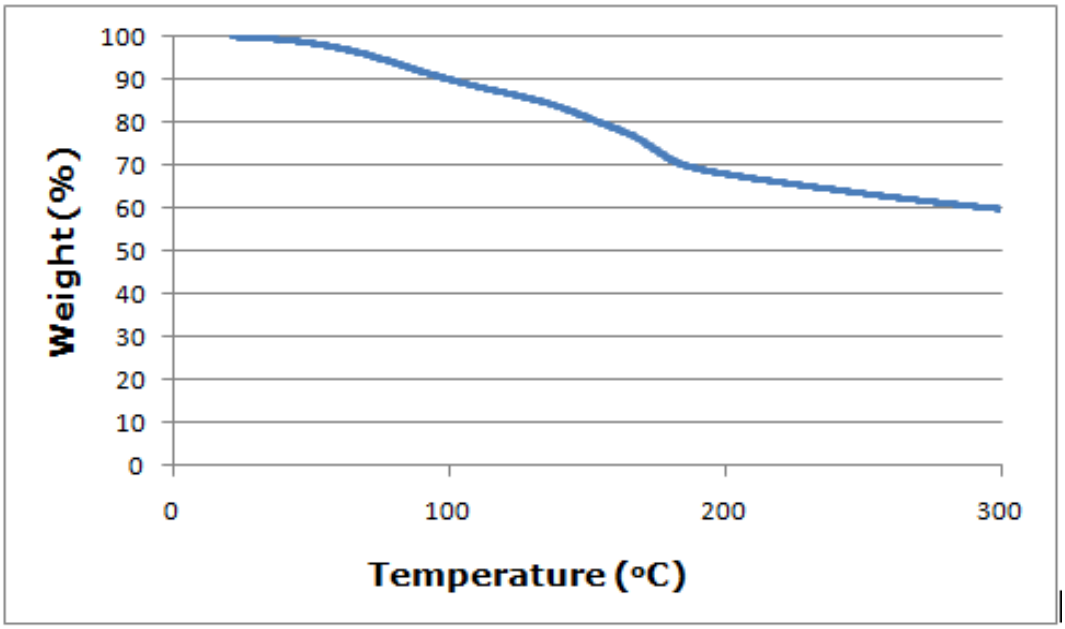

Figure F.12 TGA Result of Phosphoric Acid Impregnated Pistachio-nut Shells for T=300 °C (Impregnation Ratio= 3/1)

Table F.4 Yield Values (%) for Samples Impregnated by Phosphoric Acid (Char Activation Method)

Impregnation Ratio (H_3PO_4 / Char)	**Activation Temperature (°C)**	**Yield (%)**
1/1	300	23.2
1/1	500	20.5
1/1	700	13.7
1/1	900	7.90
2/1	300	22.2
2/1	500	19.8
2/1	700	14.1
2/1	900	8.15
3/1	300	22.7
3/1	500	21.2
3/1	700	16.4
3/1	900	13.0

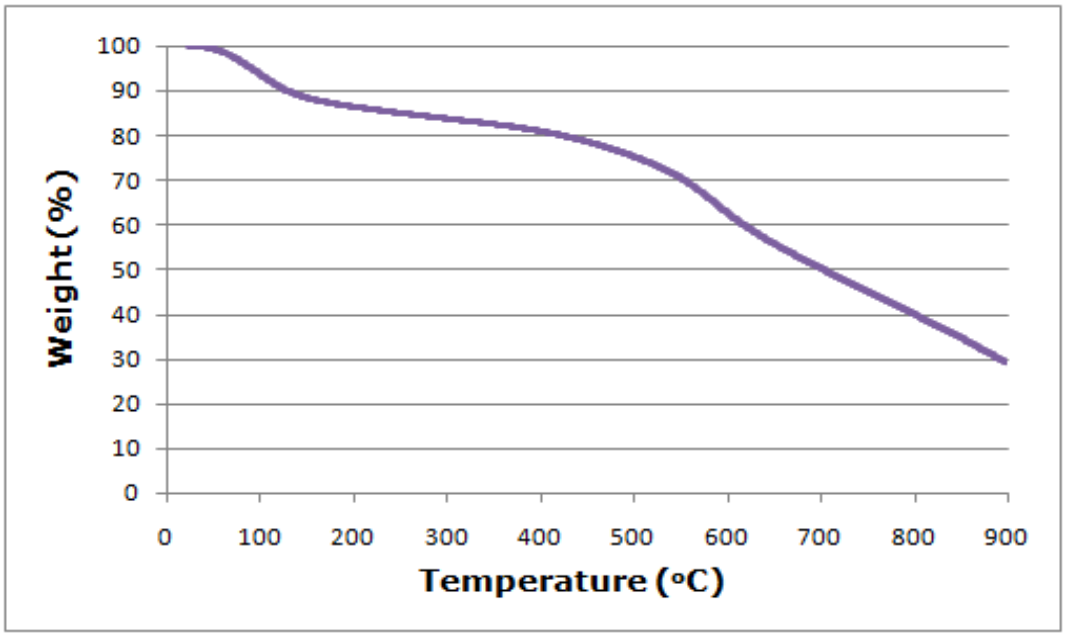

Figure F.13 TGA Result of Phosphoric Acid Impregnated Char for T=900 °C (Impregnation Ratio= 1/1)

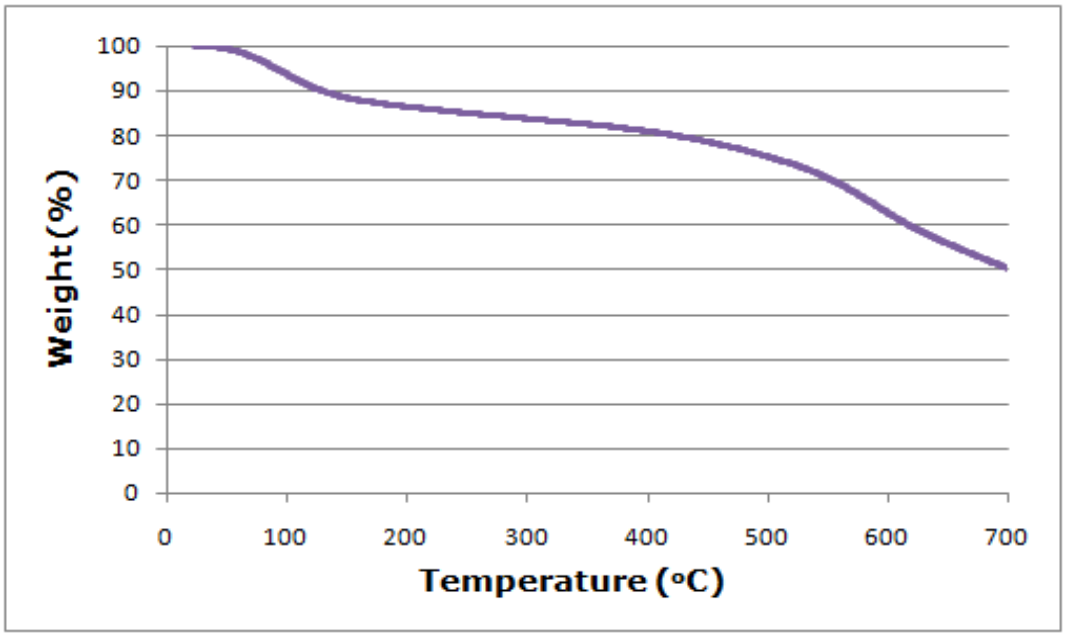

Figure F.14 TGA Result of Phosphoric Acid Impregnated Char for T=700 °C (Impregnation Ratio= 1/1)

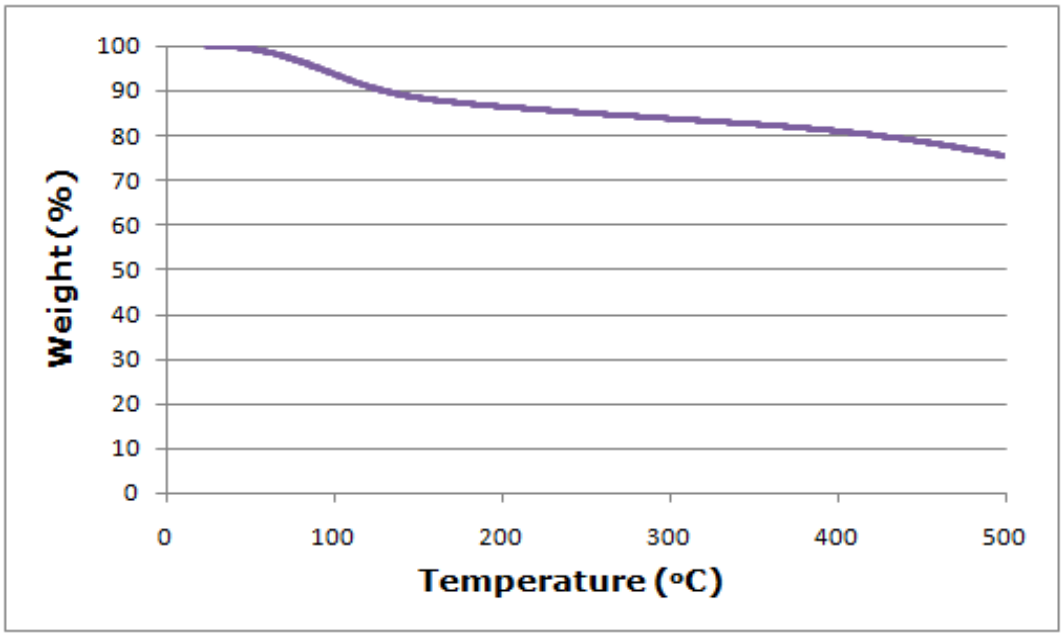

Figure F.15 TGA Result of Phosphoric Acid Impregnated Char for T=500 °C (Impregnation Ratio= 1/1)

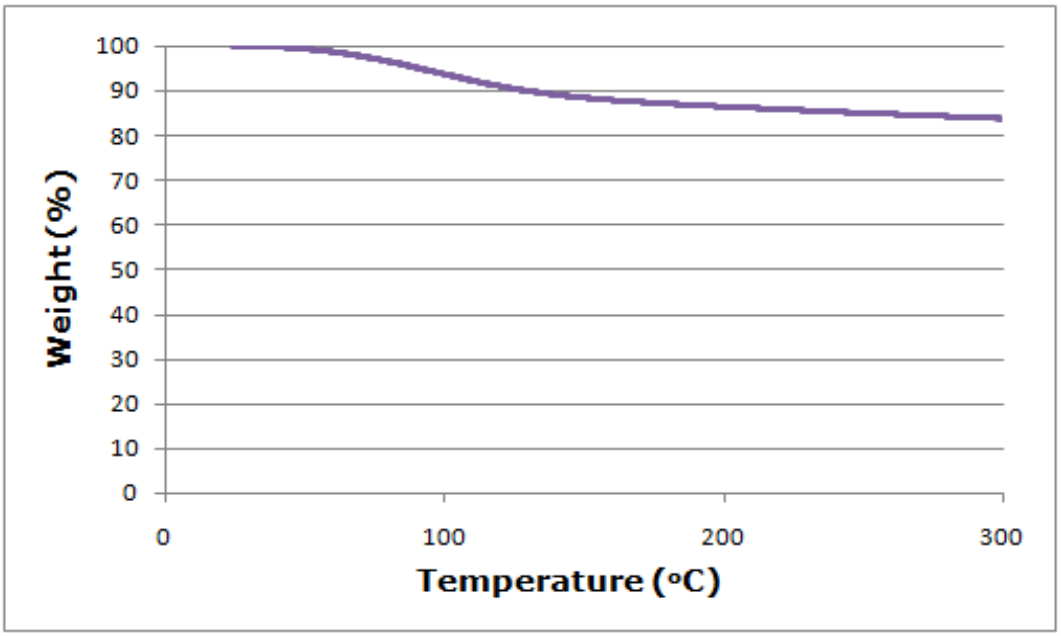

Figure F.16 TGA Result of Phosphoric Acid Impregnated Char for T=300 °C (Impregnation Ratio= 1/1)

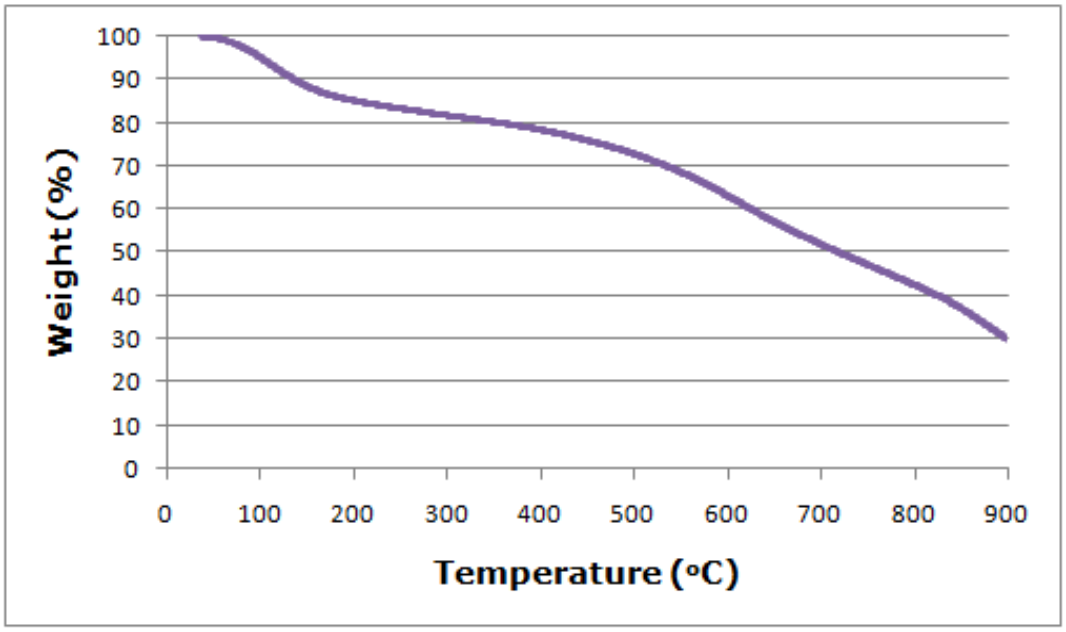

Figure F.17 TGA Result of Phosphoric Acid Impregnated Char for T=900 °C (Impregnation Ratio= 2/1)

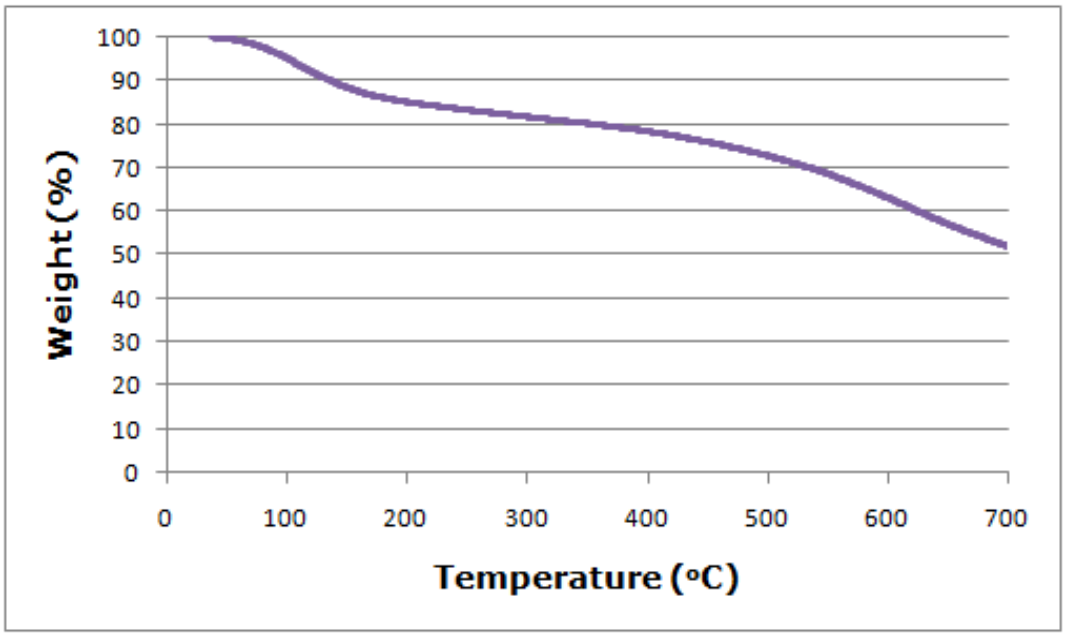

Figure F.18 TGA Result of Phosphoric Acid Impregnated Char for T=700 °C (Impregnation Ratio= 2/1)

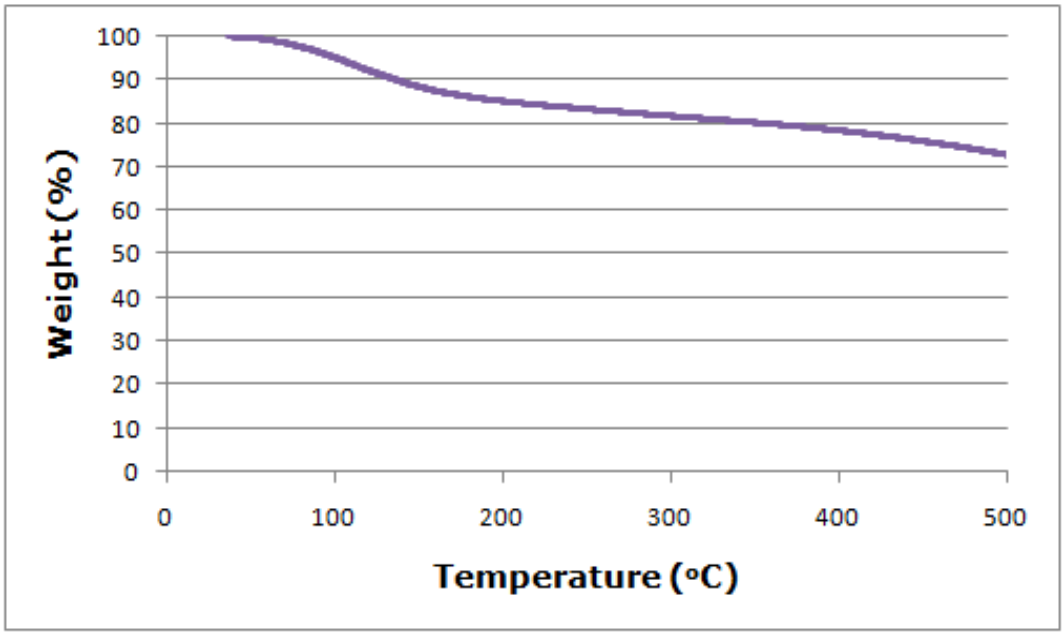

Figure F.19 TGA Result of Phosphoric Acid Impregnated Char for T=500 °C (Impregnation Ratio= 2/1)

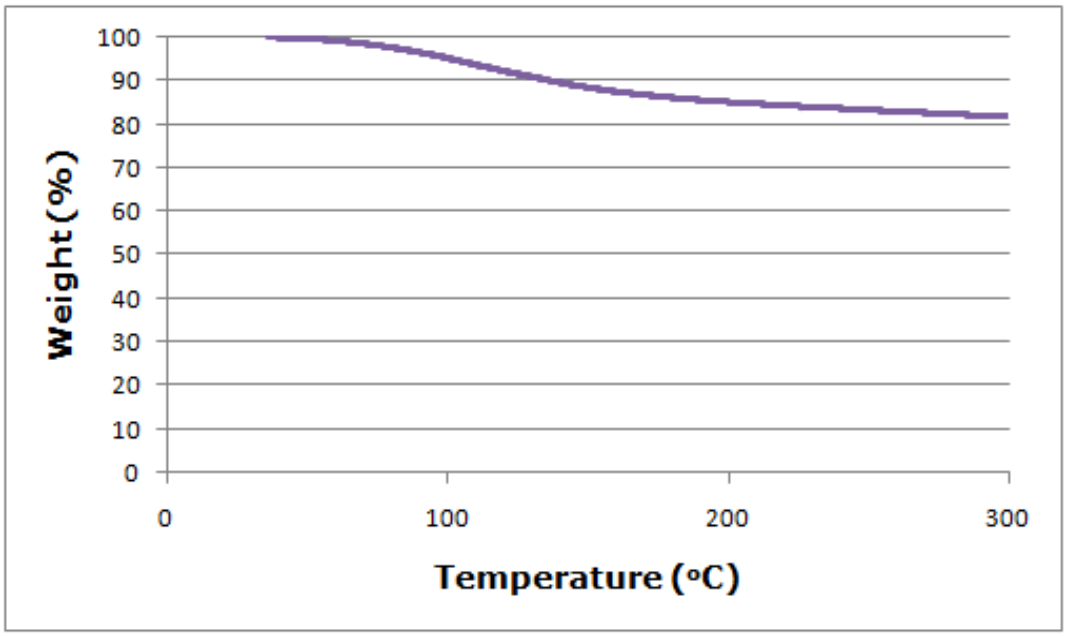

Figure F.20 TGA Result of Phosphoric Acid Impregnated Char for T=300 °C (Impregnation Ratio= 2/1)

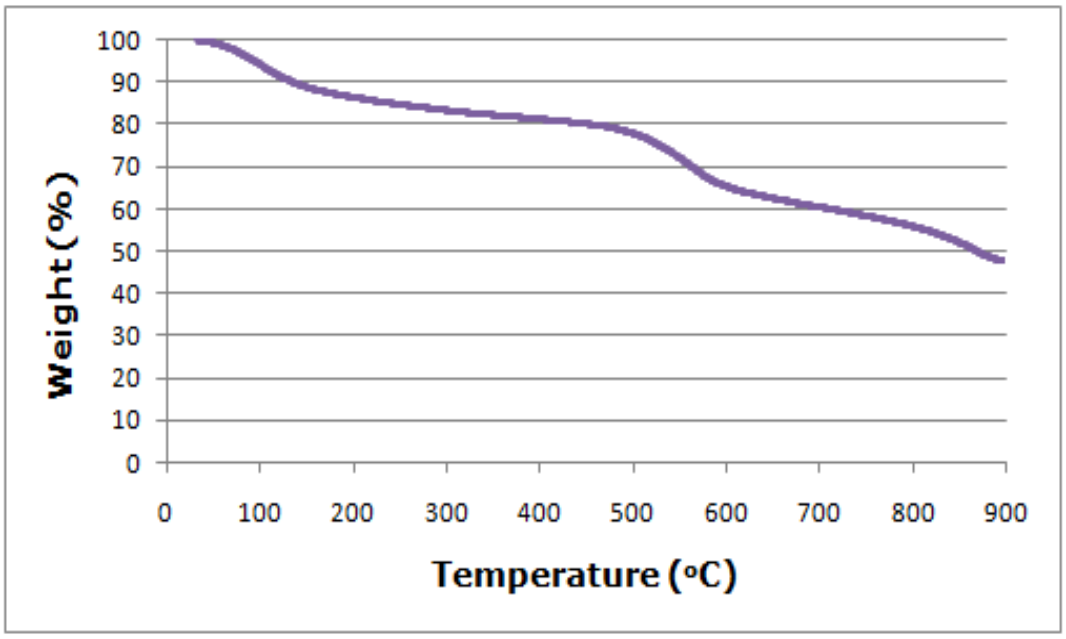

Figure F.21 TGA Result of Phosphoric Acid Impregnated Char for T=900 °C (Impregnation Ratio= 3/1)

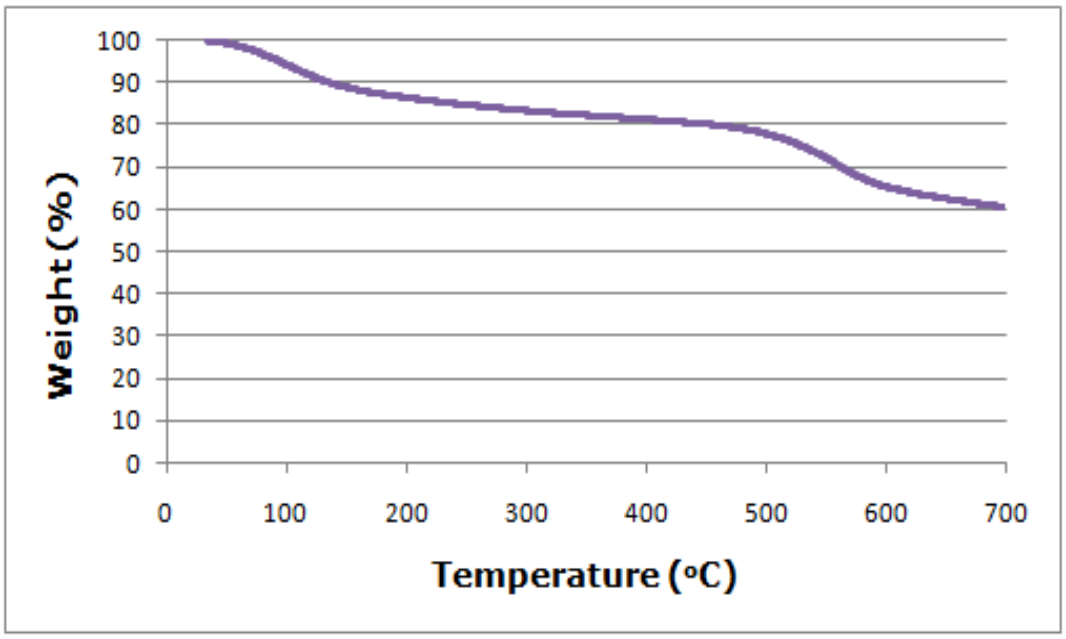

Figure F.22 TGA Result of Phosphoric Acid Impregnated Char for T=700 °C (Impregnation Ratio= 3/1)

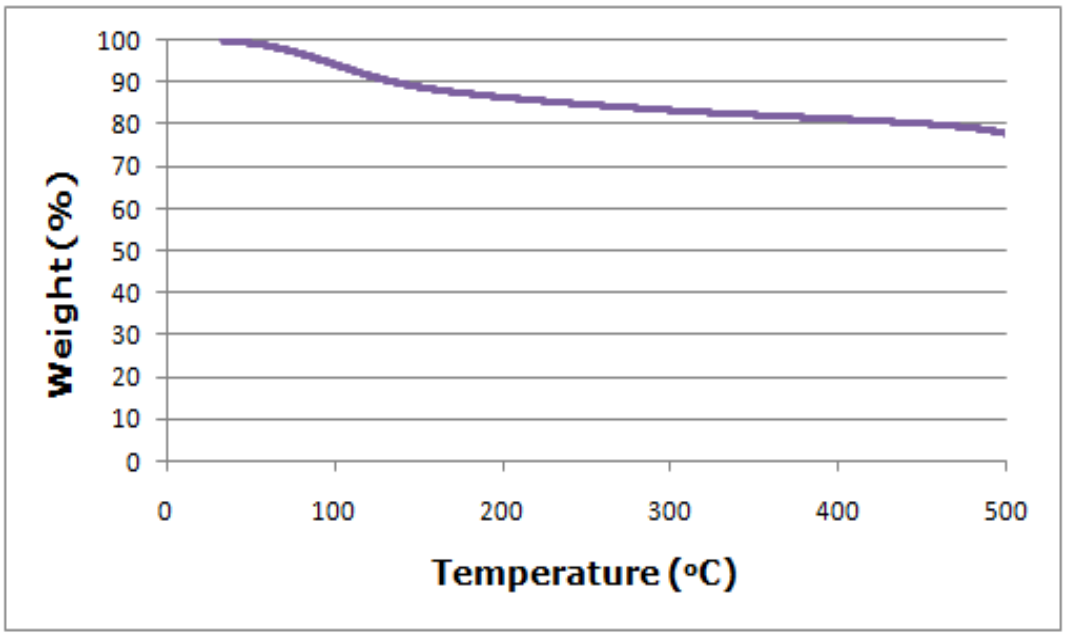

Figure F.23 TGA Result of Phosphoric Acid Impregnated Char for T=500 °C (Impregnation Ratio= 3/1)

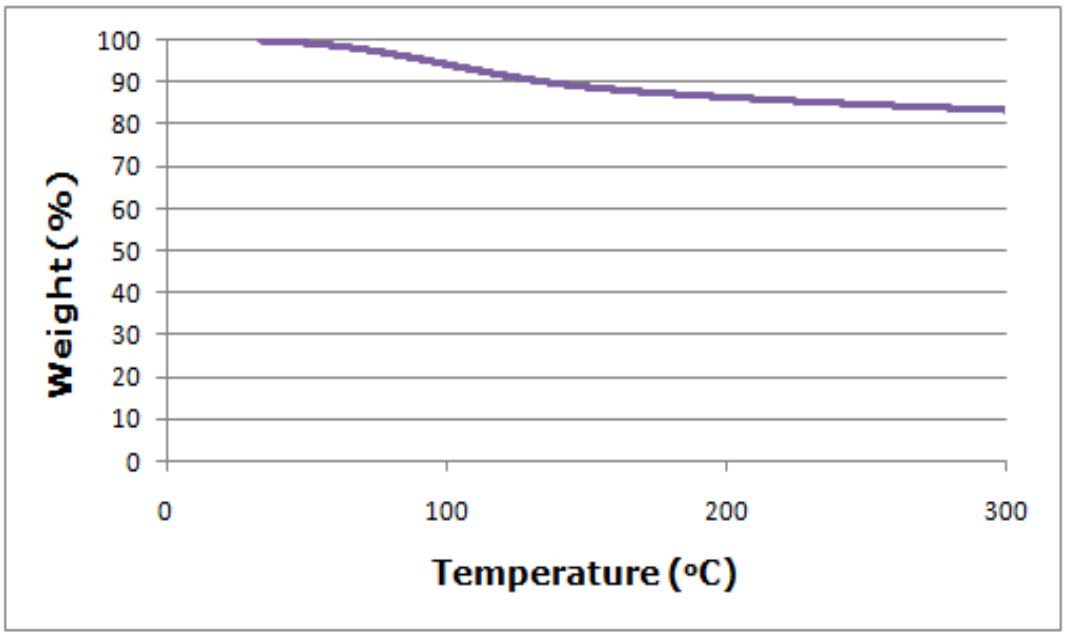

Figure F.24 TGA Result of Phosphoric Acid Impregnated Char for T=300 °C (Impregnation Ratio= 3/1)

APPENDIX G

REPEATABILITY EXPERIMENTS

Table G.1 BET Surface Area Values of Repeatability Experiments

Activated Carbon	BET Surface Area (m^2/g)	BET Surface Area (m^2/g)	% Deviation
AAR-1-300	1133	942	16.858
AAR-1-500	1293	1363	5.414
AAR-1-700	1059	1011	4.533
AAR-1-900	1286	1202	6.532
AAR-2-300	993	885	10.876
AAR-2-500	1477	1370	7.244
AAR-2-700	1354	1374	1.477
AAR-2-900	1413	1542	9.130
AAR-3-300	880	973	10.568
AAR-3-500	1640	1323	19.329
AAR-3-700	1517	1406	7.317
AAR-3-900	1573	1552	1.335